Seismic Performance of Indian RC Tall Buildings with Transfer Beam Located in Lower Seismic Zone (II)

Thesis submitted in partial fulfilment
of the requirements for the degree of

Doctor of Philosophy in ***Civil Engineering***

by

VELANI PULKIT DILIP
(20162311)
pulkit.velani@research.iiit.ac.in

International Institute of Information Technology, Hyderabad
(Deemed to be University)
Hyderabad – 500 032, INDIA

January 2024

International Institute of Information Technology

Hyderabad, India

CERTIFICATE

It is certified that the work contained in this thesis, titled **"Seismic Performance of Indian RC Tall Buildings with Transfer Beam Located in Lower Seismic Zone (II)"** by Mr Pulkit Dilip Velani, has been carried out under my supervision and to my knowledge, it is not submitted elsewhere for a degree.

Date: / /

January 2024

Advisor: Prof. Ramancharla Pradeep Kumar

Professor of Civil Engineering (on Leave)
Earthquake Engineering Research Centre
International Institute of Information Technology
Hyderabad, India – 500 032

Director
CSIR-Central Building Research Institute
Roorkee, Uttarakhand
India 247 667

Dedicated to those committed to advancing individual safety across diverse spheres.

Acknowledgement

I would like to extend my sincere appreciation to Prof. Pradeep Kumar Ramancharla, my advisor, for his unwavering support, insightful guidance, and compassionate mentorship throughout my PhD journey. His nurturing approach, coupled with occasional pushes and thoughtful actions, has been instrumental in shaping me both personally and professionally. Working under his guidance, particularly on projects like EDRI, has been a privilege that I cherish deeply. I am grateful to the Earthquake Engineering Research Centre (EERC) and the International Institute of Information Technology Hyderabad (IIIT-H) for providing the necessary infrastructure and resources essential for research. Special thanks to EERC faculty member Prof. Venkateswarulu Mandadi for his exceptional teaching, and to Dr. Sunitha Palissery and Dr. P. Pravin Kumar Venkat Rao for engaging in technical conversations and generously sharing their research journeys.

I extend my appreciation to the esteemed panel members, Dr. Vaibha Singhal from IIT Patna, Dr. Dipti Ranjan Sahoo from IIT Delhi, and Dr. Rehana Shaik from IIIT Hyderabad, for their valuable insights and constructive feedback during my thesis defence.

I am immensely grateful to Prof. Shatrunjay Rawat for his exceptional mentoring throughout this journey. He has not only provided guidance related to my research journey but also kept a vigilant eye on my overall development, fostering an environment conducive to growth in all aspects – physical, mental, and spiritual. His support and the opportunities he has offered have been instrumental in shaping me into a more well-rounded individual.

I am indebted to my PhD colleagues, who I consider as siblings in this academic journey, including Hima Sir, Dr Swajit, Dr Aniket, Dr Neelima, Dr Vyas, Dr Niharika, Bharat bhai, and Supriya. Our discussions, both technical and non-technical, have enriched my understanding of life and beyond, fostering a sense of camaraderie and mutual growth. The journey alongside M.Tech CASE students, spanning from the batches of 2017 to 2022, has been transformative in itself. From studying courses together to serving as a Teaching Assistant for many of them, this experience has instilled in me a sense of responsibility and exposed me to the wide spectrum of learning capabilities among students. I am grateful for the camaraderie and collaboration with other PhD and MS research students, as well as colleagues from various labs. Interacting with them has enriched my academic experience, providing opportunities for knowledge exchange, brainstorming sessions, and mutual support. Their diverse perspectives and expertise have broadened my horizons.

I extend my appreciation to the staff members of the Earthquake Engineering Research Centre (EERC), including Mr. Raju, Mr. Karthik, Mr. Krishna Babu, and Nagmani Madam, for their invaluable administrative support. Their dedication and assistance have played a crucial role in facilitating the smooth operation of various activities within the centre. I would like to express my gratitude to Pushpalatha Madam assistance has been instrumental in navigating various administrative processes and ensuring a seamless experience for students. Additionally, I am thankful to the entire administrative team and technical support staff for their invaluable contributions in providing logistical assistance, and ensuring the efficient functioning of the academic environment. I am deeply appreciative of the funding agency that supported my research endeavours.

I extend my heartfelt appreciation to Yuktahar Mess and the Sports facility for providing essential sustenance and opportunities for physical activity, contributing to my overall well-being during my PhD journey. Additionally, I am grateful to Vayu house, the Frisbee group, and the Volleyball group for their camaraderie and the integral role they played in fostering a healthy and joyful routine. Their support and companionship have been invaluable, enriching my experience outside of academia and contributing to a balanced lifestyle.

I am immensely grateful to the Hyderabad *Satsang* Group for their unwavering support and warm hospitality throughout my PhD journey. Specifically, I extend my heartfelt thanks to Mataji (Vimla Rawat), Bhaiya (Shatrunjay Rawat), Dr Sukhada didi, Didi (Ankita Nayak) and Bhaiya (Saurabh Nayak) and their families, Chachi (Sushila Nayak) and Chacha (Prakash Nayak) and their families, Didi (Soma) and Bhaiya (Atul Gotmare) and their families, as well as the Mehtre family (Usha, Baburao, Abhay, Akshay), and the Sharma family. Our discussions during *satsang* have been enriching, providing spiritual nourishment and a sense of belonging. The group has offered a homely atmosphere, standing by me through both the highs and lows of my journey. Their presence has been a source of immense comfort and strength, and I am deeply thankful for their unwavering support.

I am grateful to the E block Family for being wonderful neighbours, sharing in festivals and celebrations, and providing companionship to my wife. I must make a special mention of 2-year-old Arohi Shah; playing with her on a daily basis during my thesis writing provided moments of joy and respite, reminding me of the importance of balance and connection amidst academic pursuits. I extend my heartfelt appreciation to the faculty families residing in the quarters, whose warmth and camaraderie have enriched my residential experience. I am grateful to Dr. Zeel and Dr. Vineet, Anuradha Madam and family, Sheebaji and Dr. Sachinji, Dr. Naresh Manvani and Family, Dr. Prasad Krishnan and family, Dr Praful Mankar, Dr. Rehana and Family, as well as Dr. Avinsha and Family. Their presence has fostered a sense of community and belonging, making our residential environment feel like a home away from home. I am thankful for the shared moments, conversations, and support that have made my time here memorable and fulfilling.

I extend my sincere appreciation to my current company, MIDAS Research and Development Centre Pvt. Ltd., and its director, Mr. Naga Ravi, for their understanding and support. I am grateful to my manager, Mr. Nandeep, as well as my colleagues and juniors, for accommodating my commitments and providing the flexibility needed to respond to reviewer comments, prepare for my thesis defence, and navigate the demands of academia. Their support has been instrumental in balancing my professional responsibilities with my academic endeavours, and I am truly thankful for their cooperation and understanding.

I would like to extend my heartfelt appreciation to all individuals whose names I may have inadvertently missed but who have played a significant role in my PhD journey, whether directly or indirectly. Your contributions, whether through encouragement, support, or inspiration, have been invaluable and have left an indelible mark on my academic and personal growth. I am deeply grateful for your presence and influence, and I acknowledge the collective effort of all those who have contributed to shaping my path and enriching my experience.

With utmost reverence, I express my profound gratitude to my parents, Mother Pratibha Velani and Father Dilip Velani, for their unwavering support and sacrifices that have brought me to this point in my academic journey. Their encouragement and permission to pursue higher studies have been invaluable. I extend heartfelt appreciation to my siblings: my sister, Aditi Pokar, and brother-in-law, Miheer Pokar, for their moral support and understanding. Special thanks to my brother, Lawanya Velani, and his wife, Sanjana Velani, for their patience and unwavering support during my absence at home. Additionally, I am deeply grateful to my niece and nephew, Snehil and Pravanya, for their understanding and sacrifices, especially in sacrificing time with their Mama (me) due to my academic commitments. Furthermore, I extend my gratitude to my in-laws, the Dholu family, including Divya, Jagdish, and their daughter Devanshi, for their love and acceptance into their family. Their support has been a source of strength throughout my journey.

To my beloved wife, Dr. Tanvi, I express my deepest gratitude for her unwavering support, constant motivation, and selfless sacrifices throughout my academic journey. Beyond fulfilling her own responsibilities, she has often taken on additional burdens to ensure that I could focus on completing my work. Her small and significant sacrifices have been invaluable to me, and I am profoundly grateful for her unwavering love and dedication.

Finally, I express my deepest gratitude to the Almighty, who is Existent, Conscious, Blissful, Formless, Almighty, Just, Merciful, Unbegotten, Infinite, Unchangeable, Beginningless, Incomparable, the support of all, the Lord of all, All-pervading, Omniscient, and Controller of all from within. He is Evermature, Imperishable, Fearless, Eternal, Pure, and the Creator of the universe. I am humbled by the precious life He has bestowed upon me and pledge to strive to utilize it to the fullest potential.

…

Abstract

From last two decades, India is witnessing rapid urbanisation. Many tall buildings are coming up in tier I and tier II cities of India. To accommodate the functional needs of an occupant, such as car parking, within the same building, two different floor plans are needed. The requirement for unobstructed space for car parking and residential units is fulfilled by discontinuing the closely spaced vertical elements, such as structural walls and columns at certain floor levels. Elements supporting such discontinued elements are known as transfer elements, and buildings with such features are becoming popular in India. Transfer elements introduce stiffness irregularity in the structure, which is undesirable from the design code point of view. The recently introduced tall building code IS 16700 does not have detailed guidelines for analysing and designing such structures. Weather these structures are safe is the question that needs to be answered. With that question in mind, a detailed literature review is carried out to know the global practice of analysing and designing tall buildings with transfer elements located in lower seismic zones of respective countries. Overall, the literature reviewed supports the idea of constructing buildings with transfer elements in the lower seismic zone. However, these recommendations are supported by comprehensive experimental and numerical studies tailored to local seismic hazard and construction practices.

Therefore, the motivation of this study is to contribute to the understanding of the global response of RC tall buildings with transfer beams subjected to seismic activity. Particular attention is given to the residential building with RC transfer beam (TB) located in seismic zone II. Along with this, the study also attempts to evaluate the advantages and disadvantages of attaching a podium to the buildings under focus. For this purpose, residential buildings inspired by current building stock are analysed and designed using relevant IS codes. And later, the seismic performance of these buildings is evaluated using Linear Time History Analysis (LTHA) method. Three global parameters, viz., base shear, displacement and inter-storey drift ratio (IDR), and two local parameters of PMM capacity ratio and shear demand to capacity ratio, are used as performance indicators.

Assessment of these buildings revealed that the base shear values due to LTHA were observed to increase by 19-32% compared to the design base shear of buildings. However, roof displacements for all the buildings are found to be very lower. Also, displacement variation due to podium configurations were found to be negligible. The maximum IDR value did not exceed 1/5th of code limiting IDR values. Furthermore, despite the stiffness and mass irregularities near the TB level, the maximum IDR demand was found to be at the upper storeys. The PMM capacity ratio of all the

columns of different buildings does not exceed 0.30, which indicates that the brittle failure of transfer columns will not be present. Similarly, the transfer column shear demand to capacity ratio reached only 0.50.

The study found that the building performance was satisfactory under LTHA, even after qualifying for several irregularities, thus eliminating the need to revise the code limits for inter storey drift ratio. Additionally, it was found that residential buildings with RC transfer beams can perform well in seismic zone II when all analysis and design criteria are properly followed. The impact of podium configurations on the seismic resistance of buildings was found to be negligible. This implies that architects and structural engineers can choose whether or not to include a separation joint based solely on functional and execution requirements. Hence, the transfer beam feature can be allowed in seismic zone II and for zone III, IV and V further investigation is needed before it is recommended.

…

List of Publications

Journals:

1. Velani, P. D. & Pradeep Kumar, R. (2023), "Seismic Performance of RC Tall Buildings with Transfer Beam Located in Seismic Zone II", ***Indian Concrete Journal (00194565)***, 97(7), pp 16-30.
2. Velani, P. D. & Pradeep Kumar, R. (2023), "Approximate Natural Period Formula for Reinforced Concrete Tall Buildings in India – A proposal", ***Current Science (00113891)***, 124(12), pp 1412-1421. https://ischolar.sscldl.in/index.php/CURS/article/download/223032/206378
3. Velani, P. D. & Pradeep Kumar, R. (2022), "Behaviour of Tall Buildings with Transfer Storey", ***Structural Engineering Digest***, pp. 202-215, April-June 2022.
4. Velani, P. D., Patnala, N., Prakke, B., Shastry, S. L. N., & Kumar, R. P. (2022), "Tremors and built environment of Hyderabad, Telangana, India: safety of buildings using recorded ground motions", ***Current Science (00113891)***, 122(10), pp 1174-1184. doi: 10.18520/cs/v122/i10/1174-1184
5. Velani, P. D. & Pradeep Kumar, R. (2020), "Separation distance between two adjacent buildings a case study clause 7.11.3, IS 1893:2016", ***Structural Engineering Digest***, Jan-March 2020, pp. 70-78.

Conferences:

1. Velani, P. D. & Pradeep Kumar, R. (2024), "***Damping of RC Tall Buildings in India by Ambient Vibration Test***", Proc. of 18th World Conference on Earthquake Engineering, Milan, Italy 30 June – 05 July 2024.
2. Velani, P. D. & Pradeep Kumar, R. (2021), "***Seismic Performance of RC Tall Building with Structural Walls Resting on Transfer Girder***", Proceeding of 17th World Conference on Earthquake Engineering, 17WCEE 2020, Sendai, Japan. https://wcee.nicee.org/wcee/article/17WCEE/2c-0163.pdf
3. Velani, P. D. & Pradeep Kumar, R. (2018), "***Effect of Aspect Ratio and Elevation Profile on Mode Shapes of Tall Building***", Proc. of 17th International Symposium on New Technologies for Urban Safety of Mega Cities in Asia (USMCA-2018), IIIT Hyderabad, India, 12 – 14 December 2018
4. Velani, P. D. & Pradeep Kumar, R. (2017), "***New Empirical Formula for Fundamental Period of Tall buildings in India by Ambient Vibration Test***", Proc. of 16th World Conference on Earthquake Engineering, Santiago, Chile 9-13 Jan 2017. https://wcee.nicee.org/wcee/article/16WCEE/WCEE2017-218.pdf

Reports:

1. Dilsiz, A., S. Gunay, K. Mosalam, D. Prevatt, E. Gerczak, E. Miranda, C. Arteta, H. Sezen, E. Fischer, M. Hakhamaneshi, W. Hassan, B. ALhawamdeh, S. Andrus, J. Archbold, S. Arslanturkoglu, N. BEKTAS, L. Ceferino, J. Cohen, B. Duran, K. Erazo, G. Faraone, T. Feinstein, R. Gautam, A. Gupta, S. Haj Ismail, A. Jana, S. Javadinasab

Hormozabad, A. Kasalanati, M. Kenawy, Z. Khalil, I. Liou, M. Marinkovic, A. Martin, Y. Merino, M. Mivehchi, L. Moya, C. Pájaro Miranda, n. quintero, J. Rivera, X. Romão, M. Lopez Ruiz, S. Sorosh, L. Vargas, **P. Velani**, H. Wibowo, S. Xu, T. YILMAZ, M. Alam, G. Holtzer, T. Kijewski-Correa, I. Robertson, D. Roueche, A. Safiey (2023) "*StEER: 2023 Mw 7.8 Kahramanmaras, Türkiye Earthquake Sequence Preliminary Virtual Reconnaissance Report (PVRR)*", in StEER- February 6, 2023, Kahramanmaras, Türkiye, Mw 7.8 Earthquake. DesignSafe-CI. doi: 10.17603/ds2-7ry2-gv66 v1 https://www.designsafe-ci.org/data/browser/public/designsafe.storage.published/PRJ-3824

2. R. Pradeep Kumar, Aniket Bhalkikar, **Pulkit D. Velani**, Pammi Vyas, Bharat Prakke, Patnala Neelima, and Niharika Talyan (2020), *"A Primer on Rapid Visual Screening (RVS) Consolidating Earthquake Safety Assessment Efforts in India"*, National Disaster Management Authority, New Delhi, GoI. https://ndma.gov.in/sites/default/files/PDF/Technical%20Documents/RVS-Doc-11-2020.pdf
3. R. Pradeep Kumar, Swajit Singh, Aniket Bhalkikar, Patnala Neelima, **Pulkit D. Velani**, Pammi Vyas, Niharika Talyan, Hima Dasari, Keerthana Etoori, and Manoj reddy (2019), *"Earthquake Disaster Risk Index Report 50 Towns & 1 District in Seismic Zones III, IV and V"*, National Disaster Management Authority, New Delhi, GoI. https://www.ndma.gov.in/sites/default/files/PDF/Reports/EDRI_Report_final.pdf

…

Table of Contents

List of Figures

List of Tables

Abbreviations

BIS	Bureau of Indian Standards
CTBHU	Council on Tall Buildings and Urban Habitat
DIDR	Distortion Inter-storey Drift Ratio
ESA	Equivalent Static Analysis
FFT	Fast Fourier Transform
GMs	Ground Motions
IS	Indian Standards
LATBSDC	Los Angeles Tall Buildings Structural Design Council
LL	Live Loads
LTHA	Linear Time History Analysis
MRF	Moment Resisting Frame
NSE	Non-Structural Elements
PGA	Peak Ground Acceleration
RC	Reinforced Concrete
RSA	Response Spectrum Analysis
TB	Transfer Beam
TG	Transfer Girder
TP	Transfer Plate

Chapter 1. Introduction

1.1 Overview

India is prone to various natural disasters due to its unique geographical, climatic and socio-economic conditions. This disaster includes floods, droughts, cyclones, tsunamis, earthquakes, urban flooding, landslides, avalanches, and forest fires. Disaster risks in India are further compounded by increasing vulnerabilities related to changing demographic and socio-economic conditions, unplanned urbanization, and development within high-risk zones. Of the country's 36 states and union territories, 27 are disaster-prone (NDMA GoI, 2021). About 58.6% of the landmass is prone to moderate to high intensity earthquakes. In the last three decades, India has witnessed many large earthquakes, such as Khillari (30th September 1993), Jabalpur (22nd May 1997), Chamoli (29th March 1999), Bhuj (26th January 2001) and Nepal (25th April 2015) which has caused significant life loss and property loss. The primary cause of life loss is attributed to the collapse of the buildings (Ramancharla & Murty, 2014). The professionals involved in building construction should be more concerned with the safety of building infrastructure during future earthquake events.

Further, Urbanization is rapidly increasing in almost every city in India. Huge infrastructure developmental plans have been laid by government and private organizations. Urban-centric economy, slum redevelopment project (Deshpande, 2023), housing for all scheme(GoI, 2015b, 2021), and smart city mission (GoI, 2015a) are going to create an increase in the number of tall buildings in Indian towns and cities. Hence, sufficient attention must be paid to the safety of the physical infrastructure of the urban area.

Tall buildings in urban areas have a major contribution to its physical infrastructure. Usage of tall buildings is not just limited to the residential sector but also office space, trading, and hotel industry. Due to space constraints and the need for multiple functional utility usage, discontinuous vertical elements are becoming popular in urban settlements in India (Figure 1.1). The builder community tries to accommodate a maximum number of flats in a project constructed at the city's prime location. The overall flat size in such projects is designed to cater for the need of a middle-class family. This leads to a closely spaced supporting system or the adoption of a structural wall system. However, the bay width from such planning is not feasible for accommodating obstruction-free space for an assembly hall, shopping malls, indoor sports facilities, gym, parking area, commercial space for sell/rent/lease etc., within the same structure.

To have obstruction-free space use of transfer elements to support the discontinuous elements came into practice (Figure 1.2). The idea is to use large span beams, trusses or slabs in the lower storey of the tall buildings to have obstruction-free facilities listed above. Once the desired additional facilities are accommodated at initial floor levels, the typical floors with closely spaced vertical elements such as structural walls or columns are constructed. The first storey of a typical floor, which needs closely spaced elements, is supported on the transfer storey provided just below it. Such a storey has a relatively huge depth of slab, beams or truss compared to a typical storey since they have to carry a large amount of axial force and bending moments transferred by floating columns or shear walls. Transfer storey must transfer the vertical and lateral load from the upper storey to the storey below it. However, adopting such features leads to an abrupt change in the lateral stiffness of the storey. This might lead to localised damage near the transfer storey during earthquake shaking. Despite this known fact use of transfer structure is adopted in India and worldwide.

(a) (b)

Figure 1.1: Buildings with Transfer Storey (a) Hotel from Mumbai(Ahmed, 2020); (b) Upcoming twin residential apartments from Hyderabad;

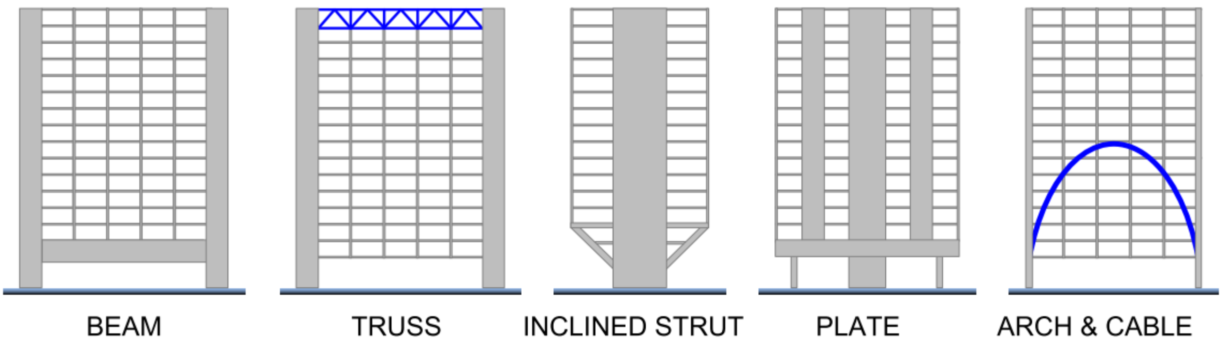

Figure 1.2: Types of transfer structures (G. X. S. Ribeiro, 2018)

The tall building code (IS 16700, 2017) of India is relatively new and does not have detailed provisions on buildings with transfer storey. Because of a lack of code provision, unregulated building stock with a transfer element is getting added to the physical infrastructure. On the other hand, vertical space above the railway station can be utilized by constructing buildings with transfer elements. The Vashi railway station commercial complex located in Navi Mumbai, Maharashtra, is an excellent example of the same (Figure 1.3). As part of the 75th independence celebration, Indian railways has launched Amrit Bharat Station Scheme (PIB Delhi, 2022), under which about 1275 railway stations (PIB Delhi, 2023) will undergo a major upgrade. Utilizing this space without the use of a transfer beam is impossible. To seize development opportunities, including those similar to this scheme, and to promote city infrastructure growth without compromising seismic safety, an in-depth literature review and code provisions on buildings with transfer storeys are carried out in Chapter 2. Based on the comprehensive study of this topic, including the analysis and design of transfer storeys and other relevant topics, the motivation, objectives, and scope of the present study are defined in the subsequent sections.

(a) Bird’s eye view of Vashi station building (VRSCCL, 2019)

(b) Inside view of building showing track, deep beams and transfer columns (Hindustan Times, 2016)
Figure 1.3: Building above railway station example of Vashi railway station Navi Mumbai, Maharshtra

1.2 Motivation and Objective of the study

The motivation of this study is to contribute to understanding the global response of RC tall buildings with transfer beams (TBs) subjected to seismic activity. Particular attention is given to the residential building having a TB.

There are two primary objectives of this study:

1. To evaluate the effect of RC TB on seismic performance of tall residential buildings located in low seismic zone (II) of India.
2. To evaluate the advantage or disadvantages of attaching podiums in buildings under focus and propose guidelines that could be incorporated in IS 16700.

1.3 Scope of the study

1. The present study is limited to assessing the performance of RC TB only. And the study does not cover other materials, such as steel or composite TBs.
2. As per IS 16700, tall building height ranges from 50 m to 250 m; however, the current work is restricted to a storey range of 20-50 floors(50-150m).
3. Further, only residential buildings are chosen for study without considering complex architectural features such as chajja, balconies and openings in structural walls.

1.4 Significance of the study

1) The insight from current work would assist the Bureau of Indian Standards (BIS) and building approval body at the municipal/town level in improving building codes and bylaws. This will not only help in regulating the development of tall buildings with TB in India but also become reference material for the non-prescriptive review process of code exceeding tall buildings.
2) The present study is probably the first study examining the seismic performance of RC residential tall buildings with transfer beams in India (seismic zone II). It is hoped that current work will lay the groundwork for future research on assessing and retrofitting existing tall buildings with transfer elements located in zones III to V.
3) The outcome of this thesis might open a new possibility for constructing tall buildings with TB above railway stations located in seismic zone II across the country, which can be directly valuable to Indian Railways for executing Amrit Bharat Station Scheme (PIB Delhi, 2022), aiming to renovate 1275 railway stations (PIB Delhi, 2023) across the nation.

1.5 Organization of the Thesis

The entire thesis consists of five chapters.

Chapter one initially gives the background of the problem, and based on the literature review done in chapter two, the study's motivation, objective, and scope are listed.

Chapter two beings by discussing damage to tall buildings in the past earthquake, followed by documenting nation-wise literature on transfer structures of several countries. Further, It also highlights the provisions published in the USA and Hong Kong codes on transfer storey. The chapter ends by comparing Indian and Chinese codes on several aspects linked with tall buildings with TB.

The numerical modelling takes the form of **Chapter three**. Initially, the details of the buildings chosen are described, followed by detailed information on the modelling and design of buildings is described in detailed. The other section discusses several code recommendations which are violated by these buildings and the reasons for violation.

Chapter four mainly focuses on the seismic performance of eighteen buildings under focus. After designing these buildings, they are subjected to eleven ground motions. The outcome of this assessment in terms of displacements, inter-storey drift ratios, base shear, PMM capacity ratio and shear demand to capacity ratio is discussed in detailed.

At last, **Chapter five** gives the conclusion of the current study along with the significance of the finding. The study's limitations and future scope have also been discussed at the end.

…

Chapter 2. Code Provisions and Literature Review

2.1 Overview

This chapter contains the behaviour of tall buildings in past earthquakes, followed by a discussion of numerical and experimental studies carried out around the world. The code provisions developed by some of these countries based on extensive research are also discussed and compared with those available in the Indian codes.

2.2 Literature review

2.2.1 Damage in past earthquakes

It is well-known that discontinuities in vertical stiffness and strength lead to damage concentration. The performance of Olive View Hospital in the 1971 San Fernando earthquake was a wakeup call for the earthquake engineering community. It has revealed the possible threats posse by buildings having a discontinuous shear wall. The olive hospital did not collapse, but two occupants in intensive care and a maintenance person working outside the building were killed. The general vertical configuration of the main building was a 'soft' two-storey layer of rigid frames supporting a four-storey (five, counting penthouse) shear wall-plus-frame structure (Figure 2.1). The second floor extends out to form a large plaza. Severe damage occurred in the soft story portion (Figure 2.2). The upper stories moved as a unit and moved so much that the columns at ground level could not accommodate such a large displacement between their bases and tops, and hence failed (FEMA 454, 2006). The largest amount by which a column was left permanently out-of-plumb was 2 feet 6 inches.

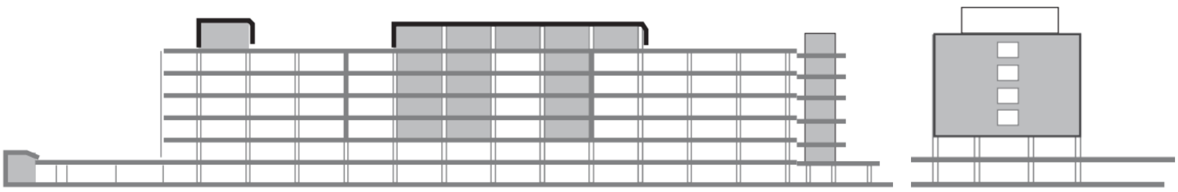
(a) **Long section** (b) **Cross section**

Figure 2.1: Olive View Hospital (FEMA 454, 2006)

Quoting Arnold (Arnold, 1984) on the reason for such damage at the hospital, he states, "*Had the columns at Olive View been more strongly reinforced, their failures would have been postponed, but it is unrealistic to think that they would have escaped damage. Thus the significant problem lies in the configuration, and not totally in the column reinforcement.*" Such practices are continued for high-rise buildings as well without knowing the consequences.

(a) Fallen stair towers and damaged basement

(b) Heavy damage to columns at the bottom storey

Figure 2.2: Damage in Olive Hospital (USGS (*Wikimedia Foundation*, 2005))

A decade back, on 27 February 2010 devasting offshore Maule, Chile earthquake of moment magnitude 8.8 shook a major part of Chile. Among many organisations, The Los Angeles Tall Buildings Structural Design Council (LATBSDC) formed a reconnaissance team to visit the areas of Santiago, Concepción and Viña del Mar areas. Based on the reconnaissance survey, they have compiled the common damages observed in the tall buildings in the regions mentioned above. One very interesting case of 16 storeys tall '*Torre del Mar*' building located at 8 Norte 380 at 3 Poniente, Viña del Mar was mentioned in their study (Carpenter et al., 2011) and is discussed here. The building was constructed in 1988, and the change of floor plan took place at level 3 of the building, causing vertical irregularity. The wider shear wall in the lower storey suddenly narrows at level 3. This sudden change in stiffness was the fundamental reason for causing damage to shear walls and columns at level 3 (Figure 2.3). The authors observed that transfer and discontinuities in the structural system, particularly at the ground floor storey, were prevalent. They also found that such building irregularities are present largely at the transition areas at the first storey from residential units above to the lobby and transitions to the parking areas below. The study recommends paying special attention to the planning and execution of such unique configurations.

(a) Exterior view with an evident change of stiffness at level 3

(b) Damage to wall and column at level 3

Figure 2.3: Torre Del Mar building (Carpenter et al., 2011)

2.2.2 Past Studies on Transfer Structure

2.2.2.1 India

There are very limited documented or published studies on building with transfer elements. Palais Royale, a popular and unique building in Mumbai, has used a 9m deep post-tensioned transfer girder (TG). Palais Royale Residential Tower (Figure 2.4) has a height of 325m, measured from the bottom of the raft to the roof, and is located in downtown Mumbai, India. The typical floor consists of a residential area with 244 columns, whereas the initial few storeys are reserved for parking area, and the sports arena has only 88 columns. Hence, up to 9m deep by 1200mm to 1500 mm wide TGs support discontinuous columns. Girders are analysed by finite element modelling using STADD-Pro commercial software. The analysis confirmed that girder behaves as a deep beam which can be designed by strut-tie model (Colaco et al., 2012).

Figure 2.4: Palais Royale, Mumbai (Under construction)

2.2.2.2 Europe

The interaction between walls supported by the beam has been an area of research as back as 1960s. A study conducted in great Britain (Coull, 1966) emphasises that the assumption of neglecting the stiffness of walls and treating the wall as a purely uniformly distributed beam load must be changed. The study redraws the reader's attention towards the 'arching' action in the wall, tending to redistribute the loads to the ends of the beams. In the same study, as part of the opening remark, the author identifies a similar problem in modern tall buildings where shear walls are discontinued. In the next decade, Green (Green, 1972) proposes the approximate method for designing beam supporting shear walls. The study gives formulae to compute complex demand with reasonable accuracy. The entire proposal is based on the finite element method, verified with experimental studies, considering important variables (Figure 2.5) such as dimensions of shear walls, beam & columns: dimensions, cross sectional area, and moment of inertia. A recent study by Ribeiro et al. reveals the importance of tackling vertical vibration in transfer storey to ensure human comfort (G. Ribeiro et al., 2022).

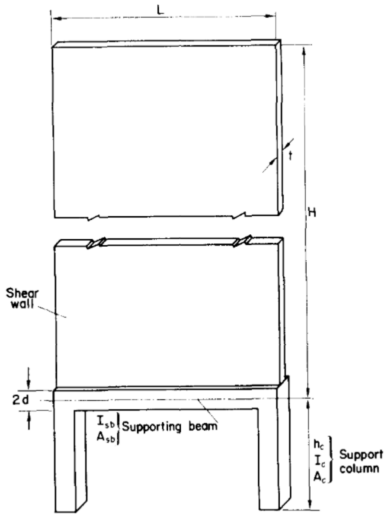

Figure 2.5: Parameters considered in Green's study [Source : (Green, 1972)]

2.2.2.3 Hong Kong and China

Hong Kong has many tall buildings with transfer elements(Ho, 2009; C. S. Li, 2005; S. Li, 2000; Puvvala, 1996; Zhang, 2000). Hence, the scientific community of this region does many numerical and experimental studies on transfer elements. Many of the work is published in the native Chinese language; hence, work published in English and easily accessible are only discussed in this section. A study by Kuang and Puvvala (Kuang & Puvvala, 1996) extended the understanding of the interaction between the shear wall and the TG. The study focuses on a continuous girder supported by three columns. The authors use the finite element analysis tool, ABAQUS, to model a typical assembly, as shown in Figure 2.6. The study reveals how the upper structural form significantly influences the behaviour of TGs, where the girder can undergo full tension or behave as an ordinary flexure beam. Significant parameters of the transfer beam-shear wall system, such as the span/depth ratio of the TB, the span of the shear wall and the stiffness of the support columns, are linked with the vertical stress, axial stress, and shear stress of transfer beam-shear wall system.

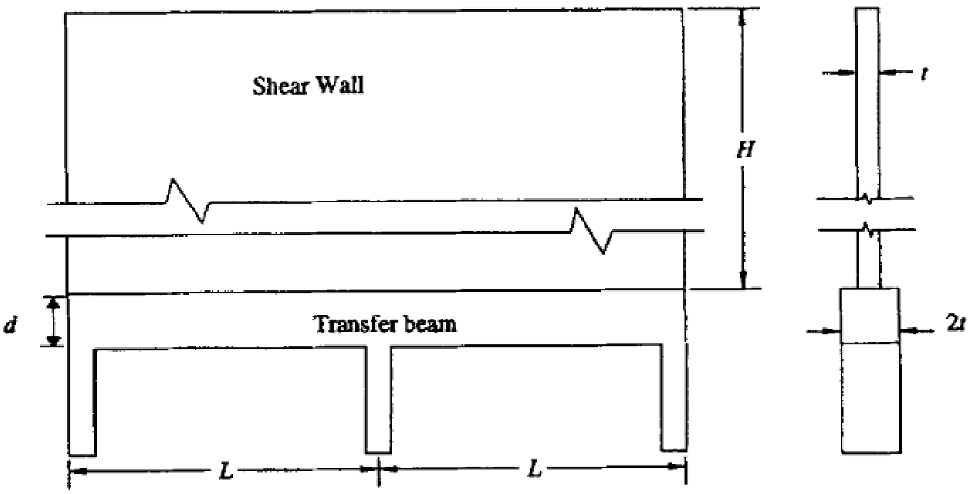

Figure 2.6: Typical two span transfer beam-shear wall assembly (Kuang & Puvvala, 1996)

Kunag and his team kept working in this area for a few more years and produced the design tables in two case studies, which can help the designer decide the size of TBs and supporting columns. Both case studies use finite element tool to compare the results obtained by the proposed tables. The first study (Kuang & Li, 2001) derived tables based on the equivalent portal method (Figure 2.7), and the second study (Kuang & Li, 2005) drew inspiration from the box foundation analogy (Figure 2.8).

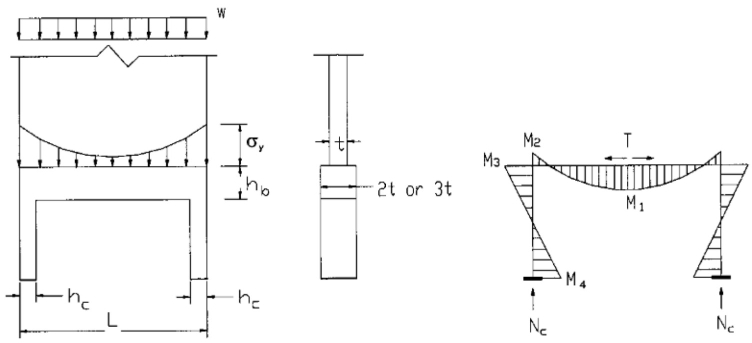

Figure 2.7: Equivalent portal frame model (Kuang & Li, 2001)

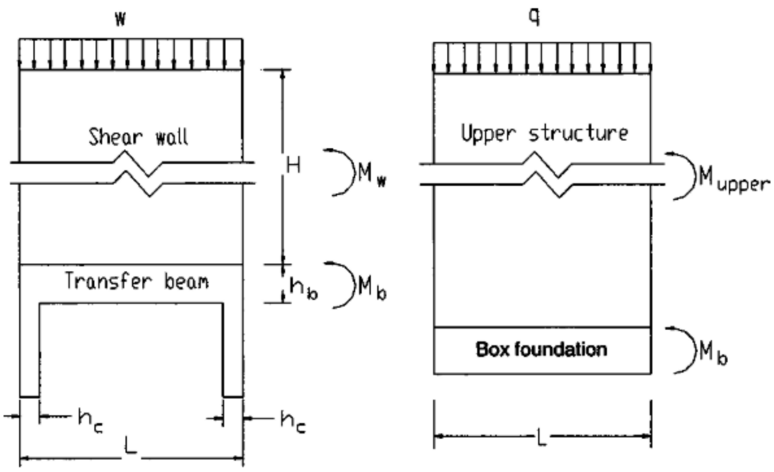

Figure 2.8: Box foundation model (Kuang & Li, 2005)

In 2006 (C. S. Li et al., 2006), One of the experimental studies aimed to assess the seismic performance of high-rise buildings with a transfer plate (TP) designed for non-seismic requirements. For this purpose, a typical reinforced concrete residential building in Hong Kong was selected. A 1:20 scale model of a building was fabricated using micro-concrete with steel wires to simulate reinforcement in concrete. The similitude laws of length ratio, modulus ratio, equivalent density ratio, time ratio, frequency ratio and acceleration ratio were fully considered in preparing the model tests. The typical characteristic strength of the micro-concrete was 2-3 MPa. Additional mass was used to satisfy the similitude law of equivalent density ratio. The building had 34 typical floors supported by a TP of 2.7m thick and a three-level podium (Figure 2.9). Shaking table tests were conducted by considering minor, moderate, major, and supermajor earthquakes. Earthquake records of the 1940 El Centro Earthquake in NS component and/or the 1952 Taft earthquake were employed in the tests. Peak accelerations of the various earthquake records were appropriately magnified or reduced to reflect different levels of earthquakes (Table 2.1). All tests assumed the same seismic intensity of VII pursuant to National Standard (GB18306-2001, 2001).

Table 2.1: Peak accelerations values adopted in shaking table test (C. S. Li et al., 2006)

Earthquake	Peak Acceleration
Minor	0.02g–0.06g
Moderate	0.08g–0.14g
Major	0.15g–0.20g
Supermajor	0.25g–0.34g

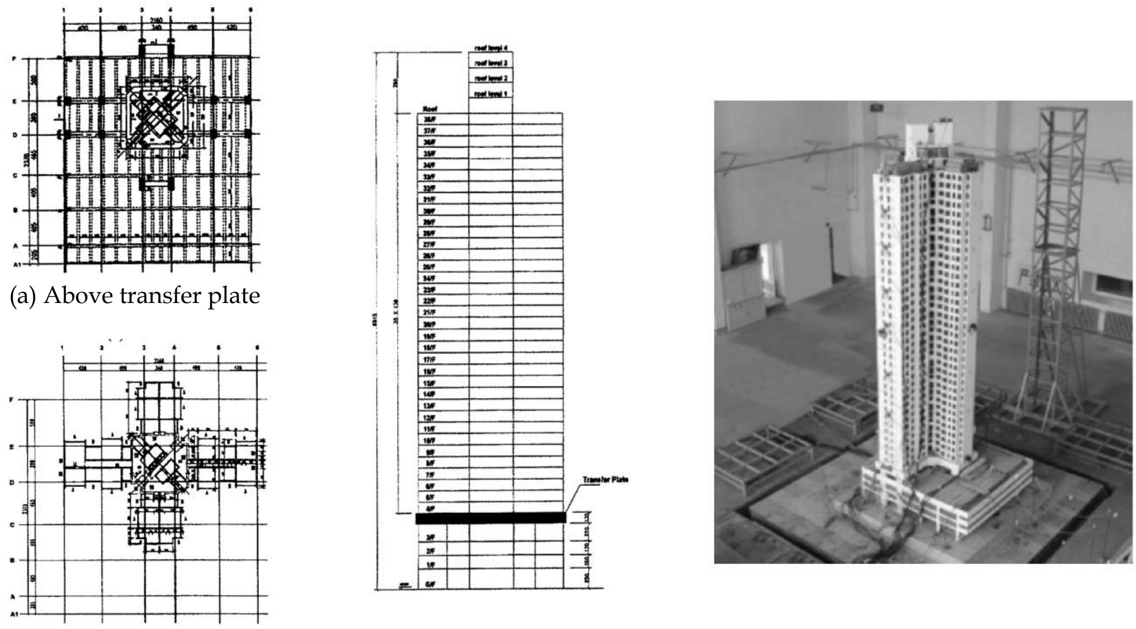

(a) Above transfer plate

(b) Below the transfer plate

(c) Elevation

(d) Microconrete prototype of building in 1:20 scale

Figure 2.9: Building details and Experimental setup of Test

The shaking table tests indicated that under frequent (minor) earthquake excitations, all the buildings remained elastic, no cracks were found in the models, and the natural frequencies of the models did not decrease. When the models were subjected to occasional (moderate) earthquakes, cracks began to occur at the tops of columns below TBs and at the base of the 1st floor columns. After rare (major) earthquakes, all the models were severely damaged. Tension failure was found on the end shear walls in the vicinity above the TP. When subjected to occasional earthquakes, damage in a building leads to changes in natural frequencies and damping. The natural frequencies in both directions were reduced by 14%. Considerable inelastic behaviour was observed when a model was subjected to rare earthquakes. At this stage, the decrease in natural frequency was in the range of 20-46%.

For many years, the multistorey buildings in Hong Kong regions have been designed without seismic provisions since many urban areas come under low to moderate seismicity region. In 2007, Zhou et al. (Zhou & Xu, 2007) demonstrated that a building with TP, designed for wind load and located in a moderate seismicity region, may also need to be explicitly designed for seismic action as well. The study arrived at this conclusion after assessing the performance criteria of a building when subjected to frequent earthquakes, design based earthquakes and maximum creditable earthquakes. The study reveals that most of the performance criteria are satisfied under the application of frequent earthquakes, but a few objectives, such as inter-storey drift ratio, could not be satisfied.

Immediately next year, Su (R.K.L. Su, 2008) published a detailed literature review on the seismic behaviour of transfer structures in low-to-moderate seismicity regions.

This paper first discussed existing seismic guidelines as per Chinese and Hong Kong codes. Then a comparative analysis of past experimental studies is done. Further, additional members' demands are discussed due to local transfer element deformation. A literature review is concluded by discussing important topics such as the design criteria for transfer structure in Chinese code, the effect of soft storey below the transfer storey, and vertical position of transfer storey. In 2009, same author (R. K. L. Su & Cheng, 2009) developed a qualitative model representing the shear concentration in the exterior wall due to TP deformation (Figure 2.10). The study reveals that this shear concertation demand arises due to a change in inter-storey drift between the exterior walls and centre wall above the transfer level. Further, authors have linked the effect of a) depth of TB, b) exterior wall thickness, c) storey height above the transfer storey, and d) vertical position of the transfer storey; with a shear concentration in the exterior wall.

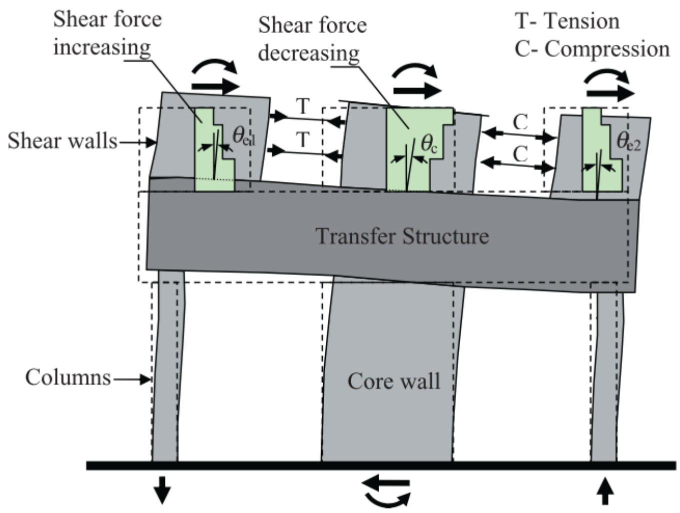

Figure 2.10: Local deformation of the transfer structure and shear concentration at the exterior

2.2.2.4 Sri Lanka

A Sri Lankan study (Balasuriya et al., 2007) on buildings with TP uncovers that careful modelling of a tall building with a transfer element can help in reducing wind induced acceleration. The author compares the linear performance of a building with and without TP and concludes that the wind induced deflection is reduced due to TP behaving as an outrigger system. The study admits that the proposed solution to reduce vibration is costly but can solve the problem of providing obstruction-free parking space at the lower storey. It is also important to note that this study does not consider the effect of earthquakes. Another study by Bandara et al. (Bandara et al., 2010) suggests a similar conclusion. The authors admit that depending upon wind and seismic demand, the TP may or may not become an economical option. However, with trial and error, the optimum location of TP can be chosen based on the procedure outlined in their study. The study by Gampathi et al. (Gampathi & Peiris, 2010) also revolves around establishing the advantage of TP and is not discussed here to avoid reptation. A few years later, Jayasinghe came up with a new study explicitly focusing on investigating the performance of TP under earthquake loading (Jayasinghe et al., 2012). Study shows that a building with TP attracts more seismic force due to an increase in the mass of a structure. However, the author firmly believes that TP should not be seen as a problem and suggests that sufficient attention should be given to the design and detailing of columns supporting TP since columns located immediately under the TPs are the areas that may suffer the worst damage.

2.2.2.5 Egypt

Egyptian study conducted in 2014 (Elawady et al., 2014) investigates the influence of the transfer storey's vertical location on a building's global response. For this, the study uses TP and TG as transfer elements and places them at different elevations. Several 3D models were analysed by linear response spectrum and non-linear time history analysis methods. The study shows that TG improves the global behaviour and reduces the straining action below the transfer storey compared to the transfer slab. This outcome is unaffected by the position of the transfer storey. It also reveals that the transfer storey's location directly influences the location of maximum inter-storey drift. Higher level transfer storey leads to domination of the fundamental mode in overall deformation, whereas lower-level transfer storey leads to higher mode effects. Another study from Egypt (Osman & Azim, 2015) emphasizes the importance of the correct modelling technique of the TP element to get accurate results. With the help of their numerical models, the Authors shows that changing modelling assumption leads to missing in capturing the true interaction between tower and podium elements. The same author in one more study (Osman & Saad, 2015) attempted to show the benefit of transfer slab (TS) when one of the columns supporting TS is removed/damaged. Study shows how progressive collapse analysis at the initial design stage can make a structure safe when one supporting column is damaged in the event of a blast. The following subsection discusses the Indian and international codes or guidelines which are directly or indirectly applicable to transfer structures.

2.2.3 Code Provisions and Guidelines

The buildings constructed following the guidelines of modern building codes have proven relatively resilient in recent earthquakes such as the 2010 Offshore Maule, Chile earthquake and the 2011 Great East Japan (Tohoku) earthquake (Naeim, et al., 2012). However, each earthquake exposes the vulnerabilities of building codes that were unrecognised or unknown previously. Hence, this section briefly summarises the current practice and methodology adopted in analysing and designing tall buildings with transfer elements worldwide.

2.2.3.1 Hong Kong, China

Hong Kong's concrete code (HK Buildings Department, 2020) has a dedicated section (section 5.5) on transfer structures. This code does not give any prescriptive clause for analysis and design of transfer structure, except restricting the inter-storey drift limit ratio to 1/700 for transfer storey. However, it specifically mentions the topics which need to be considered by the designer for the analysis of the transfer structure. The list of topics is mentioned below and is taken as it is from the code:

a) construction and pouring sequence;
b) temporary and permanent loading conditions;
c) varying axial shortening of elements supporting the transfer structure;
d) local effect of shear walls on the transfer structure;
e) stiffness of structural elements above and below the transfer structure;
f) deflection of the transfer structure;
g) lateral shear forces on the transfer structure; and
h) sidesway of the transfer structure under lateral loads.

It appears that, In Hong Kong, designers must be referring to specialist literature for analysis and design of transfer structures.

The reference book on Seismic Detailing for Concrete Buildings in Hong Kong (R. K. L. Su, 2019) is a good resource throwing light on transfer structures and other structural systems. The guideline clearly states that all structural components do not need to have ductile detailing since they remain elastic or near to an elastic state during a rare earthquake. However, the component adjoining the transfer storey needs to design for ductile detailing (Figure 2.11). Further transfer element is not recommended for a dual system. It is also advisable to avoid transfer element for regular RC frames, where high seismic force and displacement is anticipated, founded on the soil site. This is because the transfer structure might further amplify the seismic demand of the structure.

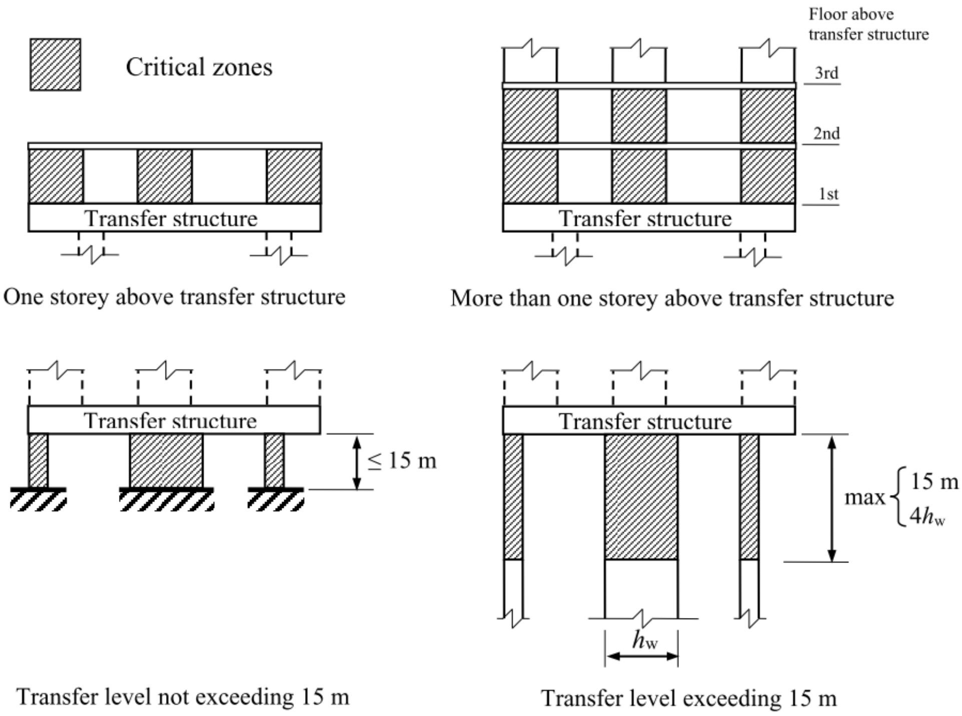

Figure 2.11: Critical zones of walls adjoining to transfer element (R. K. L. Su, 2019)

Further, The behaviour of the transfer element is studied in such detail that a separate parameter called Distortion inter-storey drift ratio (DIDR) (Figure 2.12) is derived to accurately measure gravity and seismically induced deformation in the structural wall above or below the transfer storey. The guideline reveals that DIDR can reach around 1/500 under gravity load alone. This gravity-induced shear force can use up to 40% shear deformability; hence, the guideline suggests limiting the local rotation of the transfer element at the base of the structural wall to be not greater than 1/1000 under gravity loads.

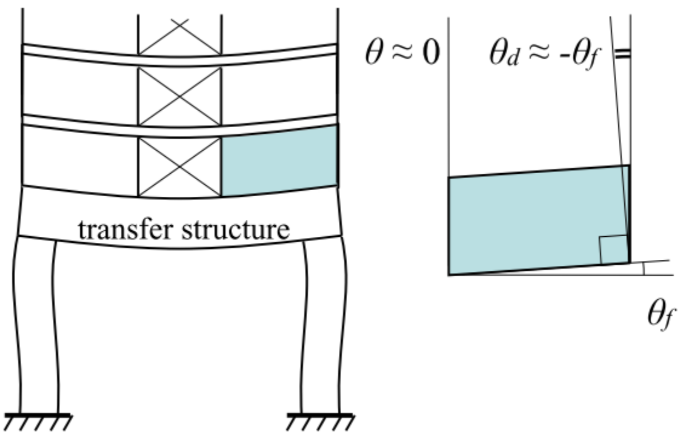

Figure 2.12: Distortion deformation in transfer structure (R. K. L. Su, 2019)

2.2.3.2 USA

A non-prescriptive performance-based guideline is more popular in the USA reflected in LATBSDC (LATBSDC, 2017) and Tall building Guideline (TBI, 2017). Such codes insist designer to consider the effect of vertical ground motion when significant discontinuities are encountered in the vertical-load-resisting system. For such cases, vertical masses (based on the effective seismic weight) shall be included with sufficient model discretisation to represent the primary vertical modes of vibration in the analysis model used to simulate the vertical response. Whereas ASCE 7-16 (ASCE 7-16, 2016) clearly outlines a separate provision for elements supporting discontinuous walls or frames, this is in addition to the basic irregularities provision of out-of-plane offset, stiffness-soft storey, stiffness extreme soft storey, in-plane discontinuity, discontinuity in lateral strength. The code states, "*The connections of such discontinuous walls or frames to the supporting members shall be adequate to transmit the forces for which the discontinuous walls or frames were required to be designed.*" Hence, Code outlines the additional load combinations for both allowable stress and strength design of members as per Eq. 2-1.

$$\begin{gathered}(1.2 + 0.2S_{DS})D + E_{mh} + L + 0.2S \\ (0.9 - 0.2S_{DS})D + E_{mh} + 1.6H\end{gathered} \quad 2\text{-}1$$

D, S and H are the dead load, snow load and lateral earth or water pressure, respectively. E_{mh} is the horizontal seismic forces effect, including the structural over-strength factor; $E_{mh}=\Omega_o Q_E$ with Ω_o being the seismic force amplification factor *(Ω_o=1.25 to 3.0)* and Q_E is the horizontal seismic forces from V or FP (equivalent lateral force procedure). S_{DS} is the design spectral response acceleration parameter at short periods.

Alternatively, ASCE 7-16 also allows the user to compute horizontal seismic load effect, including overstrength directly (eq. 2-2), where the exact demand of supporting element is derived based on the yielding capacity of the members to be supported.

$$S = S_G + S_{M_u} + S_{V_u} + S_{N_u} + S_E \quad 2\text{-}2$$

Where,

S = Combine action on Transfer element
S_G = Gravity demand
S_{Vu} = Shear demand
S_{Mu} = Bending moment demand
S_{Nu} = Axial couple demand
S_E = Seismic force in TB

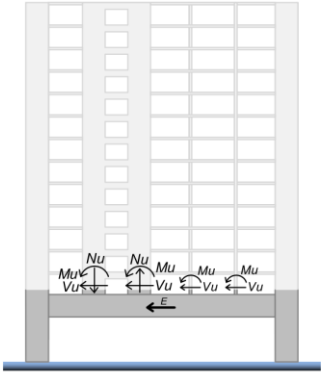

Figure 2.13: Capacity design approach as per clause 12.4.3.2, ASCE 7-16 [Image courtesy: (G. X. S. Ribeiro, 2018)]

2.3 Tall building code comparison of India and China

This section briefly summarises the current practice and methodology adopted in the analysis and design of tall buildings with transfer elements in India and China. China is chosen since India and China are the only countries with dedicated prescriptive tall building codes. And in the previous section, we have already seen that extensive numerical and experimental research is conducted and published on transfer structure by the scientific community of China.

2.3.1 Transfer structures and seismic zone

The tall building code of India (IS 16700, 2017) defines transfer structure in the terminology section. Where there is an acknowledgement of the transfer element in the form of a deep beam, truss, and thick slab (Clause 3.15 of IS 16700). However, IS 16700 or relevant associated codes like IS 456 (IS 456:2000, 2000), IS 1893 (IS 1893(Part 1):2016, 2016) and IS 13920 (IS 13920:2016, 2016) do not have any specific provisions or guidelines for any of this transfer structure element. Since a structural wall system supported by a moment resisting frame (MRF) system is not a typical structural system covered in IS 16700, buildings with transfer elements need to be designed and approved based on the performance objective as stated in annexure A of the IS 16700. On the other hand, Hong kong's concrete code (HK Buildings Department, 2020) has a section (section 5.5) dedicated to transfer structures. This code does not give any prescriptive clause for the analysis and design of the transfer structure. However, it specifically mentions the topics which need to be considered by the designer for the analysis of the transfer structure. Further, The Tall Building Code of China (JGJ 3-2010 China, 2010) has a detailed analysis and design guideline for transfer elements under section 10.2, having the title "High-rise buildings with transfer floors". The definition of transfer structure in all these three codes is tabulated in Table 2.2.

Table 2.2: Transfer structure definitions

Country/Region	Particular
India: Cl. 3.15, IS 16700 (IS 16700, 2017)	Transfer Structure: A structure, comprising horizontal deep beams, trusses or thick slabs that transfers load actions and supports vertical elements above to vertical elements below that are not aligned with each other, through flexural and shear actions. Alternatively, it can be a trussed structure that fulfils the task through axial actions in the truss members.
Hong Kong: Cl. 5.5 (HK Buildings Department, 2020)	Transfer Structure: Transfer structures are horizontal elements which redistribute vertical loads where there is a discontinuity between the vertical structural elements above and below.
China: 10.2.1 (JGJ 3-2010 China, 2010)	Transfer layer: At the bottom of the high-rise building structure, when some of the vertical members (shear walls, frame columns) of the upper floors cannot be directly connected to the ground, a structural transfer layer shall be set up to form a high-rise building structure with a transfer layer.

India and China both have broadly four categories of seismic regions. In India, it is termed “Seismic Zone”, whereas, in China, it is popular with the name “Seismic precautionary intensity”. The peak ground acceleration (PGA) values associated with them are tabulated in Table 2.3. Table 2.3 and Figure 2.14 show that the Chinese provision of intensity 6 and 7 can be compared with seismic zone II and III of India. Similarly, zone III and IV can be compared with Chinese precautionary intensity 8 and 9. Clause 10.1.2 (JGJ 3-2010 China, 2010) of the tall building code of China restricts the construction of transfer structures in intensity 9. As intensity reduces, from 8 to 6, the Chinese code becomes more liberal by reducing the number of clauses to be followed while the design of the transfer structure. For example, clause 10.2.5 of the same code links the allowable position of frame supported transfer layer (above the ground level) with the seismic intensity as a) up to 3 floors for intensity 8, b) up to 5 floors in intensity 7 and; c) appropriate floor level for intensity 6.

Table 2.3: Design Acceleration values as per Indian and Chinese seismic codes

Indian Seismic Code (IS 1893:2016)		**Chinese Seismic Code (GB 50011-2010)**	
Seismic Zone	**Peak Ground Acceleration**	**Seismic precautionary intensity**	**Design basic acceleration value of ground motion**
II	0.10 g	6	0.05 g
III	0.16 g	7	0.10 (0.15) g
IV	0.24 g	8	0.20 (0.30) g
V	0.36 g	9	0.40 g

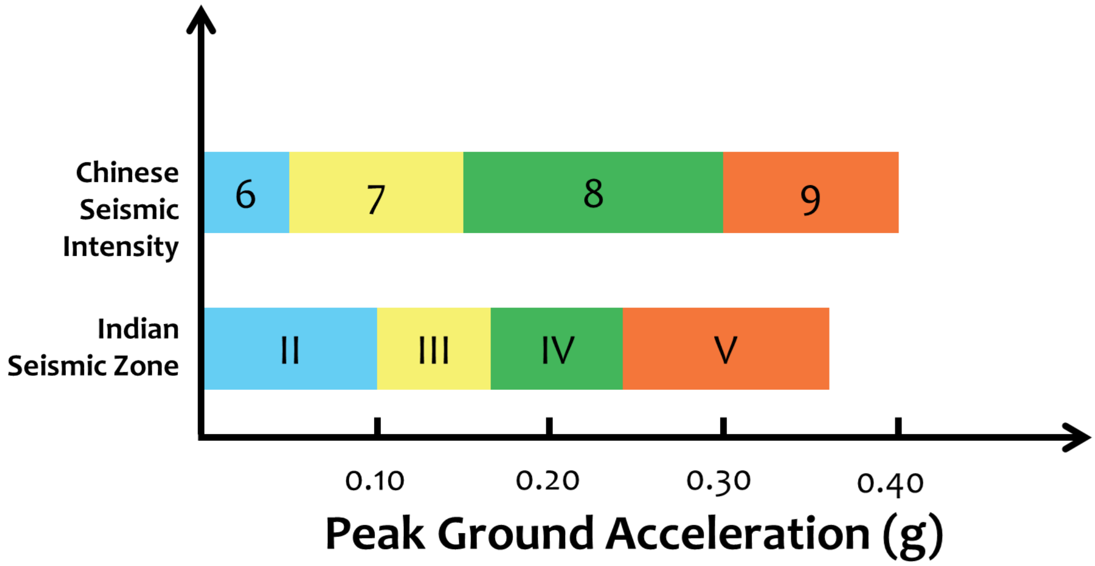

Figure 2.14: Graphical representation of Acceleration values as per Indian and Chinese seismic codes

2.3.2 *Stiffness irregularity*

The next most relevant criteria linked with the transfer element is the guideline on stiffness irregularity. To prevent stiffness irregularity, the Indian tall building code (IS 16700) allows designers to have a stiffness difference of up to 30% between two consecutive storeys, i.e. it states, "*lateral translational stiffness of any storey shall not be less than 70 per cent of that of the storey above*". The code committee must have consciously kept the scope of a 30% difference in stiffness in two consecutive storeys. The difference in stiffness must be coming out of a few unavoidable or popular geometrical features. Else this relaxation might not have been given for tall buildings. The Chinese tall building code appendix E is fully reserved for outlining the provisions for lateral stiffness of upper and lower structures of the transfer layer. Depending upon the vertical location of the transfer storey, this provision directs the designer to compute the relative storey stiffness formulae. When the transfer storey is located above the second floor, one additional formula of an equivalent lateral stiffness ratio must be computed. All these formulae are tabulated in Table 2.4.

Table 2.4: Stiffness Irregularity provision in Indian and Chinese Tall building codes

Clause Number	Formula
India: Cl 5.3, IS 16700	$k_i < 0.7k_{i+1}$ Where, k_i and k_{i+1} = Storey Stiffness of i^{th} and $i+1^{th}$ storey

Clause Number	Formula
China: Annexure E, JGJ 3-2010	First or Second Storey, $$\gamma_{e1} = \frac{G_1 A_1}{G_2 A_2} \times \frac{h_2}{h_1} \Bigg\} \geq \begin{matrix} 0.4, Gravity\ Deisgn \\ 0.5, Seismic\ Deisgn \end{matrix}$$ $$A_i = A_{w,i} + \sum_j C_{i,j} A_{ci,j} \quad (i = 1,2)$$ $$C_{i,j} = 2.5 \left(\frac{h_{ci,j}}{h_i}\right)^2 \quad (i = 1,2)$$ Where, G_1 & G_2 = Shear modulus of elasticity of storey below transfer element and above it, respectively A_1 & A_2 = Reduced Shear area section of storey below transfer element and above it, respectively A_{wi} = The sum of effective cross-section area of all shear walls in the direction of lateral load (excluding flange area) $A_{ci,j}$ = The effective area of column jth column h_i = Height of ith storey $h_{ci,j}$ = Column height for ith storey along calculation direction C_{ij} = Conversation factor of the cross-sectional area ≤ 1 Above Second Storey, $$\gamma_1 = \frac{V_i\, \Delta_{i+1}}{V_{i+1} \Delta_i} \geq 0.6$$ Where, V_i and V_{i+1} = Storey shear at i^{th} level and $(i+1)^{th}$ level Δ_i and Δ_{i+1} = Storey displacement at i^{th} level and $(i+1)^{th}$ level
China: Annexure E, JGJ 3-2010	Additional Formula for transfer storey located above second floor, $$\gamma_{e2} = \frac{\Delta_1}{H_1} \Big/ \frac{\Delta_2}{H_2} = \frac{\Delta_1 H_2}{\Delta_2 H_1} \Bigg\} \geq \begin{matrix} 0.5, Non-seismic\ design \\ 0.8, Seismic\ design \end{matrix}$$ H_1 = Height of the substructure below the transfer structure H_2 = Height of the substructure above the transfer structure ≤ H_1 Δ_1 & Δ_2 = Elastic lateral deflections of substructure below and above the transfer structure under the application of unit load, respectively.

2.3.3 *Discontinuity of Vertical Elements*

IS 16700 does not have any specific provision on the discontinuity of elements. Hence, IS 1893 is to be referred to, and this code does not allow discontinuity of columns when they are part of a lateral load-resisting system. Code is silent over discontinuity of structural wall element. A future revision of the code might prohibit discontinuity of structural walls at a lower level and link it with vertical irregularity. In the same way, clause 3.5.4 of JGJ 3-2010 also recommends the continuity of vertical, lateral load-resisting elements from top to bottom. These provisions are summarised in Table 2.5.

Table 2.5: Vertical Irregularity provision in Indian and Chinese Tall building codes

Clause Number	Clause Description
India: Cl 7.1, IS 1893:2016	**Floating or Stub columns:** Such columns are likely to cause concentrated damage in the structure, and are undesirable. A building with floating columns shall not be permitted, if the floating columns are part of or supporting the primary lateral load resisting system.
China: 3.5.4, JGJ 3-2010	During the seismic design, the vertical lateral force-resisting members of the structure should be connected continuously at the top and bottom
China: 3.4.3, GB 50011-2010	**Discontinuity of vertical lateral-force-resisting component:** The internal force of vertical lateral-force-resisting components (columns, seismic walls and seismic bracing) is transmitted downward through horizontal transmission components (beam and truss)

2.3.4 *Mass Irregularity*

Uniform mass distribution in multi-storey buildings is important since that will influence the earthquake-induced force. Sudden change in mass irregularity should be avoided; for this, both country codes have the same provision. As per IS 16700 and JGJ 3-2010, mass irregularity is said to exist when any storey's mass is more than 1.5 times the mass of the storey below. The exact wording of both codes is presented in Table 2.6.

Table 2.6: Mass Irregularity provision in Indian and Chinese Tall building codes

Clause Number	Clause Description
India: Cl 7.1, IS 1893:2016	**Mass Irregularity:** Mass irregularity shall be considered to exist, when the seismic weight of any floor is more than 150 percent of that of the floors below.
China: 3.5.6, JGJ 3-2010	The floor mass should be evenly distributed along the height, and the floor mass should not be greater than 1.5 times the mass of the adjacent lower floor.

2.3.5 *Inter-storey Drift limits*

Inter-storey drift limits are essential check to protect the non-structural elements. In India, for all Tall buildings, irrespective of it’s height and structural system, the inter-storey drift limit is restricted to 1/250. This value is further reduced to 1/500 for that storey and all storey below, if any, with stiffness irregularity. Whereas, as per JGJ 3-

2010, the upper limit for inter-storey drift is kept as 1/1000 for transfer structures of height up to 150m. Which is more stringent than current Indian limits.

2.3.6 *Additional provisions*

Apart from provisions compared in earlier sections Chinese code has a few specific provisions linked with TB that are discussed here. Clause 3.5.8, JGJ 3-2010 imposes a penalty for a storey having either stiffness irregularity and/or discontinuity of vertical lateral load resisting members by amplifying the design storey shear by factor 1.25. In Indian buildings qualifying for stiffness irregularity, the inter-storey drift limit is reduced by 50% from 1/250 to 1/500. At the same time, the discontinuity of lateral load-resisting member like columns is not allowed in IS 1893.

To increase the factor of safety of transfer elements, clause 10.2.4 of JGJ 3-2010 recommends an increase of internal forces caused due to earthquake by multiplying the coefficient in the range of 1.3-1.9. Further, clause 10.2.17 instructs the designer to consider the minimum shear force in the column supporting transfer elements as a) up to 10 columns in one layer, the design shear forces in individual columns should be taken in the range of 2-3% of base shear; b) Or for layers with more than 10 number of columns, a sum of shear force resisted by columns of one layer should be designed for 20-30% of the base shear. Further, as per clause 4.3.2-3, transfer structures located in intensity 7 (0.15g) and 8 should consider the earthquake's vertical effect if the transfer element has a span greater than 8m.

In view of all that has been mentioned so far, these studies support the notion that there is a similarity in a seismic zone between India and China (Figure 2.14). China is well aware of the adverse effect of the construction of transfer structures in higher seismicity areas; hence, such structures are restricted to intensity 8 (0.3 g) only and are not allowed for intensity 9 (0.4g). Further, additional prescriptive clauses are outlined to ensure the seismic safety of such buildings in lower to moderate intensity (up to 8). Looking at Chinese prescriptive clauses for TB, there is enough evidence to explore the suitability of TB in the lower seismic zone (II) of India.

2.4 Summary

The studies presented thus far prove that transfer elements in the form of transfer girder/beam or transfer slab/plate are very popular and widely used worldwide. In most cases, they tend to reduce the wind-induced vibration and deflection of the structure but are likely to attract greater seismic force due to an increase in mass. From a functional point of view, transfer elements give obstruction-free space, which is quite essential from the occupant's point of view. In fact, some of the modern tall buildings' structural forms have inherent transfer elements, e.g., an outrigger system.

Hence, such buildings are adopted worldwide but need rigorous and sophisticated analysis and design. Countries like China (Hong Kong) have done extensive experimental and numerical studies and incorporated outcomes into their codes and guidelines. However, they have too restricted certain forms of transfer structures in some specific seismic intensities. Similarly, the USA has chosen a performance-based design approach which needs a rigorous review process for approval of such buildings.

2.5 Research Gap

It is found that the due to need of parking space and commercial value of lower floors many tall buildings are having transfer structure configuration. And these structures are found across all seismic zone in India. The literature review addressing the seismic safety of such configuration, from Indian condition, is not done yet. Hence, it becomes necessary to carry out the seismic performance of Tall buildings with TB tailored to Indian construction practise. And to develop analysis and design provisions to regulate and promote such construction without worrying about safety.

…

Chapter 3. Numerical Structural Modelling and Analysis provision

3.1 Introduction

In the last chapter detailed discussion of studies highlighting the performance of transfer buildings is carried out. The global practise and building code provisions of some of the countries is also discussed to arrive at the objectives of the current study.

This chapter discusses the numerical study carried out to achieve the objectives mentioned in 1.2. Initially, the details of the buildings chosen are described, followed by detailed information on the modelling and design of buildings is described in detailed. The other section discusses several code recommendations which are violated by these buildings and the reasons for violation. The chapter ends with outlining a few critical observations linked with buildings with TB and violated code provisions.

3.2 Buildings under consideration

In the current parametric study, eighteen tall residential buildings are studied to achieve the objectives stated in the previous chapter. These eighteen buildings arrived based on two plans, three structural configurations and three different heights (Figure 3.1).

a) Two Plan aspect ratios:
    a. Tower 1 (27.40m x 27.34m), Plan aspect ratio = 1.00
    b. Tower 2 (60.80m x 27.34m), Plan aspect ratio = 2.22
b) Three Structural configurations:
    a. Type B: Only transfer beam
    b. Type C: Transfer beam with podium portion without retaining walls
    c. Type D: Transfer beam with podium having retaining walls
c) Three height variations:
    a. 60m, 100m and 150m

The above variables and their values were selected to represent the typically built environment buildings in metropolitan cities such as Hyderabad and Bengaluru. More details on each parameter are outlined in the following subsections.

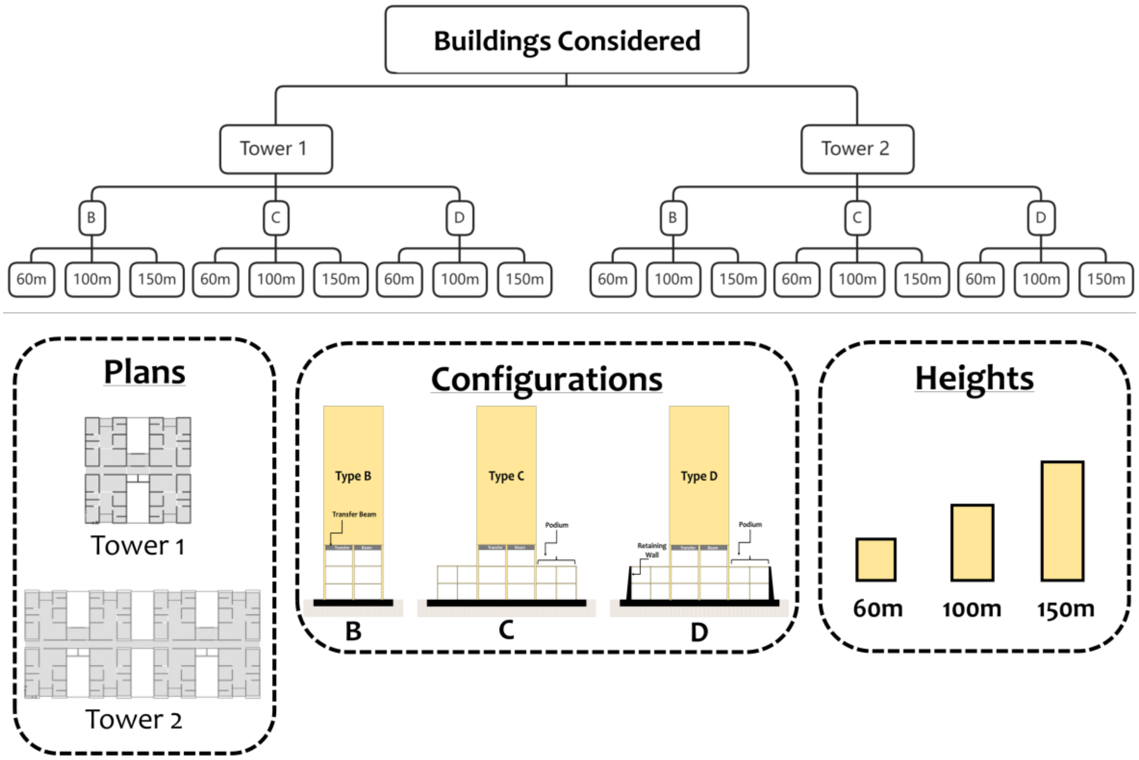

Figure 3.1: Overview of buildings considered in the study

3.2.1 Building Plans

Two residential building plans, having two different aspect ratios, 1.00 and 2.22, are considered (Figure 3.2). Both plans are inspired by a typical residential building consisting of four to ten flats on each floor. Such a flat can be identical or a combination of smaller and larger units. For the present study, *Tower 1* consists of four units, whereas *Tower 2* consists of eight identical units per floor. Each flat comprises one master bedroom, two bedrooms, one drawing room, one dining cum living area, one kitchen along with a utility area, and one sit-out. These four units in *tower 1* are connected by each other by a 2m wide passage for horizontal movement and are served by two lifts and one staircase for vertical transport. The same is the case with *tower 2*, except that there are eight units, and they are served by four lifts and two staircases to cater to the demand of eight units.

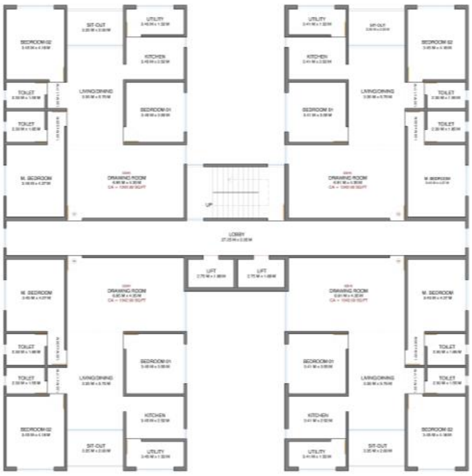

(a) Tower 1

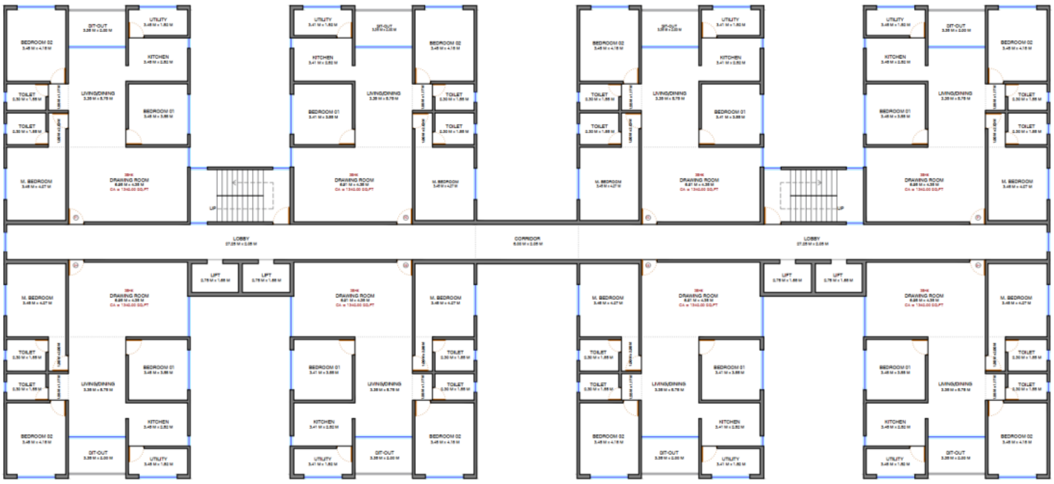

(b) Tower 2

Figure 3.2: Typical floor plans

3.2.2 *Structural configurations*

Three structural configurations, as observed in real buildings, are incorporated into the study (Figure 3.3). The first configuration, *type B*, consists of a structural wall supported by a TB, which is further supported by transfer columns. This configuration does not have any additional portion, and the main tower footprint remains the same until the foundation. *Type C* configuration is an extension of *type B*, where the podium portion gets attached to the main tower for one or more storeys, increasing the building footprint beyond the footprint of the main tower along one or both sides (Figure 3.4). This configuration is commonly found in large gated communities consisting of multiple towers within the same plot. These towers are connected by a single podium at lower levels with few expansion joints at the required lengths. *Type D* is an extension of *type C* with retaining walls in the podium portion. This configuration arises due to local topography and/or functional requirements when the soil has to be retained at the podium's boundary, making retaining walls essential.

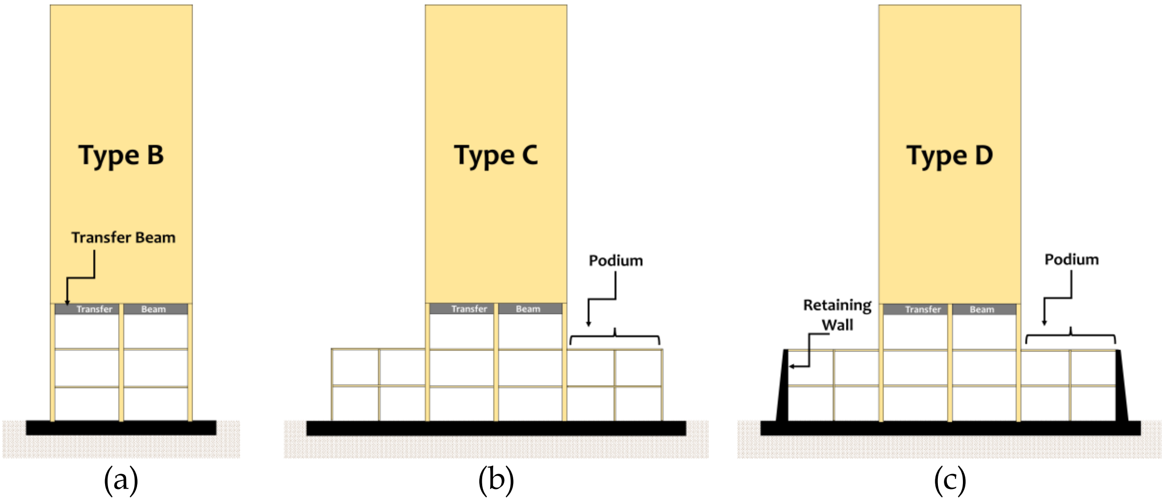

Figure 3.3: Structural Configurations considered in current study (a) Type B: Only transfer beam, (b) Type C: Transfer beam along with podium, (c) Type D: Transfer beam with podium having retaining walls

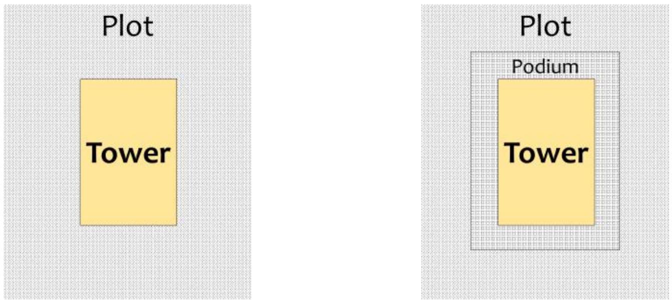

(a) Type B (b) *Type C* and *D*
Figure 3.4: Building footprints

3.2.3 Height variations

Three height variations considered in this study are ~60m, ~100m and ~150m. Assuming floor to floor height as 3m, the height range considered in the study represents buildings of 20, 33 and 50 floors, respectively. This is the typical case of buildings in metro cities; further, the height range considered also covers 50% of the height range specified by the tall building code(IS 16700, 2017) as 50-250m. The exact height of each building is tabulated in Table 3.1.

3.2.4 Location of transfer storey

For all the buildings, the structural walls terminated at the fifth storey, and the fourth storey consists of transfer beams supported by transfer columns. Following clause 8.1.3.3.k of IS 16700, the transfer beams are provided one storey above the connected floor, as shown in Figure 3.5. The transfer storey (storey 4) has a height of five meters to accommodate the transfer beam. Additionally, the spacing of transfer columns is adjusted to allow two vehicles to park comfortably, which would not be possible if the structural walls were extended to the foundation. Two sets of columns are used to support the transfer beams, one set of columns being circular and the other set being square in shape Figure 3.6.

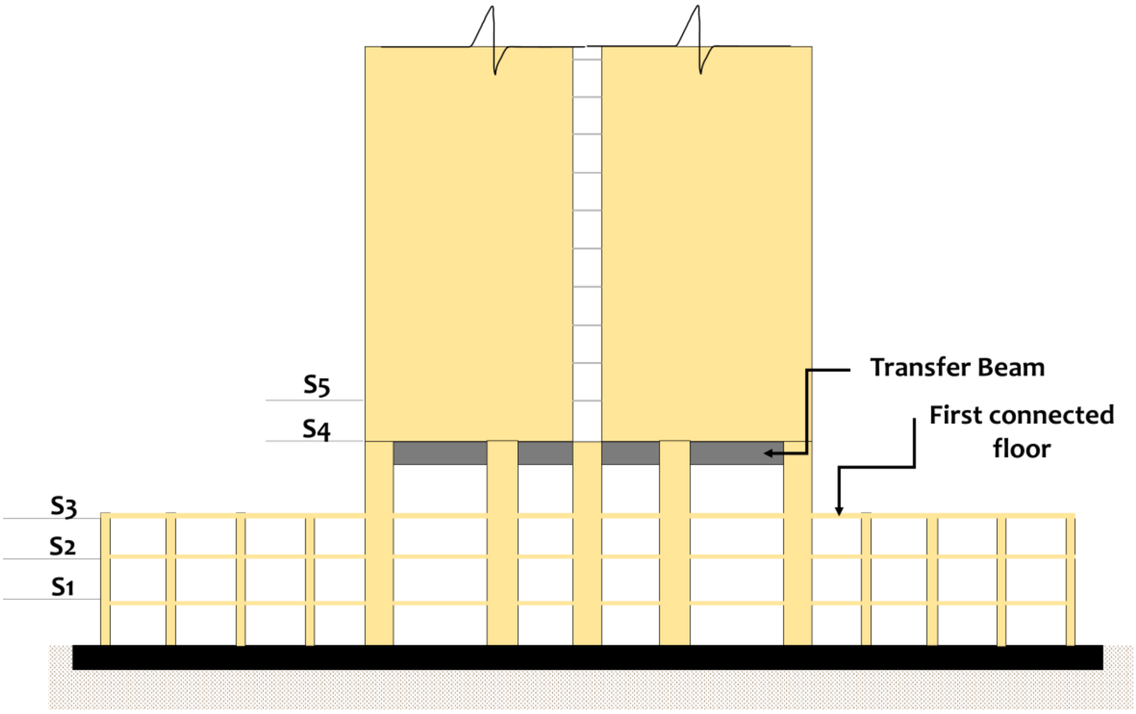

Figure 3.5: Location of Transfer beam

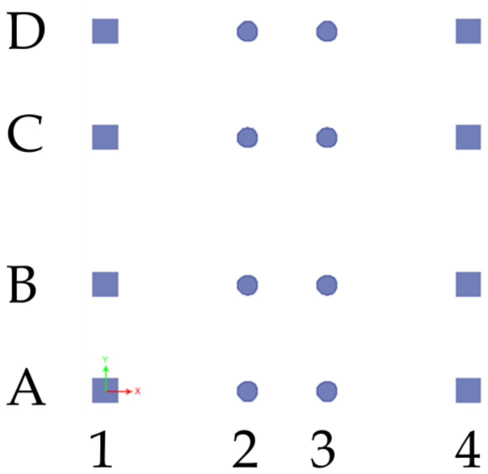

(a) *Tower 1*

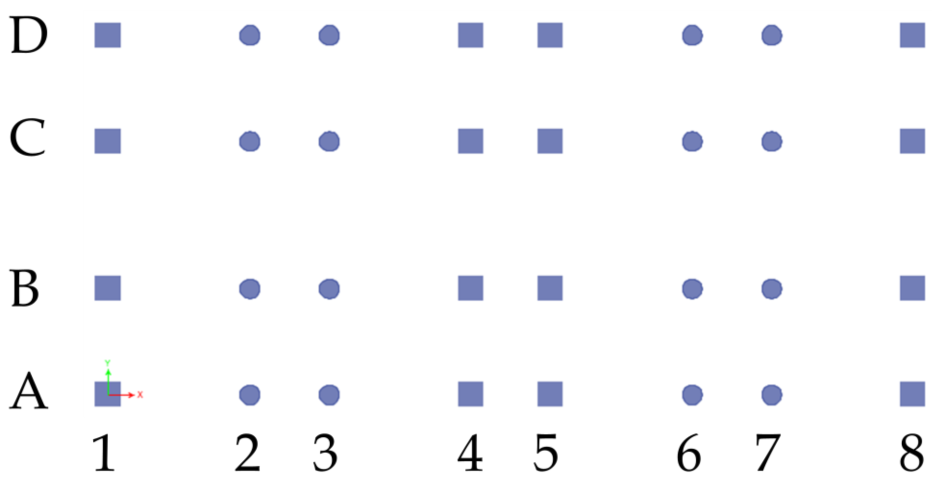

(b) *Tower 2*
Figure 3.6: Floor plan of transfer storey showing the location of transfer columns

3.2.5 *Model ID*

The building model ID is assigned in such a way that it captures all three details, which include two plans, three configurations, and three height variations, as shown in Figure 3.1. For future studies, a seismic zone is added as an additional variable. For example, model ID *T2ZIID100* indicates *T2* = plan of *Tower 2*, *ZII* = Seismic zone II (constant for all buildings), *D* = Configuration *type D*, *100* = Indicates the height of 100m. Similarly, a building with a plan of *Tower 1* without a podium (i.e., configuration *type B*) with 150m height will be identified as *T1ZIIB150*.

Table 3.1: Building plan dimensions and exact heights

Model ID	**Typical Floor Dimensions (m)**	**Podium Dimensions (m)**	**Total Height (m)**
Tower 1 buildings			
T1ZIIB60	27.40 x 27.34	-	062
T1ZIIC60	27.40 x 27.34	63.40 x 63.34	062
T1ZIID60	27.40 x 27.34	63.40 x 63.34	062
T1ZIIB100	27.40 x 27.34	-	101
T1ZIIC100	27.40 x 27.34	63.40 x 63.34	101
T1ZIID100	27.40 x 27.34	63.40 x 63.34	101
T1ZIIB150	27.40 x 27.34	-	149
T1ZIIC150	27.40 x 27.34	63.40 x 63.34	149
T1ZIID150	27.40 x 27.34	63.40 x 63.34	149
Tower 2 buildings			
T2ZIIB60	60.80 x 27.34	-	062
T2ZIIC60	60.80 x 27.34	98.85 x 62.40	062
T2ZIID60	60.80 x 27.34	98.85 x 62.40	062
T2ZIIB100	60.80 x 27.34	-	101

Model ID	Typical Floor Dimensions (m)	Podium Dimensions (m)	Total Height (m)
T2ZIIC100	60.80 x 27.34	98.85 x 62.40	101
T2ZIID100	60.80 x 27.34	98.85 x 62.40	101
T2ZIIB150	60.80 x 27.34	-	149
T2ZIIC150	60.80 x 27.34	98.85 x 62.40	149
T2ZIID150	60.80 x 27.34	98.85 x 62.40	149

3.3 Modelling and Design of buildings

The eighteen buildings discussed in the previous section are analysed and designed using a commercial finite element software called ETABS(Computer and Structures Inc., 2020). This tool is chosen since it is one of the most widely accepted in the research community (Abdelbasset et al., 2014; Y. Abdlebasset et al., 2016; Y. M. Abdlebasset et al., 2016; Ahn et al., 2020; Colaco et al., 2012; El-Abbasya et al., 2017; Elassaly & Nabil, 2017; Elawady et al., 2014; Gwalani et al., 2023; Huynh & Panahshahi, 2020; C. S. Li et al., 2006; J. H. Li et al., 2002; Looi & Su, 2018; Mwafy & Khalifa, 2017; O. El-Mahdy et al., 2022; Osman & Saad, 2015; G. Ribeiro et al., 2022; Shan et al., 2020; R. K. L. Su & Cheng, 2009; R. K. L. K. L. Su et al., 2002; Tang & Su, 2015; Yacoubian et al., 2016, 2018; Zhou & Xu, 2007) for linear analysis of tall buildings and equally popular among structural engineering community of India due to its capability of integration of Indian codes. The latest versions of IS 16700(IS 16700, 2017), IS 456(IS 456:2000, 2000), IS 875 (IS 875 (Part 1) : 1987, 1987; IS 875 (Part 2) : 1987, 1987; IS 875 (Part 3) : 2015, 2015) and IS 1893 (Part 1)(IS 1893(Part 1):2016, 2016) are extensively used for analysis and design of all these buildings.

3.3.1 Materials

The concrete and steel used in the current design are chosen based on local practice. A thumb rule of using a higher grade of material for a taller structure to have reasonable sizes of structural members is adopted. For example, for taller buildings of 150 m height, the maximum grade of concrete M70 is chosen as per clause 5.7.1.2, IS 16700. M35 and M45 are used for the remaining two groups of buildings having a height of 60 m and 100 m, respectively. Similarly, in the case of steel, for buildings of height 60 m Fe415 is used as a main reinforcement, whereas for the remaining two height categories, Fe500 is chosen. A constant grade Fe415 is used for stirrups in beams and columns. In summary, materials are chosen to strike a balance between economy and moderate section sizes. The grade of concrete and steel is kept constant for buildings of the same height to facilitate comparison of the performance of buildings due to variations in configuration (*Type B, C,* and *D*). A summary of the materials used in each building is provided in Table 3.2.

Table 3.2: Grade of concrete and Steel used in the study

Model ID	**Concrete**	**Grade of Steel**		**Model ID**	**Concrete**	**Grade of Steel**	
		Main	**Rebar**			**Main**	**Rebar**
T1ZIIB60	M35	Fe415	Fe415	T2ZIIB60	M35	Fe415	Fe415
T1ZIIC60				T2ZIIC60			
T1ZIID60				T2ZIID60			
T1ZIIB100	M45	Fe500	Fe415	T2ZIIB100	M45	Fe500	Fe415
T1ZIIC100				T2ZIIC100			
T1ZIID100				T2ZIID100			
T1ZIIB150	M70	Fe500	Fe415	T2ZIIB150	M65	Fe500	Fe415
T1ZIIC150				T2ZIIC150			
T1ZIID150				T2ZIID150			

3.3.2 *Geometry and Cracked Section*

The structural walls have a thickness of 160 mm which is derived based on the minimum thickness criteria of IS 16700 and as per the recommendation of IS 456 (Clause 21.2) for two-hour fire resistance with a reinforcement percentage of range 0.4-1.0%. The size of beams and columns are assumed initially and optimized in successive iterations based on the actual demand due to gravity and lateral loads. The sizes of beams and structural wall is given in Appendix A.2.

In the absence of non-linear analysis, cracked section properties are used to overcome the shortcoming of linear analysis and represent reduced stiffness of members in their damaged state (Murty et al., 2012). For members other than transfer elements, code recommended values are used as per IS 16700 (Table 3.3). As mentioned in the previous chapter, there are no clear guidelines for the design of TB in Indian codes; hence, ideally, such elements' behaviour shall be within the elastic range when subjected to seismic force. However, in the absence of additional load combination (as suggested in ASCE 7-16 (ASCE 7-16, 2016)) for the design of TB and to go for an over conservative approach, a reduced moment of inertia of $0.90I_g$ for columns supporting TB and $0.80I_g$ for TB is considered in the present study. These values are assumed by keeping the structural importance hierarchy in mind. The supporting member should be stronger than the member to be supported. In other words, supporting members should have lesser damage compared to members to be supported. Hence, $0.70I_g$ is used for columns and walls supported by TB. A value of $0.80I_g$ is used for TBs, and vertical members supporting TB are assigned with $0.90I_g$.

Table 3.3: Cracked RC section properties

SI No.	Structural Element	Moment of Inertia	Remark
1	Slabs	0.25 I_g	Table 6, IS 16700
2	Beams	0.35 I_g	
3	Columns	0.70 I_g	
4	Walls	0.70 I_g	
5	Transfer Beams	0.80 I_g	Assumption
6	Transfer Columns and Walls	0.90 I_g	

3.3.3 Loads

All buildings are designed for possible gravity (dead and imposed) and lateral (wind and earthquake) loads (Figure 3.7).

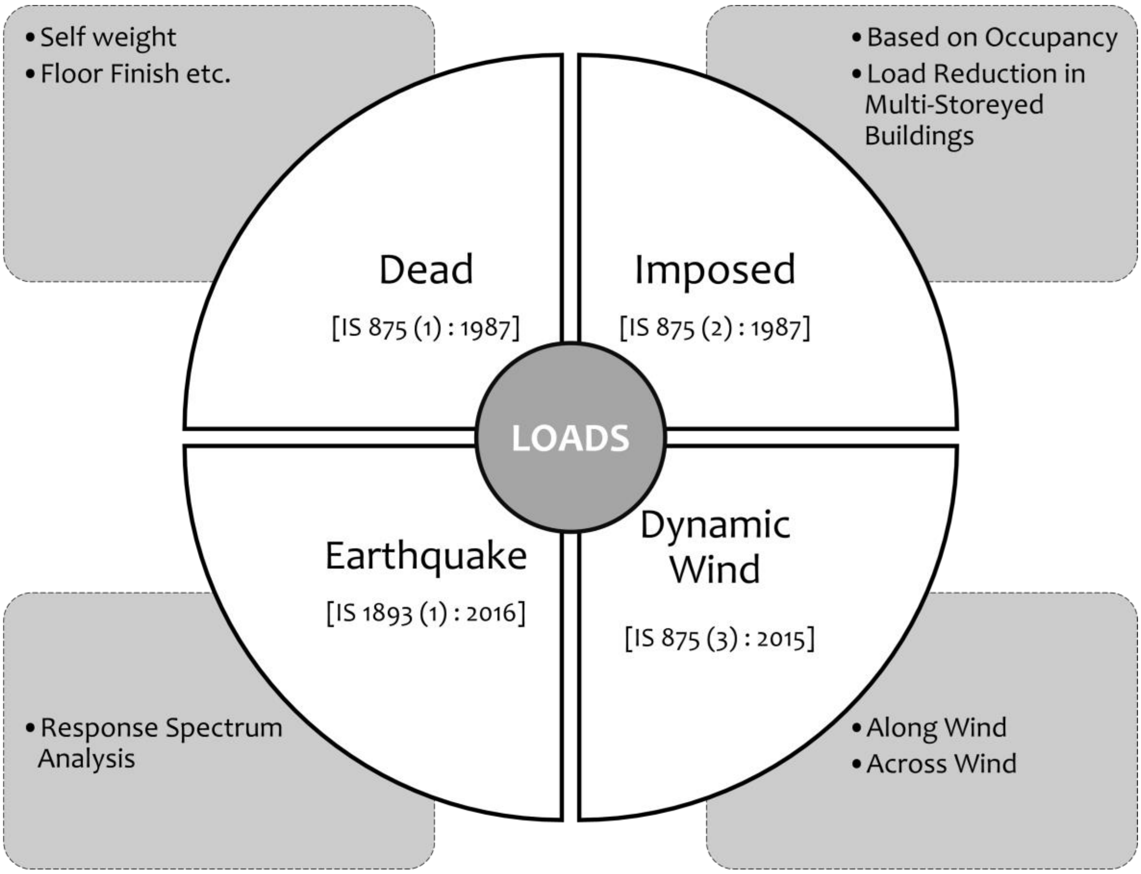

Figure 3.7: Loads considered in the design

(a) Gravity Loads

The self-weight of various members is computed based on the unit weight of concrete and steel. As per IS 875 (Part 1)(IS 875 (Part 1) : 1987, 1987), the floor finish is considered as 1.0 kN/m^2 for typical floors above the transfer storey and 1.5 kN/m^2 for storeys below TB. Loads on the roof of buildings and podium due to water proofing treatment is considered as 2 kN/m². A load of 0.5 kN/m² is applied on all floors below TB to account for various services.

Live loads (LL) are considered as per IS 875 (Part 2) - 1987(IS 875 (Part 2) : 1987, 1987). For the residential floor, LL is taken as 2 kN/m², and for balconies and passages, 3 kN/m² is applied. Light vehicular load of 5 kN/m² is applied for the podium and floors below TB. For fire fighting vehicles, a fire tender load of 20 kN/m² is applied on the podium roof. LL reduction assumption as per clause 3.2.1, IS 875 (Part 2) is also considered in the study.

(b) Lateral loads

Dynamic wind loads are applied to all structures as per IS 875(IS 875 (Part 3) : 2015, 2015). Buildings are assumed to be subjected to a basic wind speed of 50 m/sec, which is the second highest basic wind speed. The maximum basic wind speed of 55 m/sec applies only to regions covering partial or full states like Tripura, Mizoram, Assam and Leh region (Figure 3.8). Hence, assuming a basic wind speed of 50 m/sec is the worst-case scenario for tall buildings in zone II. Further, terrain category 3 is assumed to compute design wind pressure. Design wind load is computed manually using an excel sheet as per the procedure stated in IS 875 for tall buildings. The computed design forces for each floor are then applied to the buildings as user-specified loads.

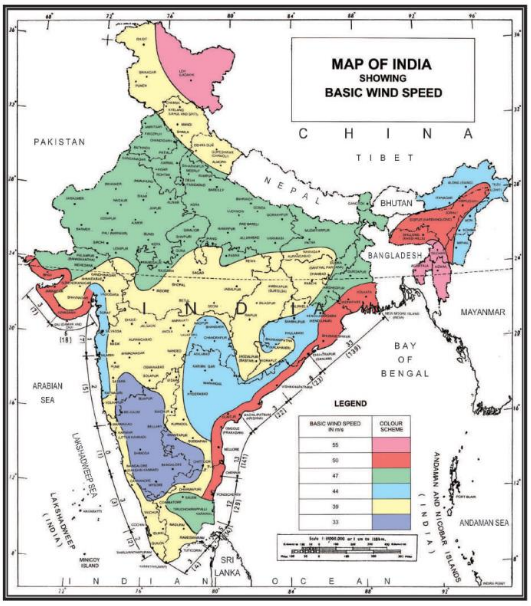

Figure 3.8: Basic wind speed (Source: IS 875(IS 875 (Part 3) : 2015, 2015))

For earthquake loads, all buildings are assumed to be in seismic zone II resting on medium soil (Type II) as per IS 1893 (IS 1893(Part 1):2016, 2016). Further, buildings are designed as ordinary structural walls and frame system; Response reduction factor R of 3 and Importance factor I of 1.2 are considered. Response spectrum analysis is used for the design of buildings. Load intensities considered under each of these load categories are summarized in Figure 3.9.

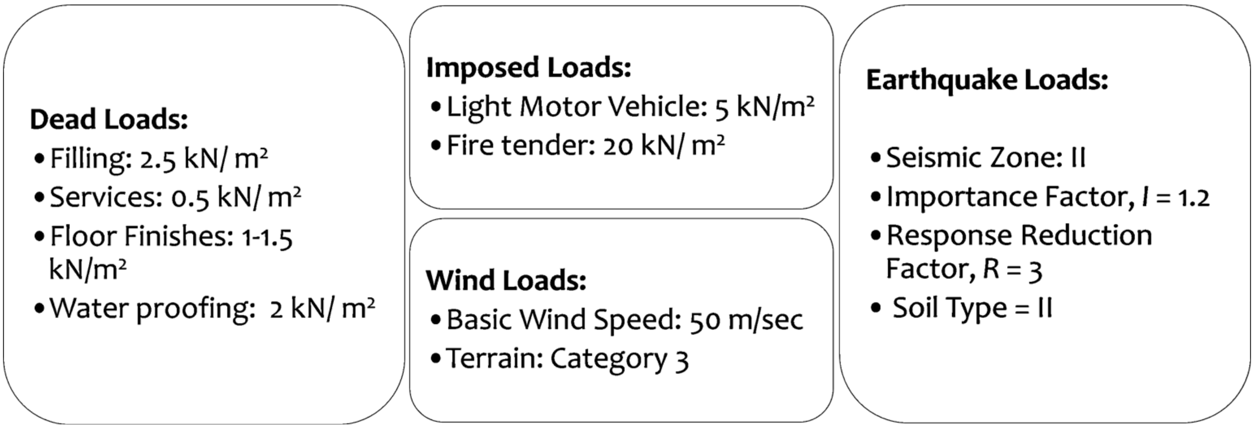

Figure 3.9: Overview of category wise load intensity

3.3.4 Other Provisions

The other important provisions applicable to tall buildings are also adopted in the analysis. For example, the P-Delta effect is considered by incorporating clause 7.2.d of IS 16700 (IS 16700, 2017). However, the limitation of software package to carry out P-Delta analysis is not address in this study.

3.3.5 Load Combinations

All the load combinations for the limit state of collapse recommended by IS 456 and IS-1893 are applied to all building models, and member design is carried out accordingly (Table 3.4). Buildings are designed for both wind load and earthquake loads. Hence, the first 24 load combinations are considered for wind load, and additional 24 load combinations for earthquake load are considered for each building.

Table 3.4: Load combinations considered in the design

SI No.	Load Combination	Number of Load combination
1	1.5 [DL + LL]	1
2	1.2 [DL + LL $\pm$ WL]	8+8
3	1.5 [DL $\pm$ WL]	8+8
4	0.9 DL $\pm$ 1.5 WL	8+8

Note:
1. *DL = Dead load; LL = Live/Imposed load; WL = Wind Load; EL = Earthquake Load*
2. *While considering earthquake effects, substitute EL for WL*

3.3.6 Modelling and Design of individual members

The slabs and structural walls are modelled as thin shell elements, while beams and columns are modelled as a line element. The software computes the flexure and shear steel for beam design based on the beam moments, shears, and load combination factors and designs them for major direction flexure, major shear, and torsion. The beam section is designed for the maximum positive and maximum negative factored moment envelopes obtained from all the load combinations. To design shear reinforcement for a particular beam, the software determines the factored shear force, the shear force that can be resisted by concrete, and the reinforcement steel required to carry the balance for a particular set of loading combinations at a specific station due to beam major shear (CSI, 2020a).

For column design, the procedure includes generating axial force-biaxial moment interaction surfaces for all different concrete section types of the model, checking the capacity of each column for factored axial force and bending moments obtained from each loading combination at each end of the column, and designing the shear reinforcement similar to beams, except considering the effect of the axial force on concrete shear capacity (CSI, 2020a).

A uniform reinforcing is given for structural walls, and the software uses P-M-M interaction for flexure design. It creates an interaction surface for that pier and determines its critical flexural demand/capacity ratio. The reinforcement is provided based on the desired demand/capacity ratio. To design for shear force, the software follows these steps: determine the factored forces P_u and V_u acting on the wall pier section, determine the shear stress τ_c that can be carried by the concrete alone, and determine the required shear reinforcing A_{sv}/S_v to carry the balance of the shear force (CSI, 2020b).

3.3.7 Scope of Modelling

The current study focuses on the global performance of tall buildings with TB; therefore, the modelling interaction of structural wall-floor slab-transfer beam is not included in the current work. It is important to note that the local interaction of these members and reinforcement detailing is crucial, and there are ongoing efforts in India in this direction, as seen in a recent study from Anna University (Balasubramanian & Jaya, 2022). Additionally, due to the lack of access to detailed drawings of an actual building and the complexity of architectural features such as chajja, overhang balcony, and openings in structural walls, these features are ignored in the current study.

3.3.8 Iterative design

Figure 3.10 and Figure 3.11 shows the ETABS models of buildings under consideration. Once the numerical model is ready with the geometry and applied loads, the typical iterative building design process consist of manual computation of code recommended natural period, modal analysis, gravity and lateral load analysis, verification of code clauses (analysis requirements), computing elements demand, checking the capacity of members against demand. This process is iterative in nature and needs to be followed until all members pass different checks (Figure 3.12).

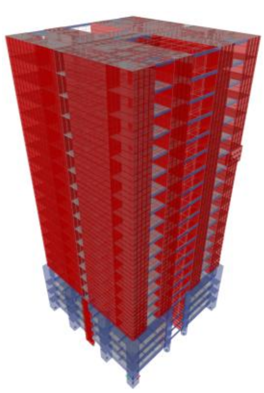
(a) T1ZIIB60

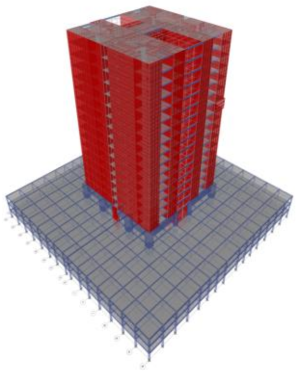
(b) T1ZIIC60

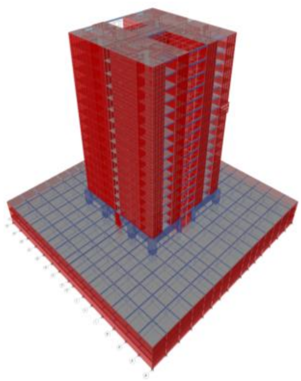
(c) T1ZIID60

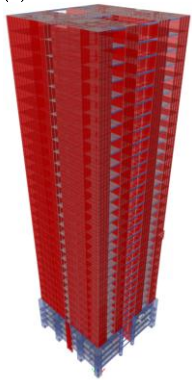
(d) T1ZIIB100

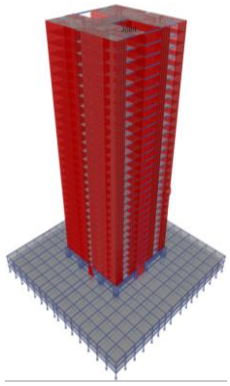
(e) T1ZIIC100

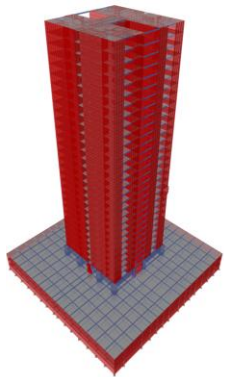
(f) T1ZIID100

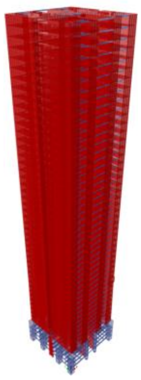
(g) T1ZII150


(h) T1ZIIC150


(i) T1ZIID150

Figure 3.10: 3D view of *Tower 1* buildings modelled in commercial software

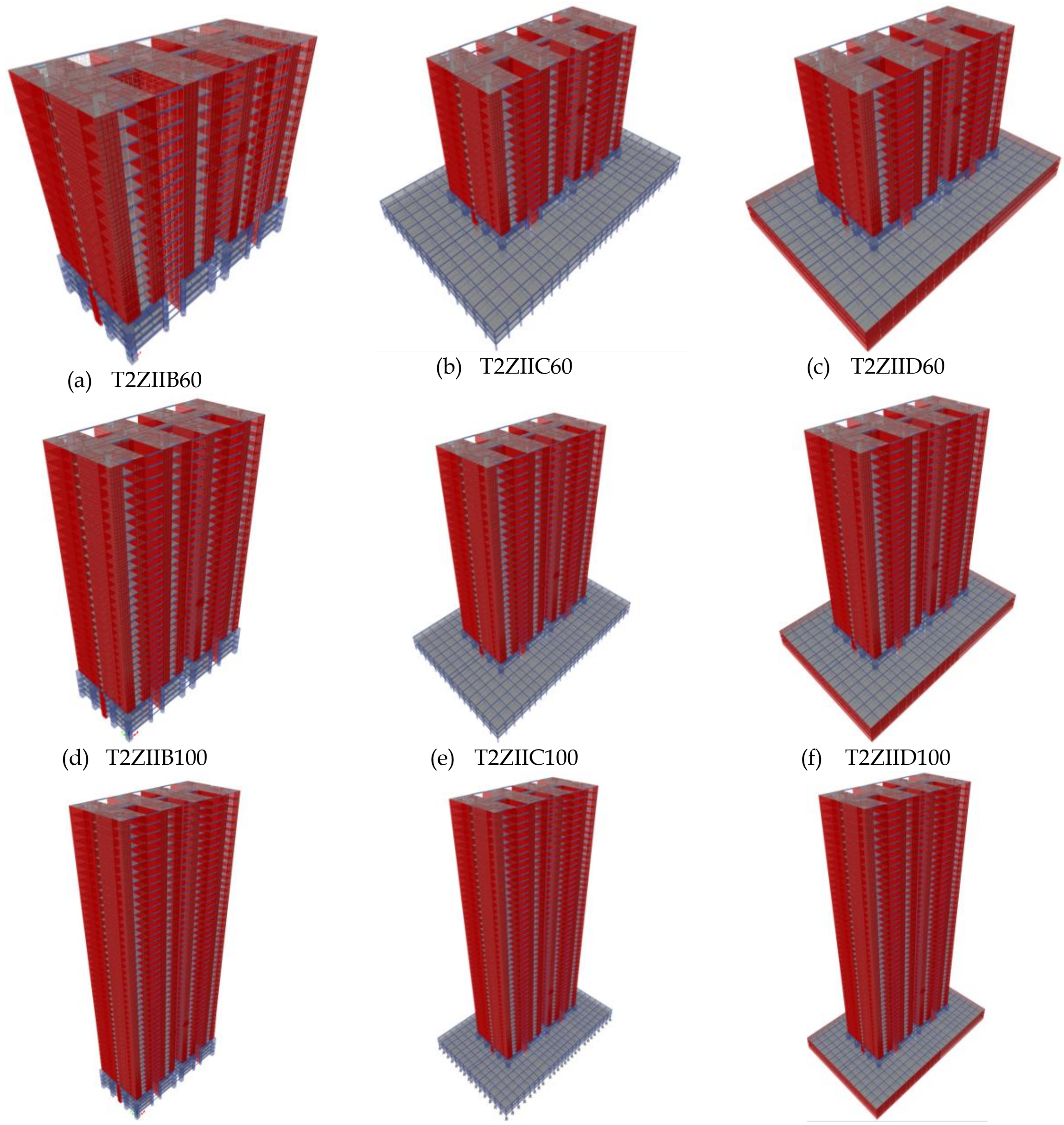

(a) T2ZIIB60 (b) T2ZIIC60 (c) T2ZIID60

(d) T2ZIIB100 (e) T2ZIIC100 (f) T2ZIID100

(g) T2ZII150 (h) T2ZIIC150 (i) T2ZIID150

Figure 3.11: 3D view of *Tower 2* buildings modelled in commercial software

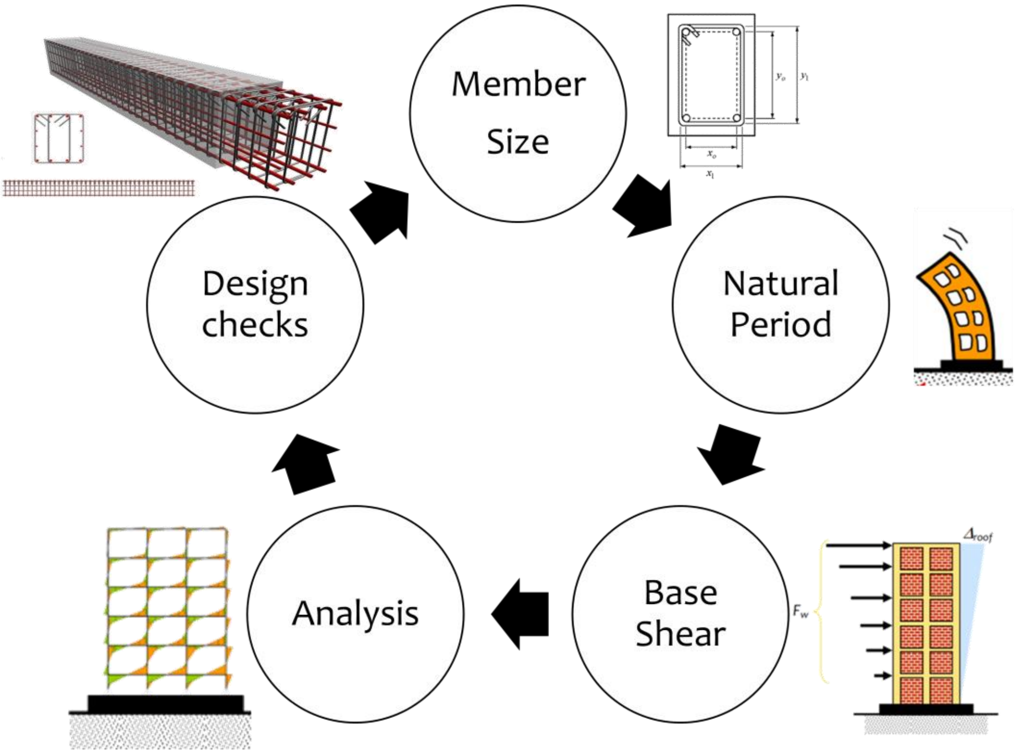

Figure 3.12: Typical iterative design of a building

3.4 Analysis Provisions

This section discusses certain code recommended provisions that buildings must adhere to during their design stage to ensure the desired performance during earthquake shaking. However, due to their configuration, the buildings under focus do not satisfy some of these provisions. Hence, they depart from the code recommended guidelines. The scope of this section is restricted to discussing only those parameters which are not in line with code recommended provisions, such as stiffness irregularity, mass irregularity, fundamental natural periods etc. The satisfied provisions are not included in the discussion.

3.4.1 Stiffness Irregularity

The response of a building to the lateral load, such as earthquakes, is greatly influenced by its lateral stiffness. Building stiffness controls the overall displacements, whereas storey stiffness influences the inter-storey drift at any particular level. Thus, it is important to have a uniform distributed stiffness along the plan and elevation of a building (Murty et al., 2012). To ensure uniform distributed stiffness along the elevation, IS 1893 defines a *soft storey* as a storey whose lateral stiffness is less than the stiffness of the storey immediately above it. The code further mandates the compulsory execution of dynamic analysis and limits the maximum inter-storey drift to 0.2% for that storey and all the storeys below it.

However, the Tall building code relaxes this aspect and allows a lateral storey difference of up to 30%. In other words, for any storey, the storey stiffness should not be less than 70% of stiffness of the storey above. Figure 3.14 shows the lateral stiffness ratios of transfer storey (storey 4) to the structural wall storey (storey 5) of *Tower 1* and *Tower 2* buildings. Storey stiffness is extracted from the numerical software package. One such example of extracted results is plotted in Figure 3.13. Two lateral direction stiffness ratios are plotted for each building, and a value less than 0.70 along Y-axis indicates qualification for stiffness irregularity. The dotted line at 0.7 separates the regular zone (above) and irregular zone (below). All bars below the dotted line indicate the presence of stiffness irregularity.

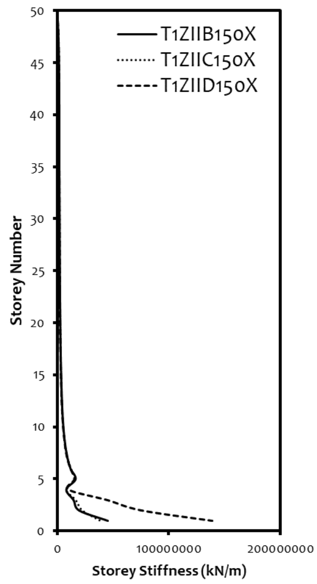

Figure 3.13: Sample Storey stiffness plot of T1_150s along X direction

It is observed that, except for three cases, the stiffness irregularity could not be eliminated for the current building plan and chosen transfer structure configuration. Attempts were made to continue a few structural walls along the Y-axis till the foundation, but that did not completely resolve the challenge. Further, the increase in structural walls continuing till the foundation will not serve the purpose of obstruction-free space.

Comparing the stiffness of configuration *types B, C* and *D* for both plans and across all three height ranges, it was observed that the effect of podium configuration on lateral stiffness is insignificant. However, a comparison of the stiffness of *type B* and *D* reveals that retaining walls (*type D*) can increase the stiffness by 10-15% along the X direction and 3-5% along the Y direction (Table 3.5). The contribution of retaining walls in increasing stiffness is less along the Y direction since many walls are continued from the top to the foundation along this direction.

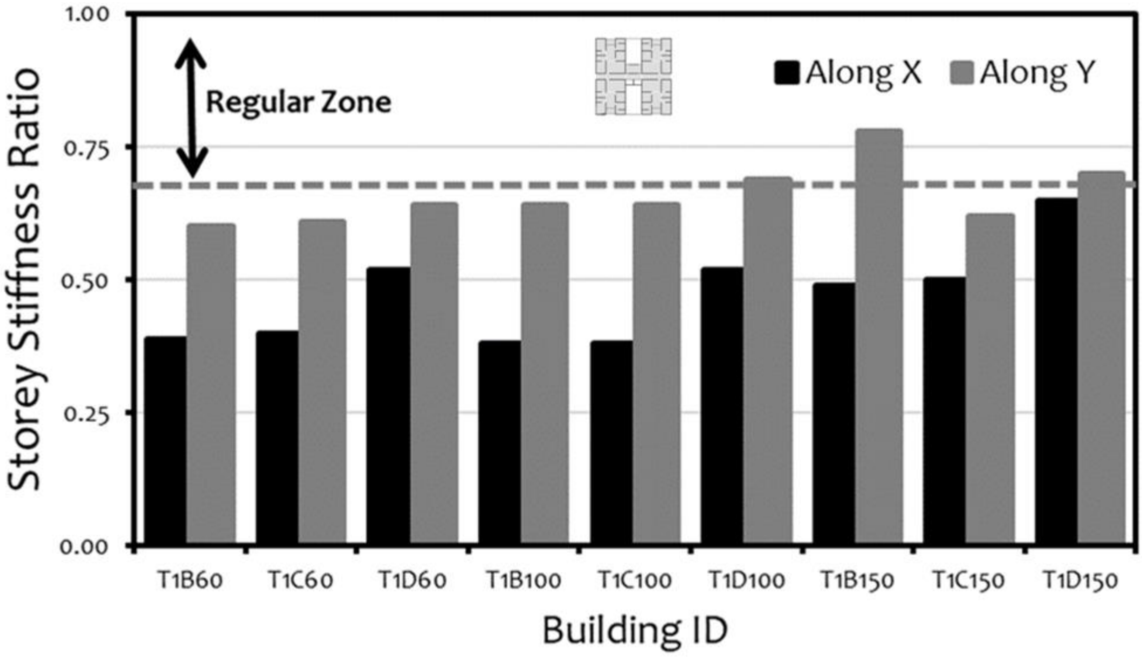

(a) Tower 1

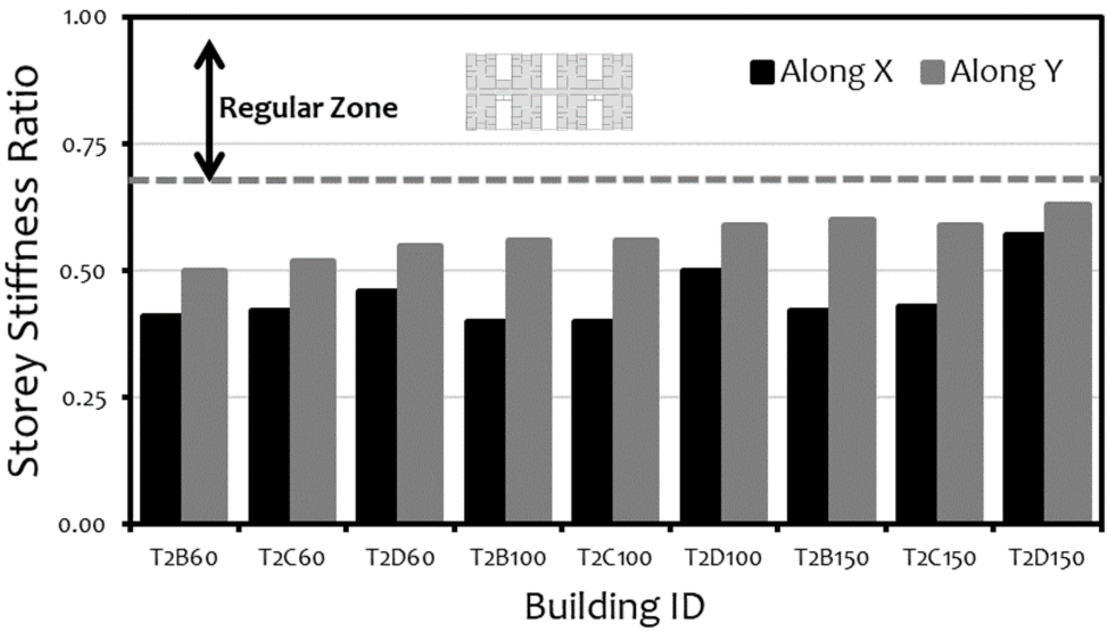

(b) Tower 2

Figure 3.14: Storey stiffness ratio plots to indicate the presence of stiffness irregularity

Table 3.5: Storey stiffness ratio of Transfer Storey/Structural wall storey for all buildings

Model ID	*TB/SW Storey*		*Model ID*	*TB/SW Storey*	
	X	*Y*		*X*	*Y*
T1ZIIB60	0.39	0.60	T2ZIIB60	0.41	0.50
T1ZIIC60	0.40	0.61	T2ZIIC60	0.42	0.52
T1ZIID60	0.52	0.64	T2ZIID60	0.46	0.55
T1ZIIB100	0.38	0.64	T2ZIIB100	0.40	0.56
T1ZIIC100	0.38	0.64	T2ZIIC100	0.40	0.56
T1ZIID100	0.52	0.69	T2ZIID100	0.50	0.59
T1ZIIB150	0.49	0.78	T2ZIIB150	0.42	0.60

Model ID	TB/SW Storey		Model ID	TB/SW Storey	
	X	Y		X	Y
T1ZIIC150	0.50	0.62	T2ZIIC150	0.43	0.59
T1ZIID150	0.65	0.70	T2ZIID150	0.57	0.63

In summary, many buildings exhibit stiffness irregularity, which necessitates the imposition of a limitation of 0.2% inter-storey drift ratio along both directions for storeys at the transfer level and all storeys below it. The implications of stiffness irregularity on inter-storey drift ratio are discussed in the next chapter.

3.4.2 Mass Irregularity

The earthquake forces are inertial forces generated at locations where mass is mobilised. The uniform distribution of mass ensures the uniform generation of inertia forces, leading to the uniform distribution of earthquake forces in members. Hence, it is important to have a uniform distribution of mass in plan and elevation (Murty et al., 2012). To ensure this, IS 1893 has a provision on *mass irregularity,* which is said to exist when the seismic weight of any floor is more than 150% of that of the floors below. The code recommends going for dynamic analysis in such qualifying mass irregularity cases, provided the building is located in zone III and above.

Unlike stiffness irregularity, when the transfer storey (storey 4) stiffness is found to be less than the storey above (storey 5) reverse case is observed for the storey mass. The transfer storey(storey 4) seismic weight was found to be more than the storey above(storey 5). This is natural since deep TB contribute more to the seismic weight of storey four than thin uniform walls contribute to storey five. Hence, as shown in Figure 3.15 a and b, the ratio of structural wall storey (storey 5) to transfer storey (storey 4) ranges between 0.4 to 0.5 for all eighteen buildings. Further, comparing the seismic mass of the transfer storey (storey 4) with the storey below (storey 3), it was observed that six buildings of *type B* are getting qualified for the mass irregularity(Figure 3.15 c and d). This indicates that mass irregularities are predominant between the transfer storey (storey 4) and the storey below (storey 3). And podium configurations (*type* C and *D*) greatly influence this asymmetric in mass. The mass ratios of all buildings are supplied in Table 3.6.

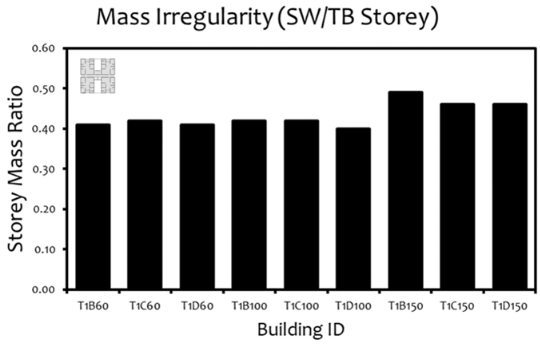

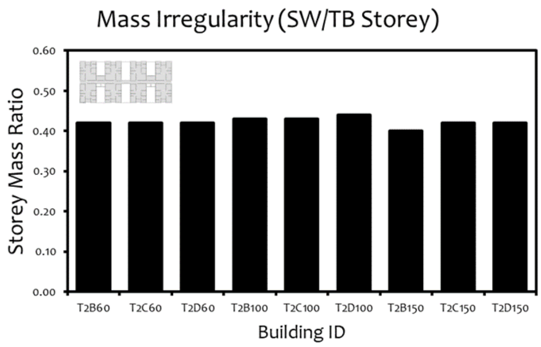

(a) Tower 1 (b) Tower 2

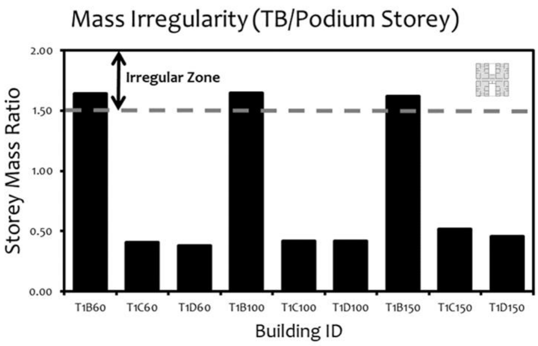

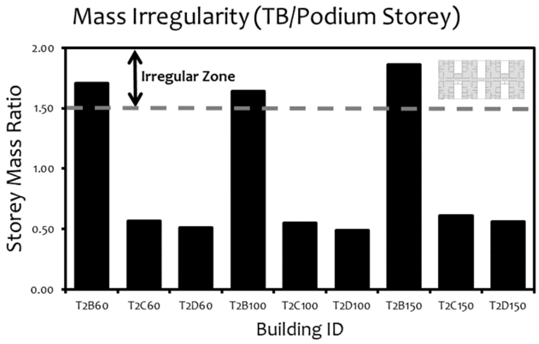

(c) Tower 1 (d) Tower 2

Figure 3.15: Storey mass ratio plots to indicate the presence of mass Irregularity

Table 3.6: Seismic Mass Ratio for all buildings

Model ID	***Mass Ratio***		***Model ID***	***Mass Ratio***	
	S5/S4	***S4/S3***		***S5/S4***	***S4/S3***
T1ZIIB60	0.41	**1.64**	T2ZIIB60	0.42	**1.71**
T1ZIIC60	0.42	0.41	T2ZIIC60	0.42	0.57
T1ZIID60	0.41	0.38	T2ZIID60	0.42	0.51
T1ZIIB100	0.42	**1.65**	T2ZIIB100	0.43	**1.64**
T1ZIIC100	0.42	0.42	T2ZIIC100	0.43	0.55
T1ZIID100	0.40	0.42	T2ZIID100	0.44	0.49
T1ZIIB150	0.49	**1.62**	T2ZIIB150	0.40	**1.86**
T1ZIIC150	0.46	0.52	T2ZIIC150	0.42	0.61
T1ZIID150	0.46	0.46	T2ZIID150	0.42	0.56

Note:
S5 = Storey 5 → Structural wall storey; S4 = Storey 4 → Transfer storey;
S3 = Storey 3 → Podium storey

3.4.3 Modal Analysis

This section discusses the fundamental natural periods and cumulative modal mass observed in the buildings' first three modes. The relationship between the fundamental lateral natural periods and the fundamental torsional period is also discussed in detail.

a) Validation of Fundamental Natural Periods:

The fundamental natural period obtained from the numerical models is compared with IS 16700:2023(IS 16700, 2023) and the Indian study(Velani & Ramancharla, 2023), as shown in Figure 3.16. The figure indicates that the natural period values are close to the code-recommended value and the proposed equation, which was derived based on an ambient vibration test of tall buildings in India. The usual case is that the natural period computed by code recommended empirical expression gives a lower value than the natural period of a numerical model, which is not observed in the current study. The reason is that the proposed tall building code expression is based on testing carried out on building stock of other countries, and the empirical equation for Indian code is being tailored.

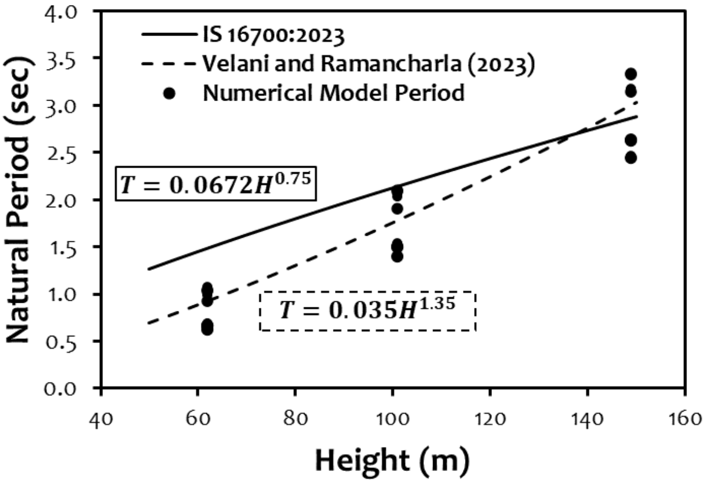

Figure 3.16: Validation of fundamental natural period of numerical model

b) Fundamental Natural Periods:

The fundamental lateral natural periods along X and Y are plotted in Figure 3.17 a and b. The fundamental natural period along X is greater than that of Y for all the buildings. The reason is that there are more structural walls along the Y direction, which is going till the foundation level, making the Y direction stiffer, which tends to reduce in the natural period. . Comparing the fundamental lateral period of *types B, C* and *D* across all three height ranges for both plan types indicates the influence of podium configuration on the fundamental natural period. The natural period is reduced due to the confinement effect of the podium configuration. The maximum decrease in the fundamental natural period due to *type D* configuration is 0.184 sec compared to the *type B* period. A Korean study observed similar results focussing on practical modelling of surrounding basement structures (Jeong et al., 2020).

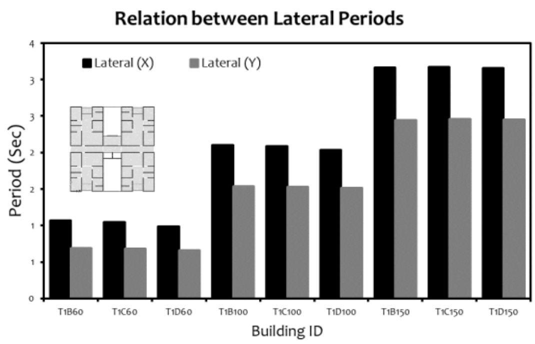

(a) Tower 1

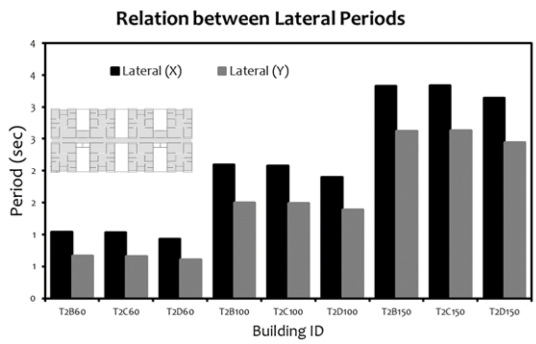

(b) Tower 2

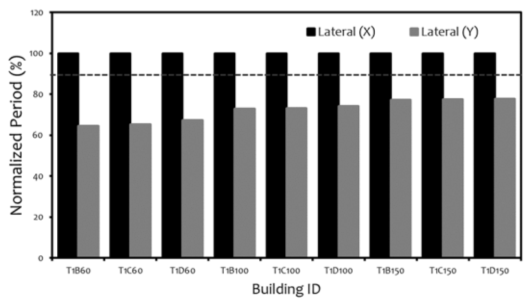

(c) Tower 1

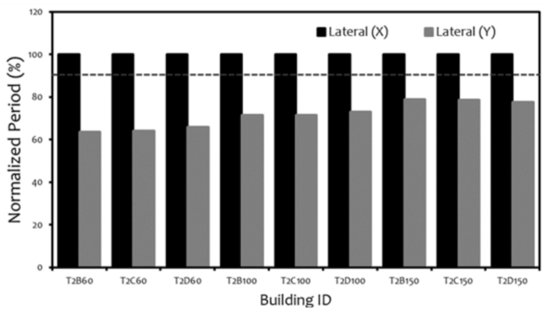

(d) Tower 2

Figure 3.17: Relation between fundamental lateral periods

Table 3.7: Fundamental lateral periods of buildings

Model ID	*Fundamental Period (Sec)*		*Model ID*	*Fundamental Period (Sec)*	
	X	*Y*		*X*	*Y*
T1ZIIB60	1.072	0.691	T2ZIIB60	1.045	0.665
T1ZIIC60	1.050	0.685	T2ZIIC60	1.033	0.662
T1ZIID60	0.985	0.663	T2ZIID60	0.929	0.613
T1ZIIB100	2.101	1.534	T2ZIIB100	2.097	1.501
T1ZIIC100	2.085	1.529	T2ZIIC100	2.083	1.489
T1ZIID100	2.037	1.512	T2ZIID100	1.900	1.390
T1ZIIB150	3.161	2.442	T2ZIIB150	3.326	2.625
T1ZIIC150	3.175	2.460	T2ZIIC150	3.340	2.630
T1ZIID150	3.157	2.452	T2ZIID150	3.140	2.441

In addition, the fundamental natural period along X and Y directions should be sufficiently apart so that they do not vibrate in phase with each other, leading to a phenomenon called *coupling* or *torsional response*. To prevent this phenomenon, the vertical irregularity number vii of Table 6 of IS 1893 has the provision of having at least 10% (of the larger period) difference in fundamental lateral natural periods for buildings in zone IV and V. Figure 3.17 c and d illustrate the normalised fundamental lateral period of all eighteen buildings. Since the natural periods along X were the maximum for all buildings, both lateral fundamental periods of each building are normalised with respect to the period along X. A dotted line along 90% marks the number of buildings with closely spaced lateral fundamental modes. The current buildings under focus were found to have lateral fundamental modes that are sufficiently spaced apart, as shown in Table 3.7 and Table 3.8.

Table 3.8: Normalized fundamental lateral periods of buildings

Model ID	*Normalized Fundamental Period (%)*		*Model ID*	*Normalized Fundamental Period (%)*	
	X	*Y*		*X*	*Y*
T1ZIIB60	100	64.5	T2ZIIB60	100	63.6
T1ZIIC60	100	65.2	T2ZIIC60	100	64.1
T1ZIID60	100	67.3	T2ZIID60	100	66.0
T1ZIIB100	100	73.0	T2ZIIB100	100	71.6

Model ID	*Normalized Fundamental Period (%)*		*Model ID*	*Normalized Fundamental Period (%)*	
	X	*Y*		*X*	*Y*
T1ZIIC100	100	73.3	T2ZIIC100	100	71.5
T1ZIID100	100	74.2	T2ZIID100	100	73.2
T1ZIIB150	100	77.3	T2ZIIB150	100	78.9
T1ZIIC150	100	77.5	T2ZIIC150	100	78.7
T1ZIID150	100	77.7	T2ZIID150	100	77.7

The relationship between lateral and torsional fundamental periods is also important for tall buildings. Clause 5.5.1 of IS 16700 insists designers to ensure that the fundamental torsional period is less than 0.9 times the smaller of the fundamental translation modes. Figure 3.18 a and b show the fundamental lateral and translation periods of all the buildings, while the percentage difference between fundamental torsion and minimum fundamental lateral period can be identified in Figure 3.18 c and d. For the current study, around four buildings have a fundamental torsional period that exceeds one of the fundamental lateral periods, and about four buildings have a difference of at least 10%. For the remaining ten buildings, the torsion period is less than the lateral period but does not have a difference of 10%.

Nevertheless, none of the buildings qualifies for torsional irregularities as specified by type i plan irregularity of Table 5 of IS 1893. According to this clause, a building is said to have torsional irregularity if the torsional period is greater than the lateral period plus if *the maximum horizontal displacement of any floor in the direction of the lateral force at one end of the floor is more than 1.5 times its minimum horizontal displacement at the far end of the same floor in that direction*. The actual values and normalised values of periods are tabulated in Table 3.9 and Table 3.10.

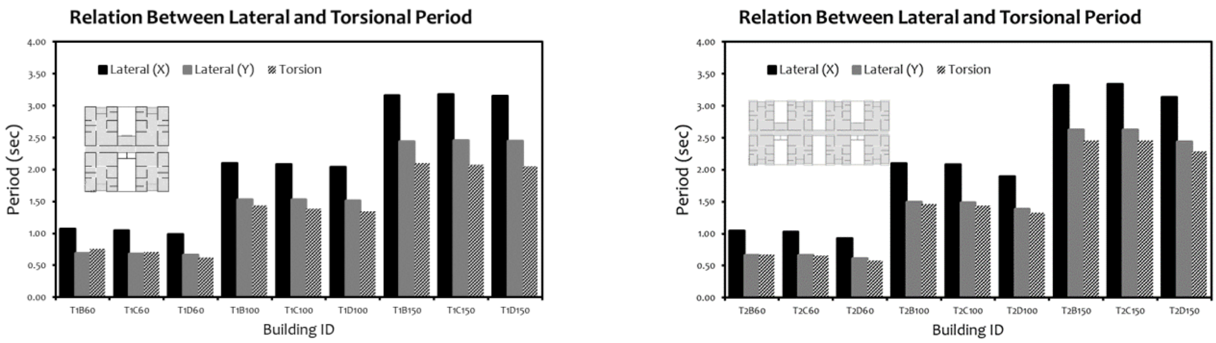

(a) Tower 1

(b) Tower 2

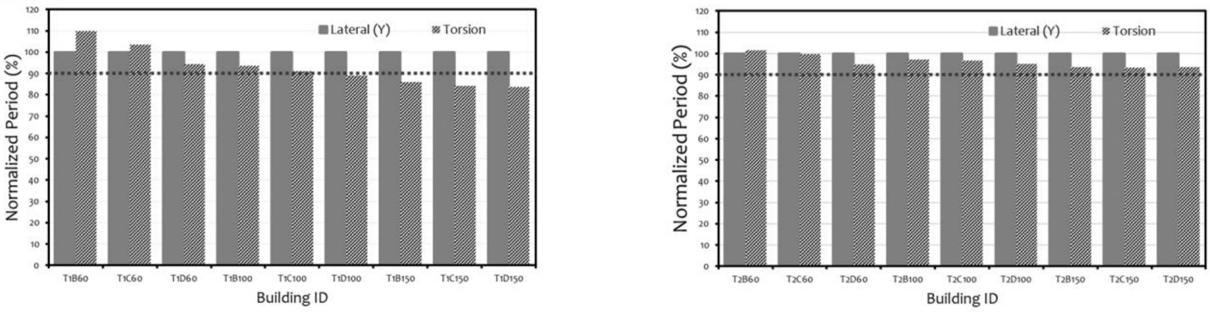

(c) Tower 1 (d) Tower 2

Figure 3.18: Relation between lateral and torsional fundamental periods

Table 3.9: Fundamental lateral and torsional periods of buildings

Model ID	*Fundamental Period (sec)*			*Model ID*	*Fundamental Period (sec)*		
	X	*Y*	*θ*		*X*	*Y*	*θ*
T1ZIIB60	1.072	0.691	**0.759**	T2ZIIB60	1.045	0.665	**0.675**
T1ZIIC60	1.050	0.685	**0.709**	T2ZIIC60	1.033	0.662	0.660
T1ZIID60	0.985	0.663	0.625	T2ZIID60	0.929	0.613	0.582
T1ZIIB100	2.101	1.534	1.435	T2ZIIB100	2.097	1.501	1.460
T1ZIIC100	2.085	1.529	1.391	T2ZIIC100	2.083	1.489	1.439
T1ZIID100	2.037	1.512	1.345	T2ZIID100	1.900	1.390	1.324
T1ZIIB150	3.161	2.442	2.101	T2ZIIB150	3.326	2.625	2.457
T1ZIIC150	3.175	2.460	2.072	T2ZIIC150	3.340	2.630	2.457
T1ZIID150	3.157	2.452	2.053	T2ZIID150	3.140	2.441	2.287

Table 3.10: Normalized Fundamental minimum lateral and torsional periods of buildings

Model ID	*Normalized Fundamental Period (sec)*			*Model ID*	*Normalized Fundamental Period (sec)*		
	X	*Y*	*θ*		*X*	*Y*	*θ*
T1ZIIB60	155	100	**110**	T2ZIIB60	157	100	**102**
T1ZIIC60	153	100	**104**	T2ZIIC60	156	100	**100**
T1ZIID60	149	100	**94**	T2ZIID60	152	100	**95**
T1ZIIB100	137	100	**94**	T2ZIIB100	140	100	**97**
T1ZIIC100	136	100	**91**	T2ZIIC100	140	100	**97**
T1ZIID100	135	100	89	T2ZIID100	137	100	**95**
T1ZIIB150	129	100	86	T2ZIIB150	127	100	**94**
T1ZIIC150	129	100	84	T2ZIIC150	127	100	**93**
T1ZIID150	129	100	84	T2ZIID150	129	100	**94**

c) Modal Mass of first three modes:

The cumulative modal mass in the first three lateral modes of a building indicates irregular modes of oscillation in two principal plan directions. The seventh vertical irregularity of Table 6 from IS 1893 insists designer to ensure that the cumulative modal mass participating in the first three lateral modes is greater than 65% for buildings in zone II and III. Figure 3.19 and Table 3.11 have this data for buildings under focus and indicate that, except for three buildings, all other buildings have a modal mass greater than 65%. Those three buildings are exempt from this provision as it does not apply to buildings with large podiums, and these buildings have a podium.

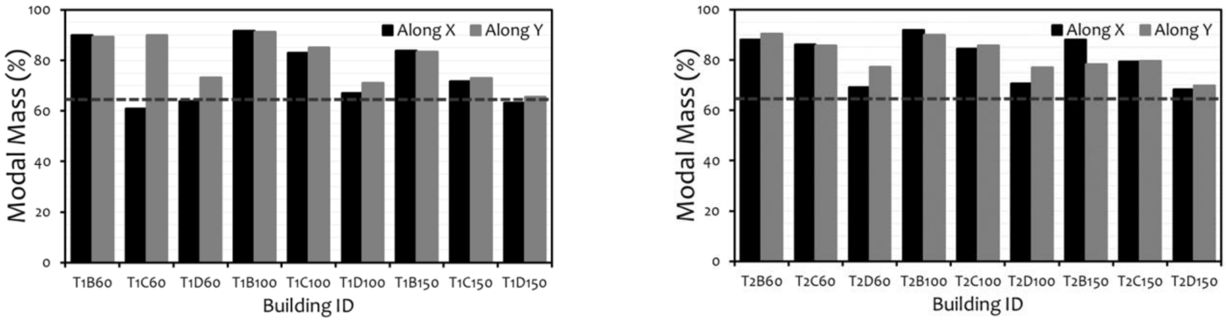

(a) Tower 1 (b) Tower 2

Figure 3.19: Cumulative modal mass in the first three modes

Table 3.11: Cumulative modal mass in the first three modes of buildings

Model ID	***Cumulative Modal Mass(%)***		***Model ID***	***Cumulative Modal Mass(%)***	
	X	*Y*		*X*	*Y*
T1ZIIB60	90	89	T2ZIIB60	88	90
T1ZIIC60	**61**	90	T2ZIIC60	86	86
T1ZIID60	**64**	73	T2ZIID60	69	77
T1ZIIB100	92	91	T2ZIIB100	92	90
T1ZIIC100	83	85	T2ZIIC100	84	86
T1ZIID100	67	71	T2ZIID100	71	77
T1ZIIB150	84	83	T2ZIIB150	88	78
T1ZIIC150	72	73	T2ZIIC150	79	80
T1ZIID150	**63**	66	T2ZIID150	68	70

d) Higher mode effect:

In the design phase, the higher mode effect is considered in the study by carrying out modal analysis. At this stage, the effect of higher modes on the overall performance of structure depends upon the modal mass (Figure 3.20 a), participation factor and corresponding S_a/g values (Figure 3.20 a). It is observed that modal mass of fundamental mode is about 55% and remaining modal mass is distributed across rest of the mode. Further, S_a/g values for second and third mode is higher compared to fundamental natural mode. In this way higher mode effect, i.e. influence of higher modes (second and above) on the global response of the building, is considered in the design of all towers. However, the effect of higher mode is accurately captured when structures goes into nonlinearity, further, it's effects change from one ground motion to another ground motion. This non-linear part of higher mode effect is not covered in this thesis.

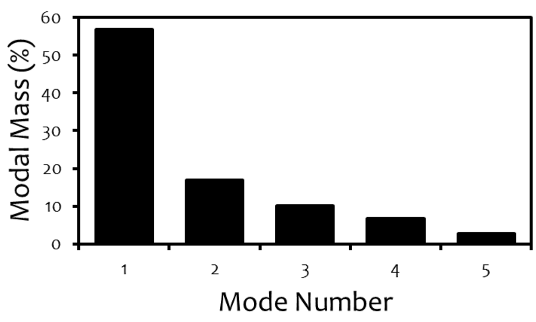

(a) Modal Mass

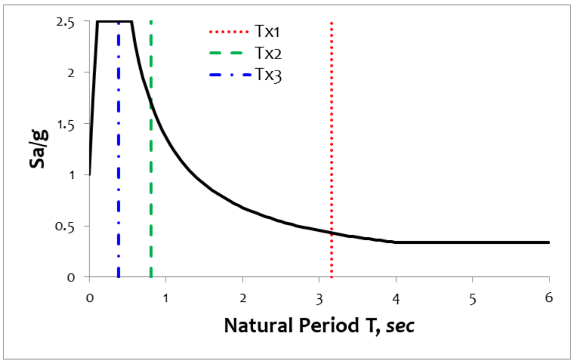

(b) S_a/g value

Figure 3.20: Higher mode effect for T1ZIIB150

3.4.4 *Design Base Shear due to Earthquake Load*

The design base shear is calculated using response spectrum analysis (RSA) and equivalent static method (ESA). If the base shear calculated from RSA is less than that calculated from ESA, the RSA base shear is scaled to the ESA base shear to determine the final design base shear. The process of computing the RSA base shear involves modelling the building, conducting modal analysis, and arriving at the base shear. In contrast, the computation of the ESA base shear is iterative in nature. First, the fundamental lateral natural period is calculated using the empirical formula suggested by the code for RC structural wall buildings as per equations 3-1 and 3-2.

$$T_a = \frac{0.075\, h^{0.75}}{\sqrt{A_W}} \geq \frac{0.09\, h}{\sqrt{d}} \tag{3-1}$$

$$A_w = \sum_{i=1}^{N_w}\left[A_{wi}\left\{0.2 + \left(\frac{L_{wi}}{h}\right)^2\right\}\right];\ L_{wi}/h\ \leq 0.9 \tag{3-2}$$

Where A_{wi} is the effective cross-sectional area of i^{th} wall in first storey, L_{wi} is length of structural wall at first storey along the direction under consideration, N_W is the number of walls in the considered direction and h is the height of a building in metre. This natural period cannot be less than the natural period computed by equation 3-3. Hence, with help of h and d (width of the building at the lowermost level along the direction of shaking under consideration) is computed. The natural period is then verified against the natural period computed by the empirical formula for RC bare frame building (equation 3-4) to ensure it does not exceed the bare frame period. Finally, an additional check is performed to ensure that the selected natural period is not greater than the natural period computed by ETABS. Once the natural period is determined, the corresponding ESA base shear can be derived.

$$T_a = \frac{0.09\, h}{\sqrt{d}} \tag{3-3}$$

$$T_a = 0.075h^{0.75} \quad \text{3-4}$$

Figure 3.21 shows the design base shear coefficient (A_h) computed based on various parameters of the buildings. All the buildings were observed to have V_b greater than the minimum base shear prescribed by codes for different heights [Table 5 and Clause 6.3.3, IS 16700]. However, no clear pattern was observed in the design base shear coefficient for buildings with similar or different heights. This is primarily because the S_a/g value changes with the natural period, which is governed by code recommendations. Therefore, it is difficult to comment on the influence of podium configuration on the design base shear.

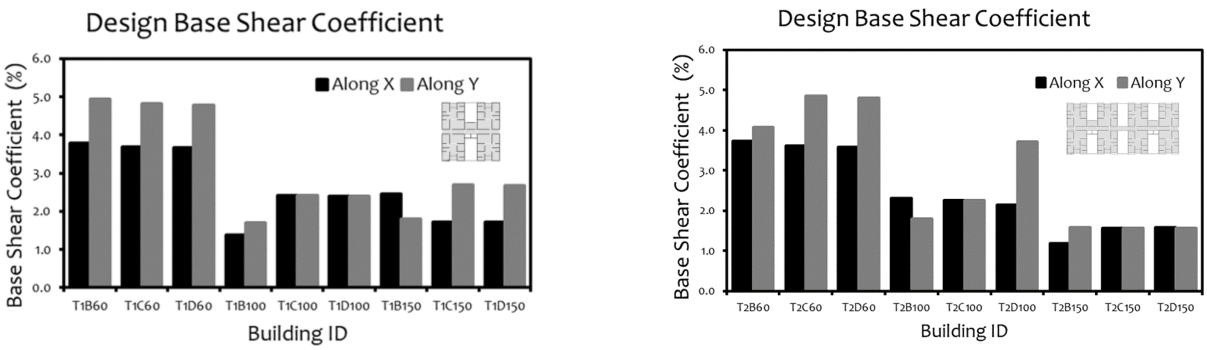

(a) Tower 1 (b) Tower 2

Figure 3.21: Design base shear

3.4.5 Design Base Shear due to Wind Load and Earthquake Load

As discussed earlier, the dynamic wind loads for Tall buildings are computed as per IS 875 Part III 2015 and applied to the model. Figure 3.22 compares the base shear coefficient of all towers for earthquake and wind load. It is found that only two towers (T2C150 and T2D150), along only one direction (along Y), have wind load base shear greater than earthquake load base shear. Hence, the current study only discusses earthquake loads and it's effect.

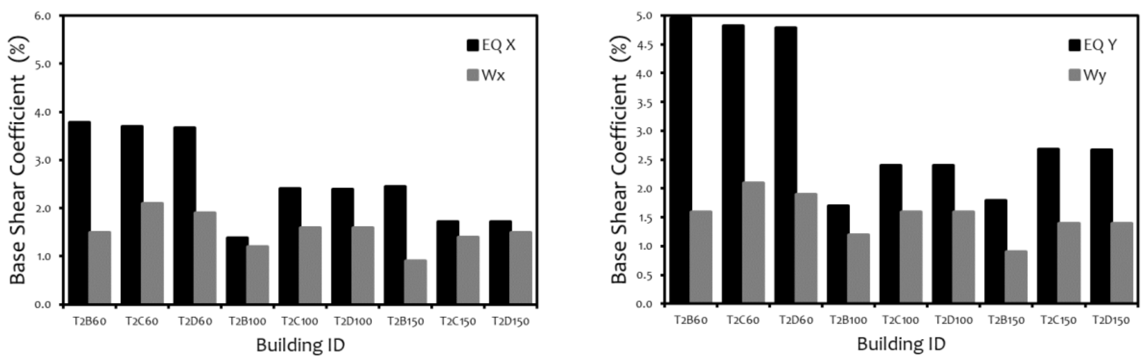

(a) Tower 1 along X (b) Tower 1 along Y

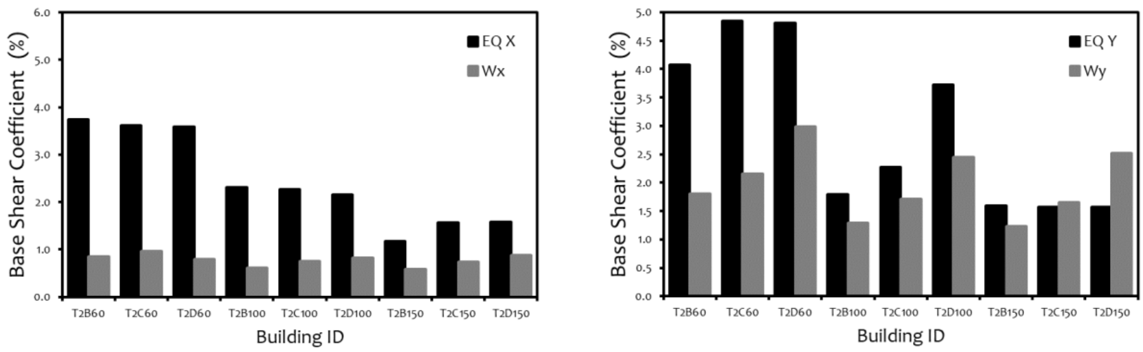

(c) Tower 2 along X (d) Tower 2 along Y

Figure 3.22: Base shear coefficient comparison between earthquake and wind load

3.5 Summary

The current study considered eighteen RC tall buildings based on i) two plans, ii) three structural configurations and iii) three height variations. The plans are typical residential buildings commonly found in city of Hyderabad and Bengaluru. Whereas structural configurations consist of transfer beam-only (*type B*), transfer beam with podium portion without retaining walls (*type C*), and transfer beam with podium having retaining walls (*type D*). Three different height variations represent buildings of 20, 33, and 50 floors, respectively. The structural walls terminate at the fifth storey, and storey four consists of transfer beams supported by transfer columns. The model ID is assigned to each building, capturing the details of the plan, configuration, height, and seismic zone. This same ID will be referred in successive chapters.

These eighteen buildings are modelled and designed using the finite element software ETABS(Computer and Structures Inc., 2020). The software is chosen due to its acceptance in the research community for linear analysis of tall buildings and its popularity among the structural engineering community in India. The buildings are designed using the latest versions of IS 16700, IS 456, IS 875 (Part 1), IS 875 (Part 2), and IS 1893 (Part 1). The grades of concrete and steel used in the design are chosen based on local practice, and a thumb rule of using a higher grade of material for taller structures to have reasonable sizes of structural members is adopted. The buildings are designed for possible gravity (dead and imposed) and lateral (wind and earthquake) loads. The load combinations recommended by IS 456 and IS-1893 are used for both wind and earthquake loads. The slabs and structural walls are modelled as a thin shell element, and beams and columns are modelled as a line element. The scope of the modelling is limited to the global performance of tall buildings with transfer beams, and the interaction of structural wall - floor slab - transfer beam is not included. The individual elements such as beams, columns and structural walls are designed for governing load of axial, shear, moment, and torsion. The iterative design process involves manual computation of code recommended natural period, modal analysis, gravity and lateral load analysis, verification of code clauses, computing elements demand, and checking the capacity of members against demand is followed.

After studying several provisions that departure from the code recommended value, the following salient observations are made:

a) Stiffness irregularity:
    a. It cannot be completely eliminated and brought to 70%. However, continuing a few structural walls until the foundation can be helpful. But this has to be checked on case to case basis as it may create a challenge to getting obstruction free space.
    b. The increase in storey stiffness due to *type C* configuration is insignificant for the current study. However, the *type D* configuration increased stiffness by 10-15% along the X direction and 3-5% along the Y direction. The increase in stiffness depends on the number of walls continuing from the top and the amount of retaining walls in the podium.
b) Mass irregularity:
    a. Mass irregularity has to be checked at two locations. One between the lowest typical storey and the transfer storey and the second one between the transfer storey and the storey below it.
    b. The mass irregularity was found to be between the transfer storey (storey 4) by the storey below it (storey 3) only for non-podium (*type B*) buildings. This also indicates that podium configurations (*type* C and *D*) can eliminate mass irregularities at this location.
c) Fundamental Natural Periods:
    a. The fundamental natural period along the X direction was found to be more for all buildings, as the Y direction was stiffer due to many continuous structural walls running from the top to the foundation. They were also found to have a sufficient gap of more than 10% between them for all buildings. The influence of podium configurations (*type C* and *D*) on fundamental lateral periods was found to be insignificant.
    b. The fundamental torsional period was found to be more than the fundamental lateral period for four buildings, and ten buildings had a torsional period very close to the minimum fundamental lateral period. Only four building has a torsional period sufficiently away from the lateral period. However, none of these buildings qualified for torsional irregularity as per IS 1893, where apart from the torsional period, the displacement relationship of an extreme end of a building also needs to be satisfied.
d) Cumulative Modal mass in first three modes:

a. Except for three buildings, all buildings have a cumulative modal mass >65% in the first three modes. The three buildings that do not have a 65% modal mass cannot come under this requirement since they all have a podium.

e) Design base shear

a. It was clearly evident that there is no specific pattern for a design base shear since it is highly sensitive to the code recommended natural period expressions. In several cases, the code recommended natural period was greater than the software computed period, which indicates the inadequacy of the code recommended natural period expression.

Table 3.12: Summary of code compliance

Building ID	*Stiffness Irregularity (Cl 5.3a, IS 16700:2017)*		*Mass Irregularity (T6 ii, Cl 7.1, IS 1893(1):2016)*	*Torsion and Lateral Period Relationship (Cl 5.5.1, IS 16700:2017)*
	Along X	*Along Y*		
T1ZIIB60	Y	Y	Y	Y
T1ZIIC60	Y	Y	N	Y
T1ZIID60	Y	Y	N	Y
T1ZIIB100	Y	Y	Y	Y
T1ZIIC100	Y	Y	N	Y
T1ZIID100	Y	Y	N	N
T1ZIIB150	Y	N	Y	N
T1ZIIC150	Y	Y	N	N
T1ZIID150	Y	N	N	N
T2ZIIB60	Y	Y	Y	Y
T2ZIIC60	Y	Y	N	Y
T2ZIID60	Y	Y	N	Y
T2ZIIB100	Y	Y	Y	Y
T2ZIIC100	Y	Y	N	Y
T2ZIID100	Y	Y	N	Y
T2ZIIB150	Y	N	Y	Y
T2ZIIC150	Y	Y	N	Y
T2ZIID150	Y	N	N	Y

Note: Y = Yes; N = No

Table 3.13: Summary of Analysis provisions

Parameters	*Overall*	*Effect of Podium Configurations*
Stiffness Irregularity	It cannot be eliminated	*Type D* configuration increases stiffness by 10-15% along the X direction

		and 3-5% along the Y direction
Mass Irregularity	It cannot be eliminated	*Type D* configuration increases stiffness by 10-15% along the X direction and 3-5% along the Y direction

…

Chapter 4. Seismic Performance of Buildings

4.1 Introduction

The previous chapter discussed a detailed description of building modelling and design. This was followed by a discussion of some important code recommended analysis provisions that could not be met. This chapter focuses mainly on the seismic performance of eighteen buildings designed in the previous chapter. After the design, these buildings are subjected to eleven ground motions using LTHA. The outcome of this assessment in terms of displacements, inter-storey drift ratios, base shear, and PMM capacity ratio, as well as shear demand to capacity ratio for transfer columns, are discussed in detail.

4.2 Methodology

An overview of the methodology adopted to know the seismic performance of tall buildings with TB and to comment on their appropriateness in seismic zone II is shown in Figure 4.1. The first two steps, i.e. the selection of buildings and the step-by-step procedure of building design, have already been discussed in sections 3.2 and 3.3 of Chapter 3. Once the building design is complete, the buildings are assessed using the Linear Time History Analysis (LTHA) method. The performance of buildings due to eleven ground motions adopted in LTHA is discussed in detail to outline the recommendations.

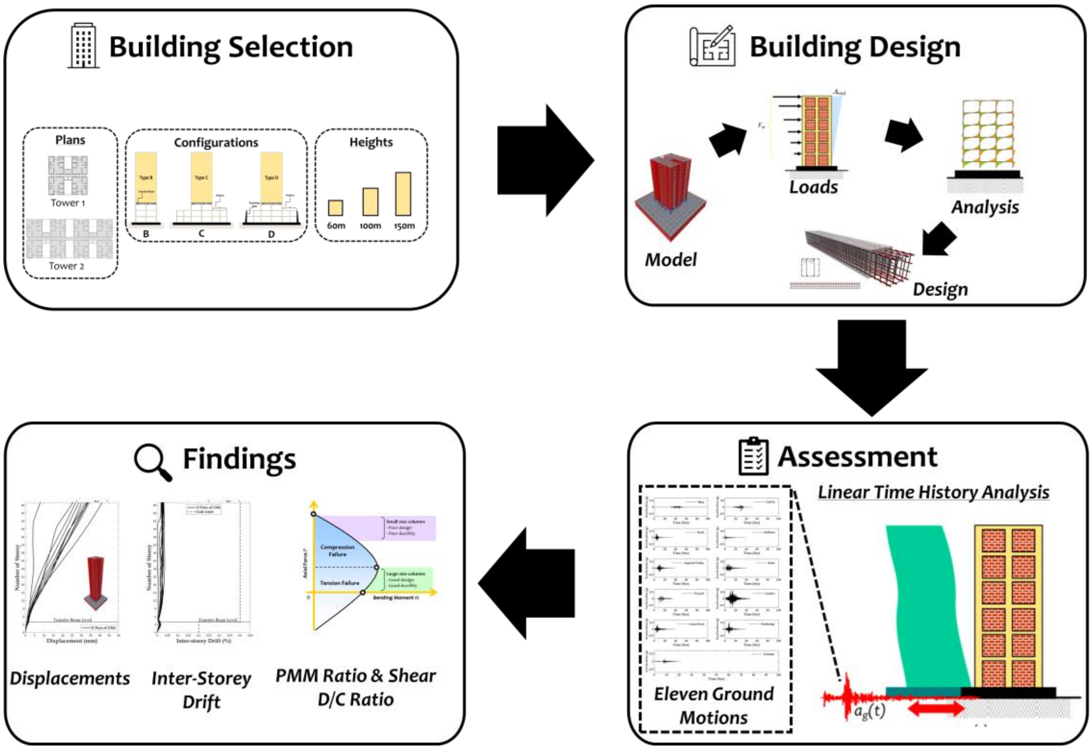

Figure 4.1: Methodology of current work

4.2.1 *Linear Time History Analysis (LTHA)*

In a LTHA, the structural behaviour is assumed to be elastic, i.e. the stiffness and strength of the structure do not change during the earthquake. It involves selecting ground motions and applying them to a structural model to compute the response of buildings in terms of forces and deformations.

a) Ground Motions

For the present study, eleven ground motions are chosen. Ideally, ground motions are selected to represent the time history that the building is likely to experience at its location. In other words, as a first step, ground motions should be selected to have similar source mechanism, magnitude, focal depth, epicentral distance, characteristics of the path through which the seismic waves travel, and soil strata on which the structure is founded. However, the current study focuses on zone II, which is spread over a larger region; hence, narrowing down to these factors representing the entire zone II is difficult. Further, only a limited number of large Indian earthquakes are recorded and publicly available. Therefore, except for the Bhuj earthquake, significant earthquakes that occurred outside India are chosen for this study. Table 4.1 gives details of all these ground motions along with their characteristics, viz., amplitude, predominant period, and significant duration. The signature and Fast Fourier Transform (FFT) of all these ground motions are plotted in Figure 4.2 and Figure 4.3, respectively.

Table 4.1: Details of ground motions considered and their characteristics

Sr No.	*Name of Earthquake (Country)*	*Station*	*Date*	*Peak Ground Acceleration (g)*	*Predominant Period (sec)*	*Significant duration (sec)*
1	Bhuj (India)	Ahmedabad	January 26, 2001	0.1060	0.07-1.23	16.97
2	Chi-Chi (Taiwan)	TCU045	September 20, 1999	0.3610	0.81-1.78	11.78
3	Friuli (Italy)	TOLMEZZO(000)	May 06, 1976	0.3513	0.47-0.53	04.24
4	Hollister (USA)	USGS STATION 1028	April 09, 1961	0.1948	0.37-1.37	16.53
5	Imperial Valley (USA)	USGS STATION 5115	October 15, 1979	0.3152	0.43-0.61	08.92
6	Kobe (Japan)	KAKOGAWA (CUE90)	January 16, 1995	0.3447	1.14-2.05	12.86
7	Kocaeli (Turkey)	YARIMCA (KOERI330)	August 17, 1999	0.3490	1.14-5.12	15.62
8	Landers (USA)	000 SCE STATION 24	June 28, 1992	0.7803	0.07-0.10	13.73

Sr No.	*Name of Earthquake (Country)*	*Station*	*Date*	*Peak Ground Acceleration (g)*	*Predominant Period (sec)*	*Significant duration (sec)*
9	Loma Prieta (USA)	090 CDMG STATION 47381	October 18, 1989	0.3674	1.08-2.56	11.37
10	Northridge (USA)	090 CDMG STATION 24278	January 17, 1994	0.5683	0.68-0.91	09.06
11	Trinidad (USA)	090 CDMG STATION 1498	August 24, 1983	0.1936	0.27-0.40	07.80

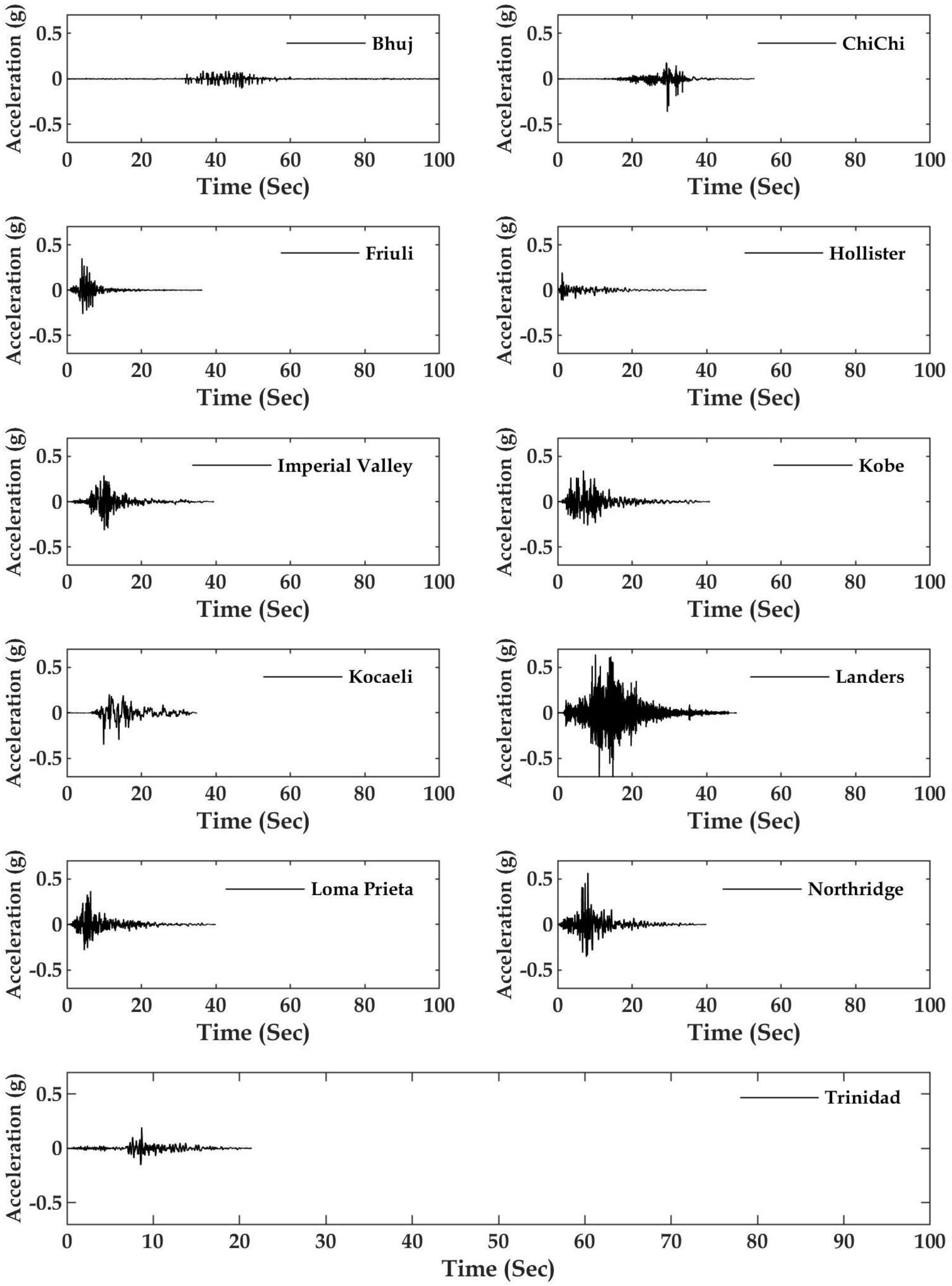

Figure 4.2: Time history plots of all Ground Motions

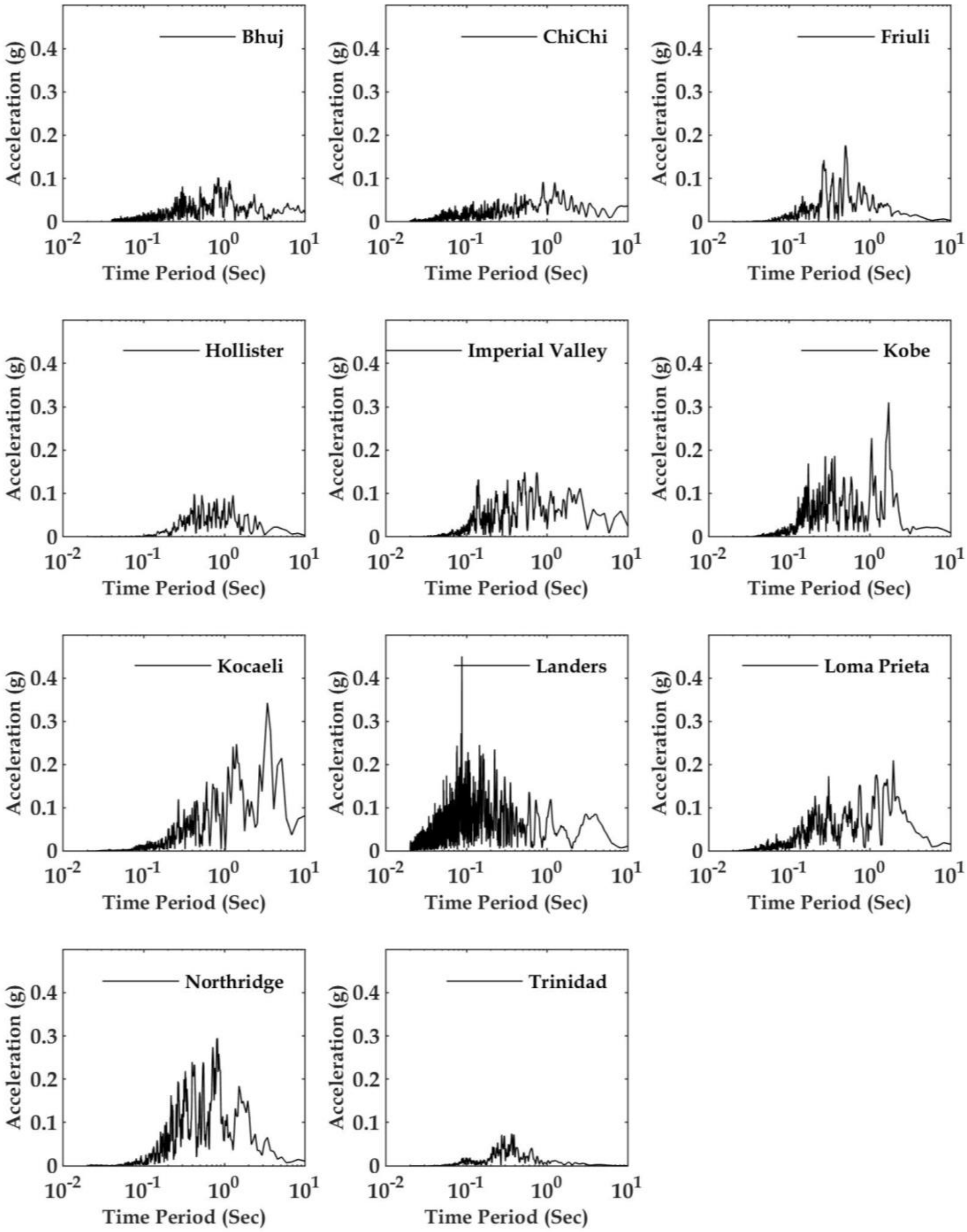

Figure 4.3: Fourier Spectrum Plots of all the Ground Motions

b) Ground motion scaling

Clause 7.7.4 of IS 1893 (IS 1893(Part 1):2016, 2016) indicates that the designer shall choose an *appropriate ground motion*. The same clause defines *appropriate ground motion* as *preferably compatible with the design acceleration spectrum in the desired range of natural periods.* Apart from this, the code is silent on giving further details. In the absence of guidelines from BIS, ASCE 7-16 (ASCE 7-16, 2016) guidelines are followed to make eleven ground motions *appropriate*. The spectral matching method is adopted to modify ground motions such that they become compatible with the design acceleration spectrum (Figure 4.4 a) for medium soil as given in IS 1893. This technique consists of using different modification factors for different periods and, in some cases, adding or subtracting additional energy wavelets to the ground motions so that the response spectra of the modified ground motions more or less match the target spectra. A SeisoMatch (Seismosoft, 2020) tool is used to perform this task, and modified ground motions compatible with the design spectra are shown in Figure 4.4 b.

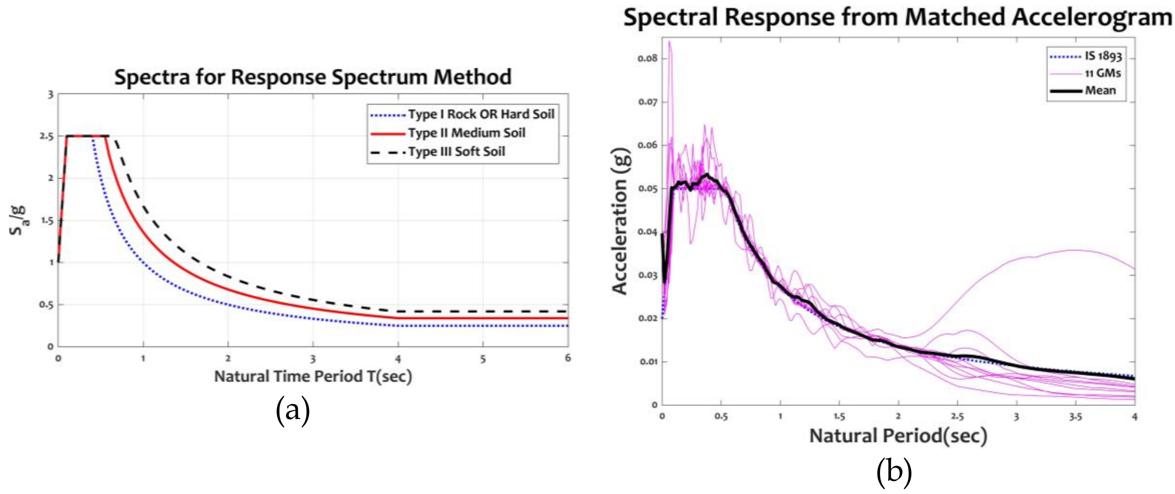

Figure 4.4: Ground motion scaling (a) Input Design spectra as per IS 1893 (b) Response spectra of scaled ground motions

Ground motions are matched for a specific period ranges that ensure the selected ground motions accurately represent the design hazard at the building's fundamental response period. To do this, ASCE 7-16 gives two formulae for upper bound and lower bound periods. The upper bound period consists of two times the maximum fundamental lateral natural period as per equation 4-1. The modification factor two is applied to capture the period elongation effects during the earthquake. And the lower bound period is selected based on the minimum of the lateral period needed for 90% modal mass participation. However, this value can not exceed 20% of the minimum fundamental lateral natural period (equation 4-2). This lower bound period captures the higher mode response.

$$T_{upper} \geq 2\{T_{x_1}, T_{y_1}\}_{max} \tag{4-1}$$

$$T_{lower} = \{T_{x_i}, T_{y_i}\}_{min,\, 90\%\, modal\, mass} \leq 0.2\{T_{x_1}, T_{y_1}\}_{min} \tag{4-2}$$

Table 4.2: Spectral matching period range as per ASCE 7-16 (ASCE 7-16, 2016)

Model ID	***Period (Sec)***		***Model ID***	***Period (Sec)***	
	Upper bound	***Lower bound***		***Upper bound***	***Lower bound***
T1ZIIB60	2.144	0.083	T2ZIIB60	2.090	0.060
T1ZIIC60	2.100	0.120	T2ZIIC60	2.066	0.070
T1ZIID60	1.970	0.069	T2ZIID60	1.858	0.063
T1ZIIB100	4.202	0.167	T2ZIIB100	4.194	0.172
T1ZIIC100	3.770	0.265	T2ZIIC100	4.166	0.117
T1ZIID100	4.070	0.101	T2ZIID100	3.800	0.047
T1ZIIB150	6.322	0.043	T2ZIIB150	6.652	0.158
T1ZIIC150	6.350	0.130	T2ZIIC150	6.680	0.114
T1ZIID150	6.314	0.060	T2ZIID150	6.280	0.047

The upper and lower bound periods for all buildings are tabulated in Table 4.2. The same has been plotted in Figure 4.5. The comparison of the upper bound and lower bound periods for the building with the same height indicates that the influence of podium configurations (*type C & D*) is negligible. This is inevitable since the fundamental lateral natural periods were more or less the same (Figure 3.17), and so is the case with modal mass participation, which resulted in a similar lower bound period with an insignificant difference.

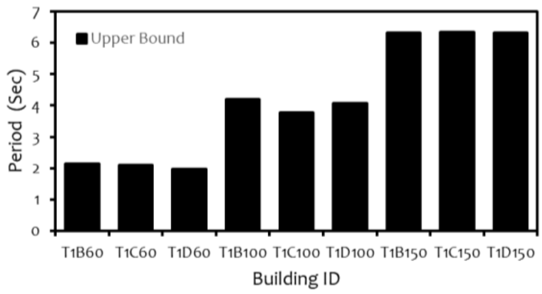

(a) Tower 1

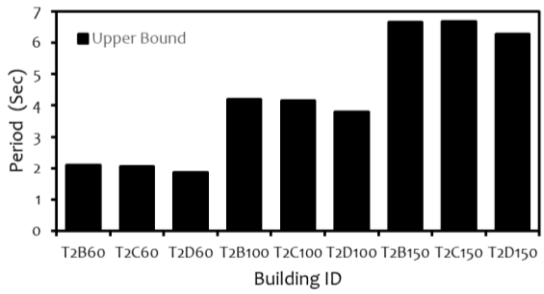

(b) Tower 2

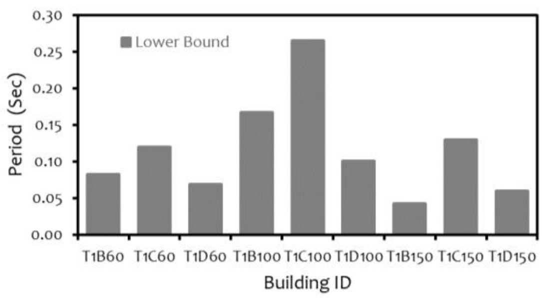

(c) Tower 1

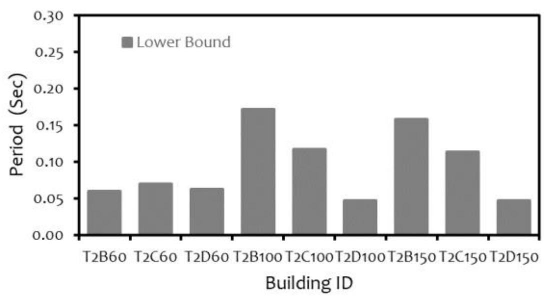

(d) Tower 2

Figure 4.5: Spectral matching period range as per ASCE 7-16(ASCE 7-16, 2016) (a) Tower 1 upper bound, (b) Tower 2 upper bound, (c) Tower 1 lower bound, (d) Tower 2 lower bound

Once the upper and lower bound period has been computed for each building, the eleven ground motions for each building are modified. Figure 4.6 summarises the spectral matching procedure from the computation of period range to the outcome of modified ground motions.

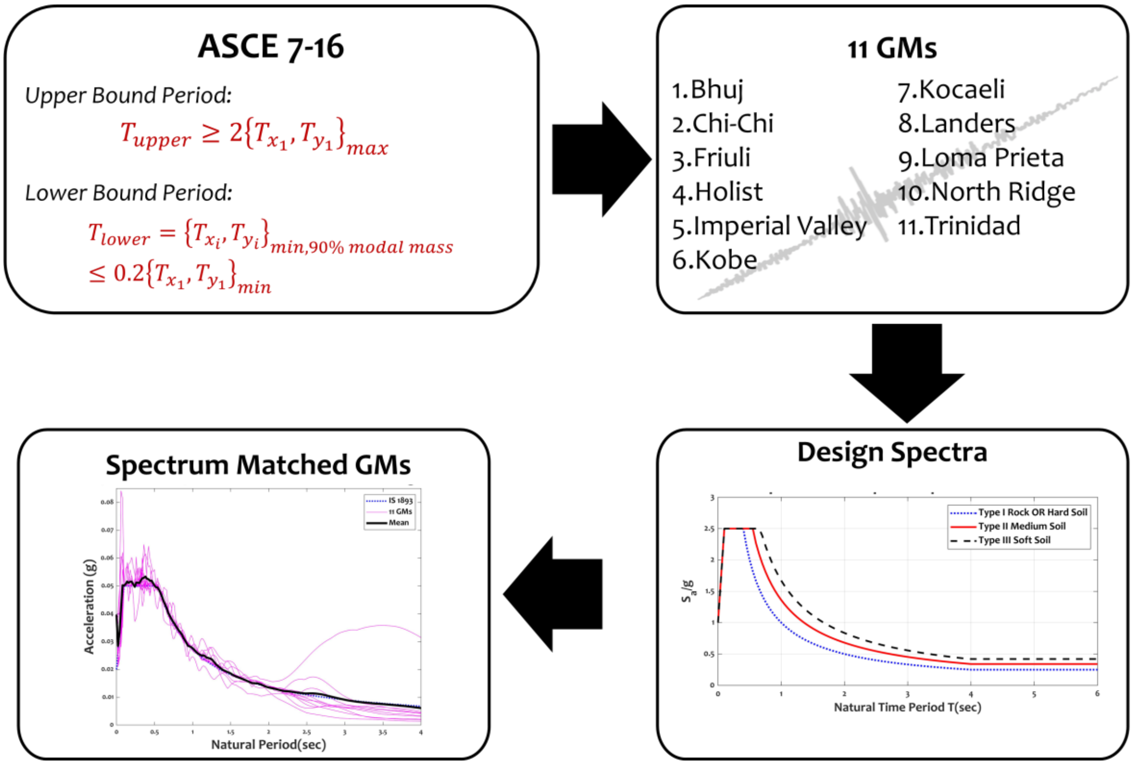

Figure 4.6: Overview of Ground Motion Scaling Procedure

4.2.2 *Evaluation parameters*

The modified ground motions are applied in the lateral direction of a building at the foundation level. As a next step, the linear response to these time histories using cracked section property (Table 3.3) is evaluated. For the evaluation, three global parameters, viz. base shear, displacements and inter-storey drift ratio, and two local parameters for transfer columns, viz., PMM capacity ratio and shear demand/capacity ratio, are considered as performance indicators for buildings with transfer beams.

4.3 Results

4.3.1 *Base Shear*

Figure 4.7 and Figure 4.8 illustrates the difference between the design base shear from RSA and the maximum base shear obtained from LTHA for *Tower 1* and *2* buildings, respectively. Figure 4.7 c and Figure 4.8 c shows the ratio of seismic demand (LTHA) to capacity (RSA) base shear. For *Tower 1* buildings, these values range from 0.57 to

1.19, whereas for *Tower 2* buildings, they range from 0.53 to 1.32. The variation in the base shear among various ground motions and between LTHA base shear and RSA base shear is obvious since, despite the modification of ground motion based on the response spectrum matching procedure, there will be a slight uniqueness of each ground motion. This leads to a difference in the base shear between the RSA and LTHA methods.

Out of eighteen buildings, only seven have a ratio greater than one. The values less than one indicate the possibility of the building performing better during earthquake shaking since they are designed for higher seismic base shear. However, the distribution of base shear, also known as storey shear, does influence the performance of the building, hence few more indicators of the performance of buildings are discussed in further subsections. The values of Figure 4.7 and Figure 4.8 are listed in Table 4.3, Table 4.4 and Table 4.5.

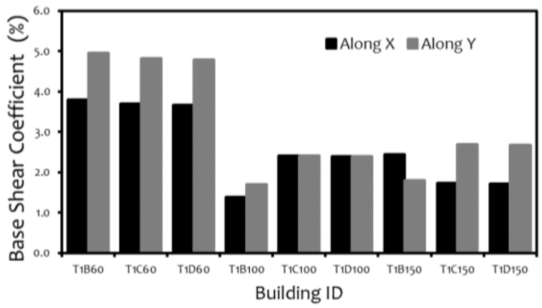

(a) Capacity: Design Base Shear (RSA)

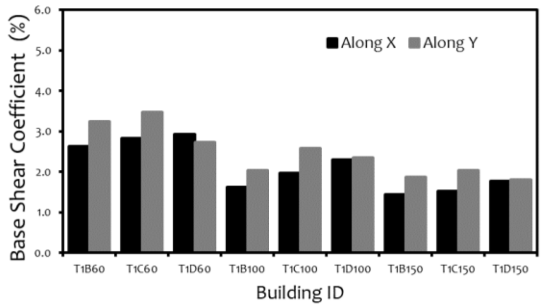

(b) Demand: Max. LTHA Base Shear

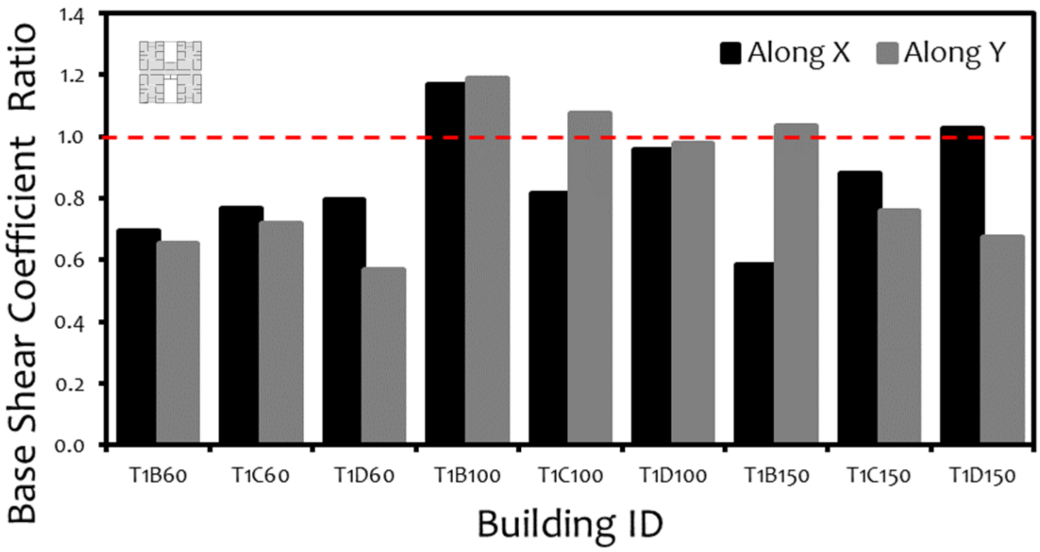

(c) Base Shear Demand / Capacity Ratio

Figure 4.7: Design (RSA) and LTHA base shear for *Tower 1* buildings

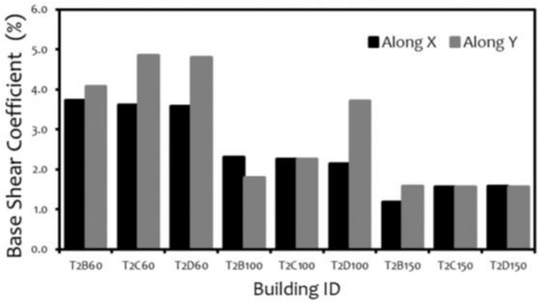

(a) Capacity: Design Base shear

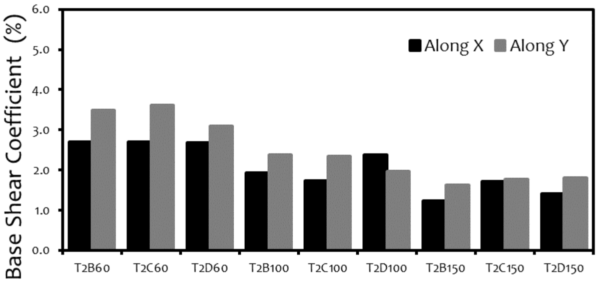

(b) Demand: Max. LTHA Base Shear

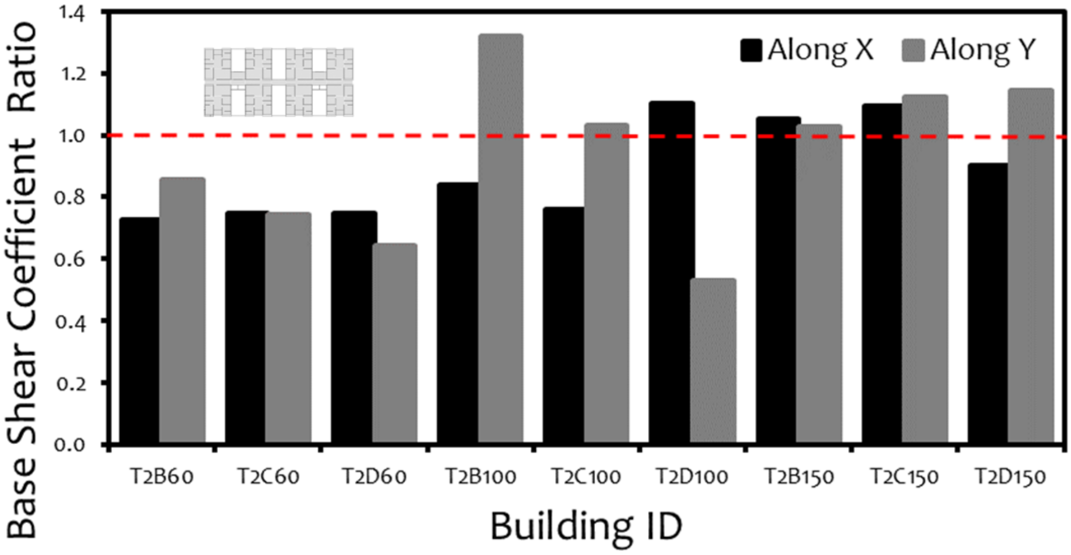

(c) Base Shear Demand/Capacity Ratio

Figure 4.8: Design (RSA) and LTHA base shear for *Tower 2* buildings

Table 4.3: Maximum LTHA base shear coefficient

Model ID	***Max. LTHA Base Shear Coefficient (%)***		***Model ID***	***Max. LTHA Base Shear Coefficient (%)***	
	X	*Y*		*X*	*Y*
T1ZIIB60	2.6	3.2	T2ZIIB60	2.7	3.5
T1ZIIC60	2.8	3.5	T2ZIIC60	2.7	3.6
T1ZIID60	2.9	2.7	T2ZIID60	2.7	3.1
T1ZIIB100	1.6	2.0	T2ZIIB100	1.9	2.4
T1ZIIC100	2.0	2.6	T2ZIIC100	1.7	2.3
T1ZIID100	2.3	2.3	T2ZIID100	2.4	2.0
T1ZIIB150	1.4	1.9	T2ZIIB150	1.2	1.6
T1ZIIC150	1.5	2.0	T2ZIIC150	1.7	1.8
T1ZIID150	1.8	1.8	T2ZIID150	1.4	1.8

Table 4.4: Design base shear coefficient (RSA)

Model ID	***Design (RSA) Base Shear Coefficient (%)***		***Model ID***	***Design (RSA) Base Shear Coefficient (%)***	
	X	*Y*		*X*	*Y*
T1ZIIB60	3.8	5.0	T2ZIIB60	3.7	4.1
T1ZIIC60	3.7	4.8	T2ZIIC60	3.6	4.9
T1ZIID60	3.7	4.8	T2ZIID60	3.6	4.8
T1ZIIB100	1.4	1.7	T2ZIIB100	2.3	1.8

Model ID	*Design (RSA) Base Shear Coefficient (%)*		*Model ID*	*Design (RSA) Base Shear Coefficient (%)*	
	X	*Y*		*X*	*Y*
T1ZIIC100	2.4	2.4	T2ZIIC100	2.3	2.3
T1ZIID100	2.4	2.4	T2ZIID100	2.2	3.7
T1ZIIB150	2.4	1.8	T2ZIIB150	1.2	1.6
T1ZIIC150	1.7	2.7	T2ZIIC150	1.6	1.6
T1ZIID150	1.7	2.7	T2ZIID150	1.6	1.6

Table 4.5: Base shear Demand (LTHA) to Capacity (RSA) Ratio

Model ID	*Base Shear Demand/Capacity Ratio*		*Model ID*	*Base Shear Demand/Capacity Ratio*	
	X	*Y*		*X*	*Y*
T1ZIIB60	0.7	0.7	T2ZIIB60	0.7	0.9
T1ZIIC60	0.8	0.7	T2ZIIC60	0.7	0.7
T1ZIID60	0.8	**0.6**	T2ZIID60	0.7	0.6
T1ZIIB100	**1.2**	**1.2**	T2ZIIB100	0.8	**1.3**
T1ZIIC100	0.8	**1.1**	T2ZIIC100	0.8	1.0
T1ZIID100	1.0	1.0	T2ZIID100	**1.1**	**0.5**
T1ZIIB150	0.6	1.0	T2ZIIB150	**1.1**	1.0
T1ZIIC150	0.9	0.8	T2ZIIC150	**1.1**	**1.1**
T1ZIID150	1.0	0.7	T2ZIID150	0.9	**1.1**

4.3.2 Displacements

The displacement profile for building T1Z2C150, when subjected to modified ground motions, is plotted in Figure 4.9. The maximum roof displacement along the X-direction is found to be 42mm, and the minimum is found to be 17mm. Similarly, 27mm and 12mm are found to be maximum and minimum displacements along the Y direction, respectively. The additional structural walls along the Y direction reduce the displacements along the Y direction compared to that along X. Closer inspection of displacements near the podium and transfer level (Figure 4.9 c & d) indicates no drastic change in the displacements at these levels. Also, displacement amplitude is less due to higher stiffness and proximity to ground level. The displacement plots of LTHA for the rest of the buildings also have the same outcome and are plotted in the Appendix (Figure B.7 to Figure B.12).

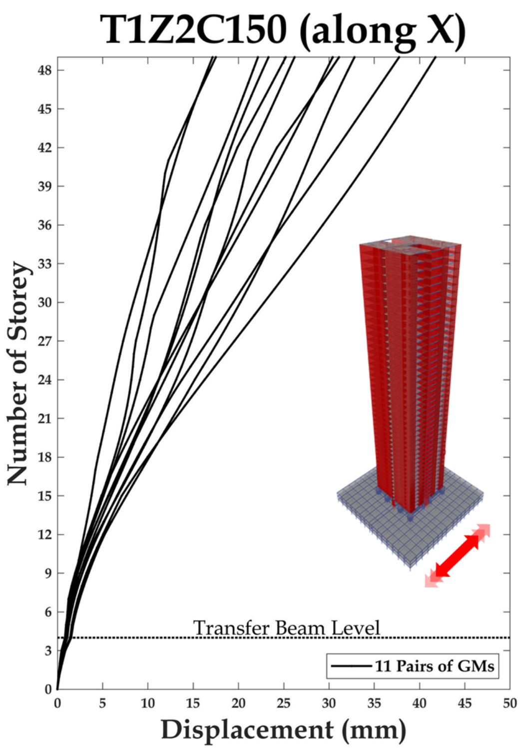

(a) Along X

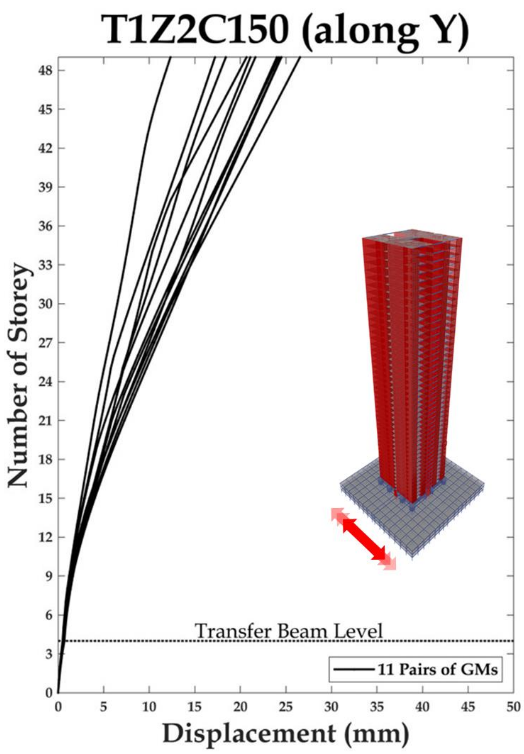

(b) Along Y

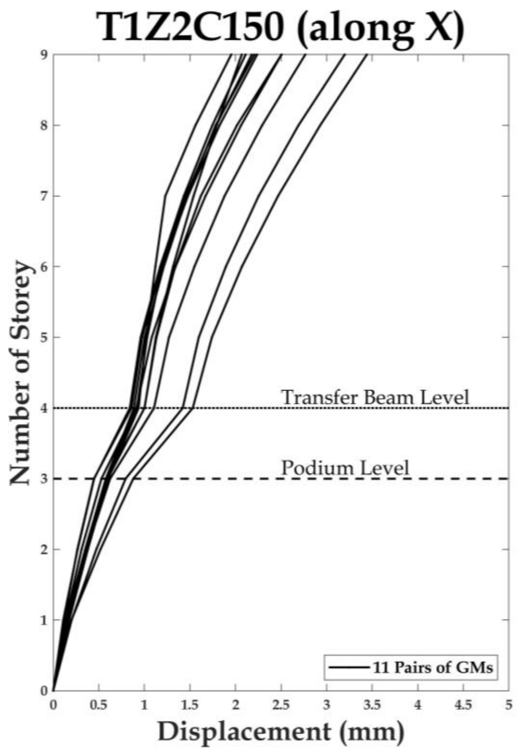

(c) Along X: Lower Levels

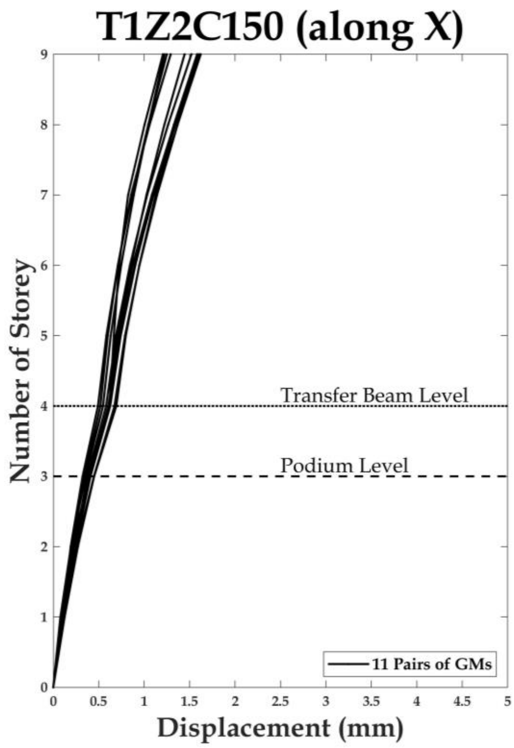

(d) Along Y: Lower Levels

Figure 4.9: LTHA displacement profile for T1Z2C150

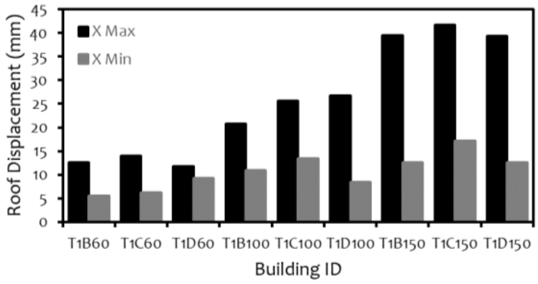

(a) Tower 1 (Along X)

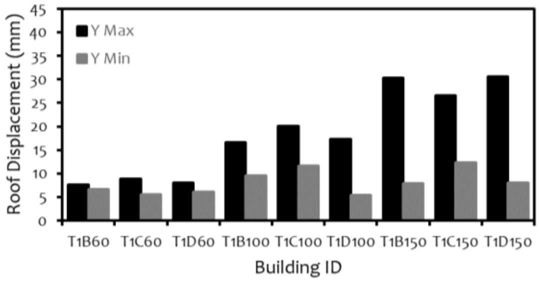

(b) Tower 1 (Along Y)

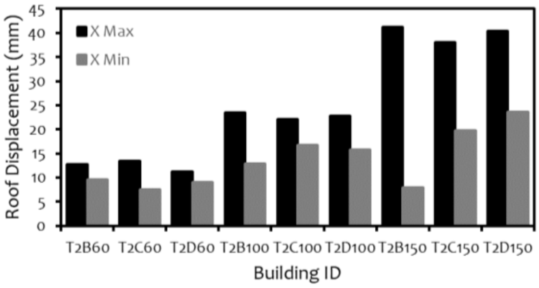

(c) Tower 2 (Along X)

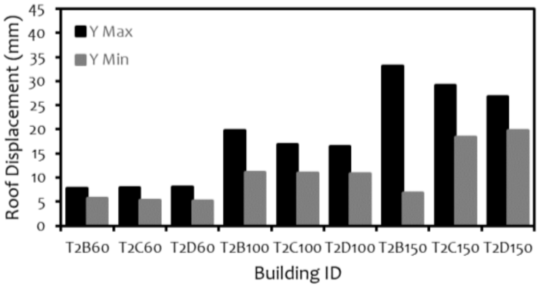

(d) Tower 2 (Along Y)

Figure 4.10: Maximum and Minimum LTHA Roof Displacements

The roof displacements of all the buildings due to LTHA are plotted in Figure 4.10 and tabulated in Table 4.6 and Table 4.7. Comparing LTHA displacements of buildings of similar height, it is observed that they have a more or less similar response to the ground motions. This indicates that the podium configurations (*type C* & *D*) do not affect the displacements of buildings of the same height.

Table 4.6: Maximum and Minimum LTHA Roof Displacements

Model ID	***LTHA Roof Displacements (mm)***				***Model ID***	***LTHA Roof Displacements (mm)***			
	X Max	*X Min*	*Y Max*	*Y Min*		*X Max*	*X Min*	*Y Max*	*Y Min*
T1ZIIB60	13	6	8	7	T2ZIIB60	13	10	8	6
T1ZIIC60	14	6	9	6	T2ZIIC60	13	8	8	5
T1ZIID60	12	9	8	6	T2ZIID60	11	9	8	5
T1ZIIB100	21	11	17	10	T2ZIIB100	24	13	20	11
T1ZIIC100	26	13	20	12	T2ZIIC100	22	17	17	11
T1ZIID100	27	8	17	5	T2ZIID100	23	16	16	11
T1ZIIB150	39	13	30	8	T2ZIIB150	41	8	33	7
T1ZIIC150	42	17	27	12	T2ZIIC150	38	20	29	18
T1ZIID150	39	13	31	8	T2ZIID150	40	24	27	20

Table 4.7: Maximum and Minimum LTHA Roof Displacements Range

Group Name	***LTHA Roof Displacement Range (mm)***				***Group Name***	***LTHA Roof Displacement Range (mm)***			
	X Max	*X Min*	*Y Max*	*Y Min*		*X Max*	*X Min*	*Y Max*	*Y Min*
T1_60s	12-14	06-09	08-09	06-07	T2_60s	11-13	08-10	08-08	05-06

Group Name	LTHA Roof Displacement Range (mm)				Group Name	LTHA Roof Displacement Range (mm)			
	X Max	X Min	Y Max	Y Min		X Max	X Min	Y Max	Y Min
T1_100s	21-27	08-13	17-20	05-12	T2_100s	22-24	13-17	16-20	11-11
T1_150s	39-42	13-17	27-31	08-12	T2_150s	38-41	08-24	27-33	07-20

Note:
T1_60s = T1Z2B60, T1Z2C60, T1Z2C60 *T2_60s = T2Z2B60, T2Z2C60, T2Z2C60*
T1_100s = T1Z2B100, T1Z2C100, T1Z2C100 *T2_100s = T2Z2B100, T2Z2C100, T2Z2C100*
T1_150s = T1Z2B150, T1Z2C150, T1Z2C150 *T2_150s = T2Z2B150, T2Z2C150, T2Z2C150*

4.3.3 IDR (Inter-storey Drift Ratio)

Inter-storey drift (ID) refers to the relative displacement or deformation between adjacent floors of a building or structure during seismic events or other dynamic loads. The inter-storey drift ratio (IDR) is calculated by dividing the maximum ID by the height of the storey. For example, if the maximum ID between two adjacent floors of a building is 100 mm, and the height of each storey is 3 meters, the IDR would be 100/3000 = 0.0333 or 3.33%.

Excessive IDR can compromise the structural integrity of a building, leading to excessive damage or collapse of a building. The performance of non-structural elements (NSE) is also linked with an amplitude of IDR, as higher IDR can lead to damage to partition walls and cladding. Further, IDR is also monitored to ensure the comfort and safety of the occupants of a building. As higher IDR may lead to a toppling of objects and/or may cause motion sickness. Finally, IDR is also used as a seismic performance indicator to assess the building's performance and identify members needing strengthening or modification.

Figure 4.11 shows the IDR profile of all the towers for LTHA along the X and Y directions. The more clear figure of each plot can be referred at Figure B.13 to Figure B.18. In addition to IDR plots, a code specified IDR limit of 0.4% is also shown with a dotted line. One of the latest amendments to IS 1893 imposes a limit of 0.2% of IDR where stiffness irregularities are present in the structure. None of the buildings' IDR crosses the 0.04% value, indicating that the IDR of all eighteen buildings is well within the code specified limit. Interestingly, despite irregularity introduced due to TB and podium, all buildings are performing well in terms of IDR. The IDR are relatively small first reason is due to the higher stiffness of the structural system. And the second reason is lower seismic demand. Together with this, the building has a uniform distribution of stiffness and mass. All this together results in relatively less displacements and inter-storey drift in buildings. Similar IDR have also been reported in past literature (Y. M. Abdlebasset et al., 2016; Lu et al., 2012).

Figure 4.12 shows the IDR of T1_150s (i.e. T1Z2B150, T1Z2C150, T1Z2D150), and Figure 4.13 shows the IDR of T1Z2C150. Close observation of the IDR profile of these figures along the X and Y directions reveals that the IDR along Y is less than the IDR along X. This observation holds true for the rest of the buildings. This indicates that the greater number of continuous walls along the Y direction reduces the amplitude of the IDR profile of the building. Figure 4.13 b and e also show that the maximum IDR of a building occurs at upper storeys and not at lower levels. A similar observation is made for the rest of all buildings.

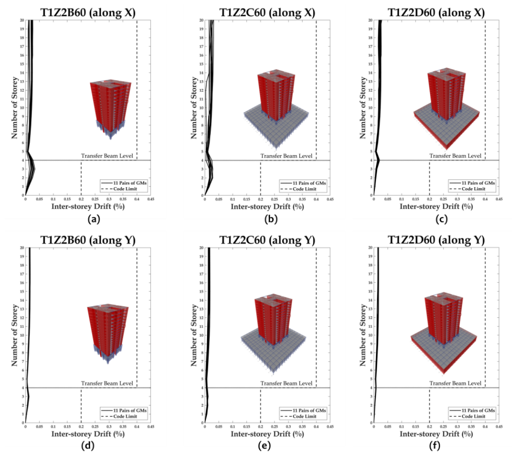

(i) T1_60s

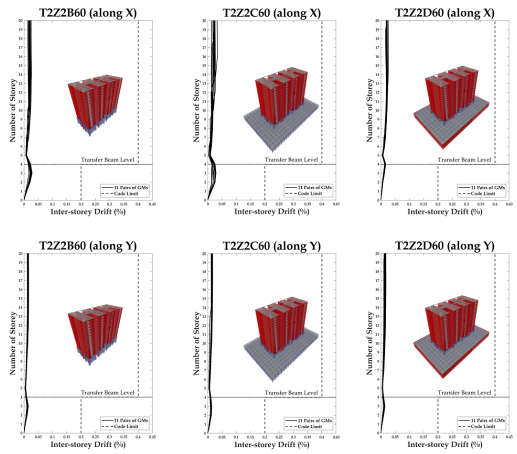

(ii) T2_60s

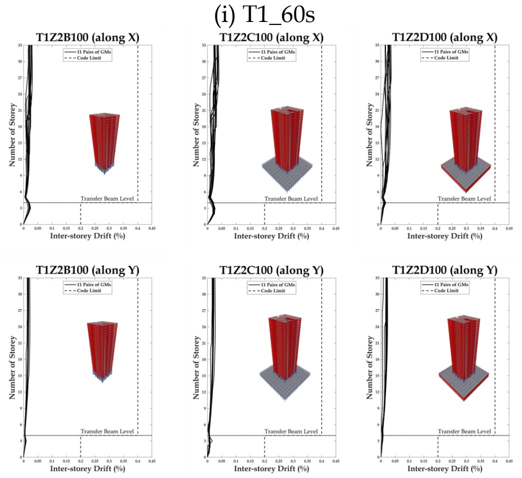

(iii) T1_100s

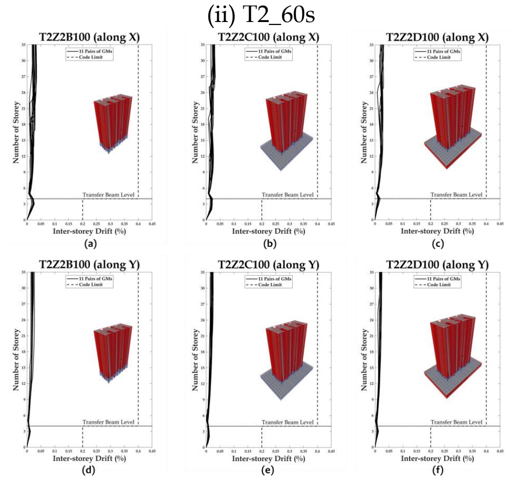

(iv) T2_100s

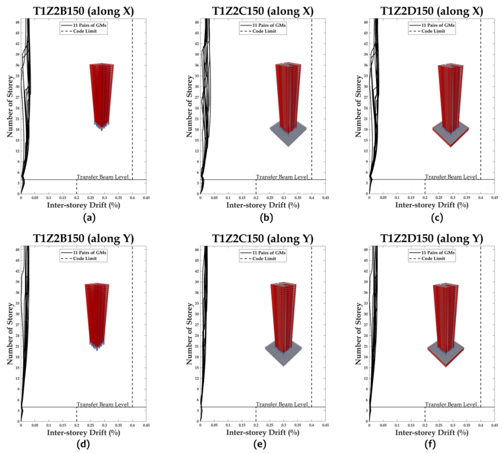

(v) T1_150s

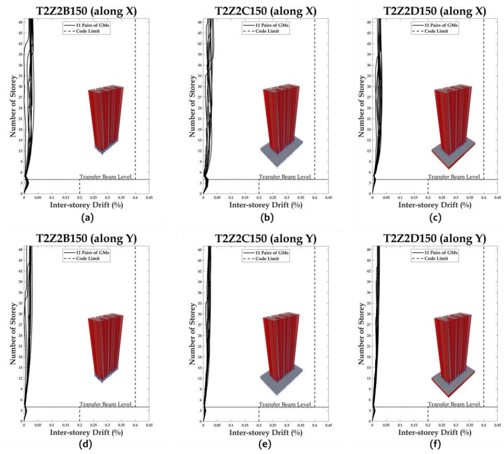

(vi) T2_150s

Figure 4.11: IDR for all buildings

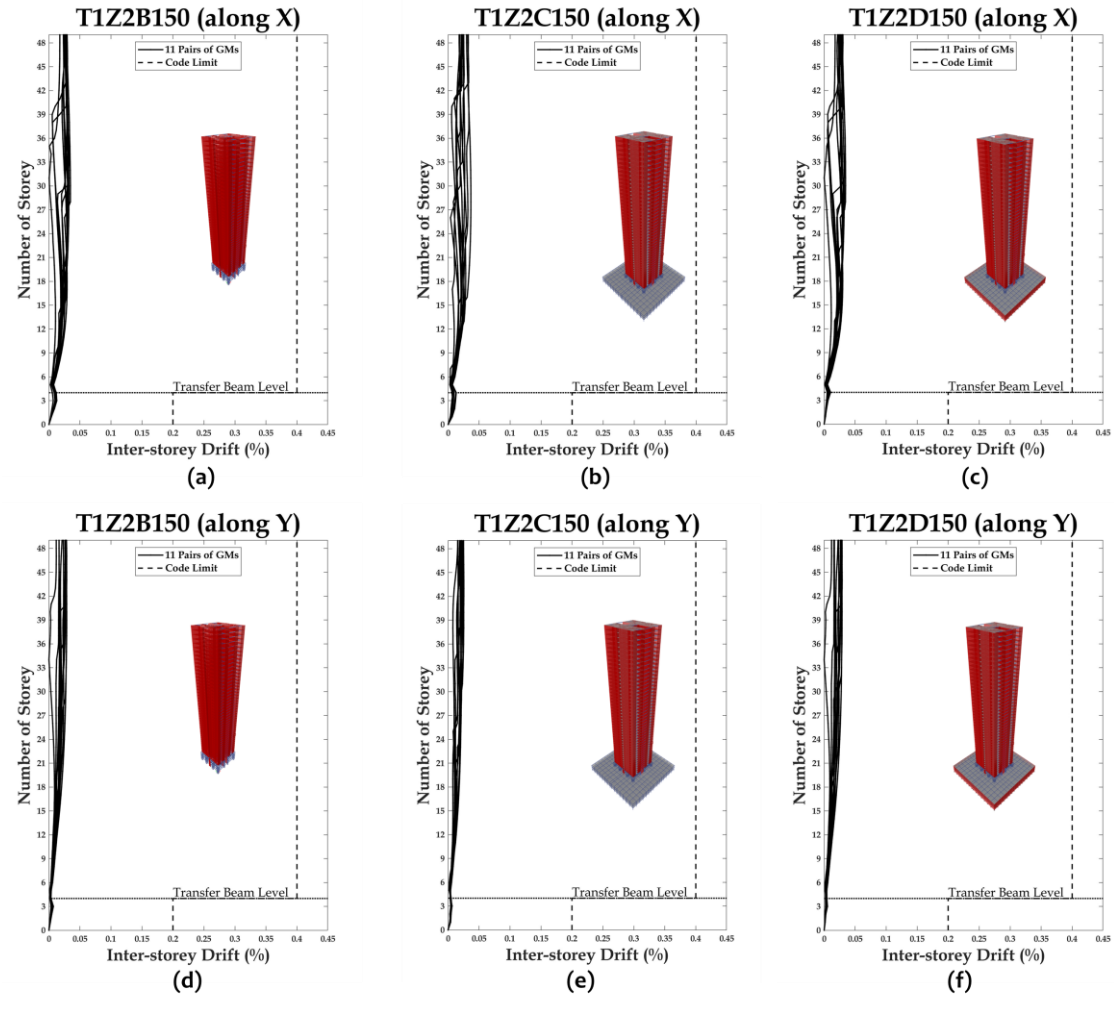

Figure 4.12: IDR for T1_150s

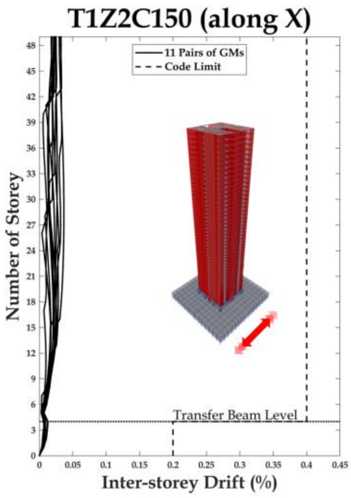

(a) With code limit (X)

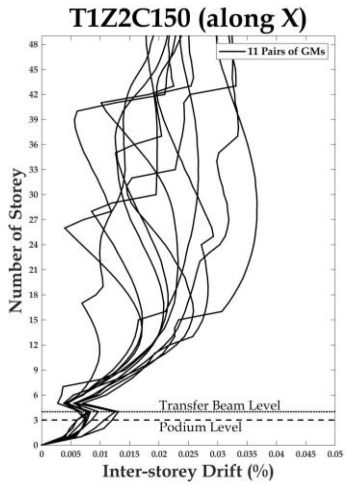

(b) Without code limit (Y)

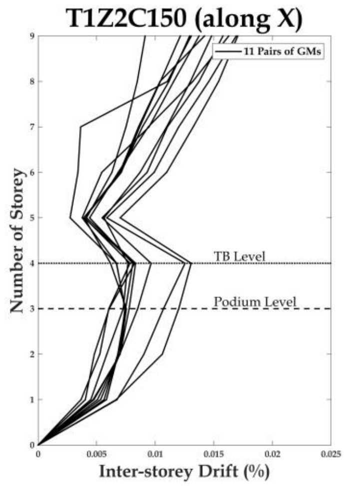

(c) Lower Storey(X)

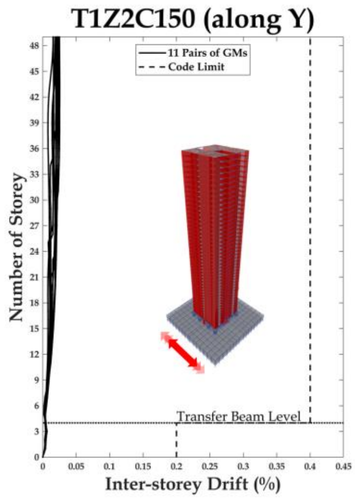

(d) With code limit (Y)

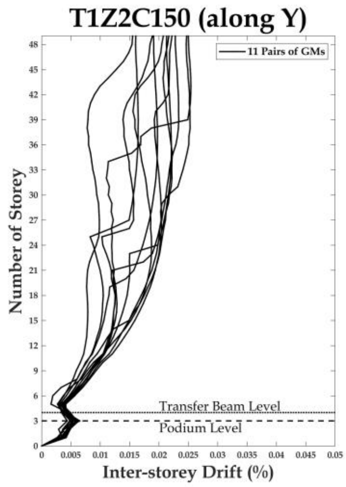

(e) Without code limit (Y)

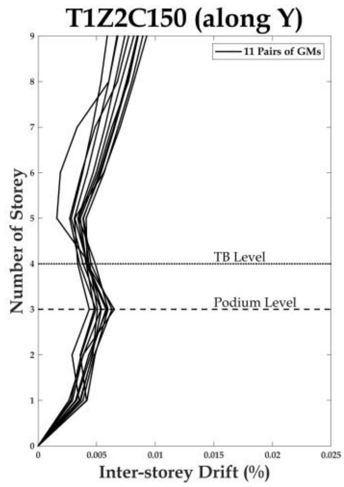

(f) Lower Storey(Y)

Figure 4.13: LTHA IDR profile for T1Z2C150

Figure 4.13(c and f) shows the IDR near the transfer storey for T1Z2C150; Figure 4.14 shows the effect of podium configurations in IDR demands in lower storeys of T1_60s and Figure 4.15 for the rest of all buildings. These figures are plotted to compare the maximum IDR near the vicinity of a TB level (storey 4). Though the overall IDR values are well within a code defined limits, the slight influence of podium configurations (*type C* & *D*) is observed in IDR values when IDR values are compared for four lower levels, viz., a floor above TB level (storey 5), TB level (storey 4), storey 3/podium level, and storey 2/level below podium level. What is striking about the figures is that all the buildings of *type B* configuration have a maximum IDR at a floor below TB level, i.e. storey 3. This indicates that a storey below TB level (storey 3) will have a higher IDR demand without podium configuration.

Further, for all buildings of *type C* configuration, the difference between IDR demand at TB level and Podium level is drastically reduced. This indicates that the podium configuration of *type C* reduces IDR demand at the podium level due to increased stiffness due to podium members (Figure 4.14). However, in most cases, LTHA IDR demand was slightly higher for the podium level than the TB level. Similarly, close observation of IDR of all the buildings of *type D* configuration shows that adding retaining walls in the podium further increases the stiffness of the podium level. Hence IDR demand at the TB level (storey 4) is greater than IDR demand at the podium level (except for four buildings along the Y direction). However, for buildings of similar height, the amplitude of maximum IDR tends to reduce from configuration *B* to *D* (Figure 4.14). The detailed plots of IDR for lower levels are provided in Figure B.19 to Figure B.24.

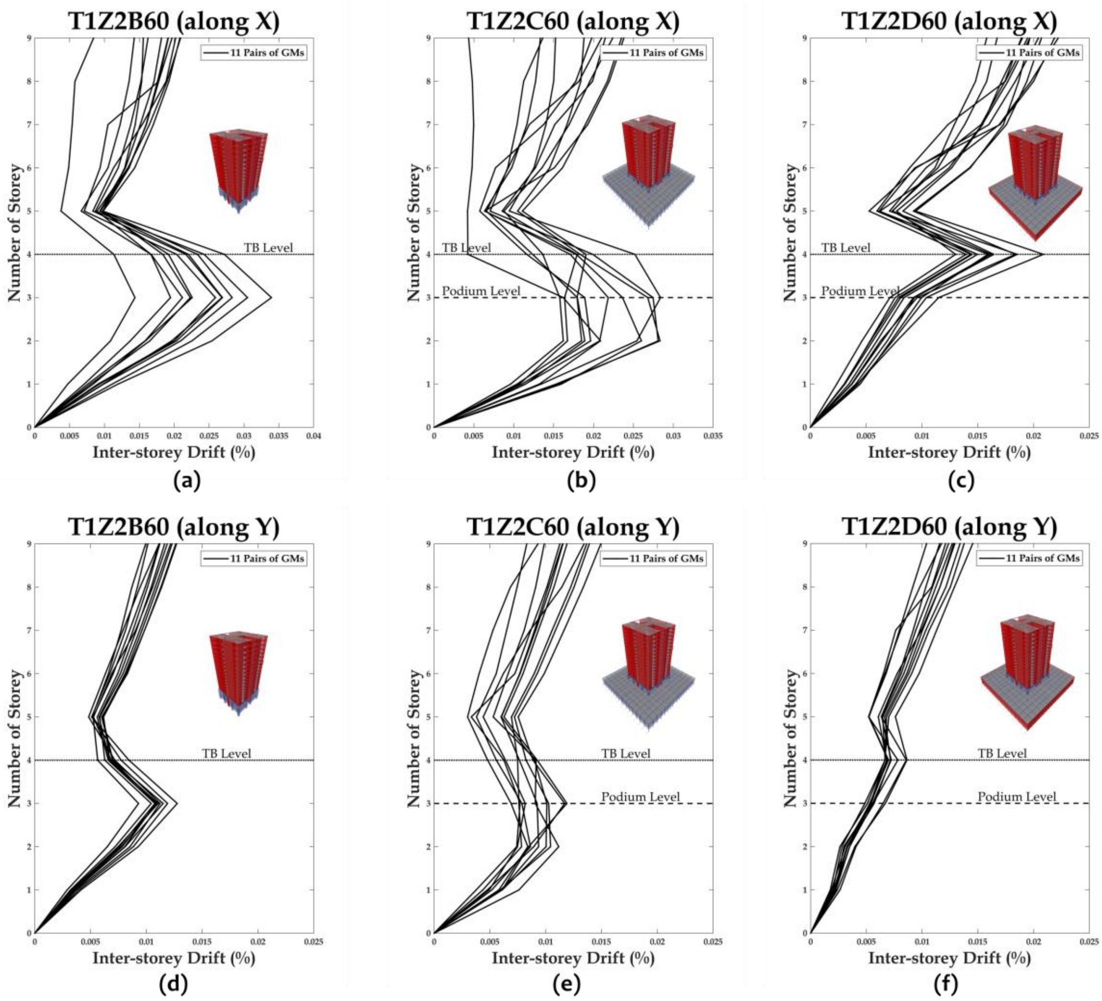

Figure 4.14: IDR demand in T1_60s at lower level showing the effect of podium configurations

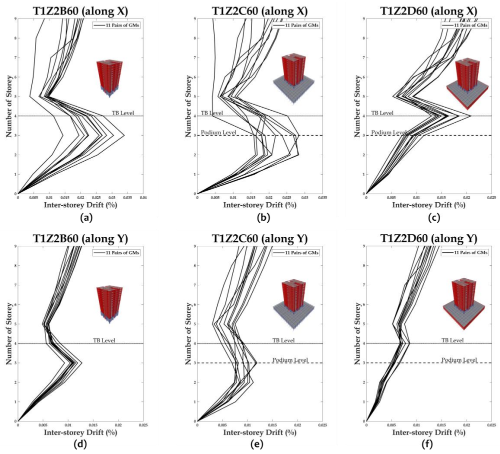

(i) T1_60s

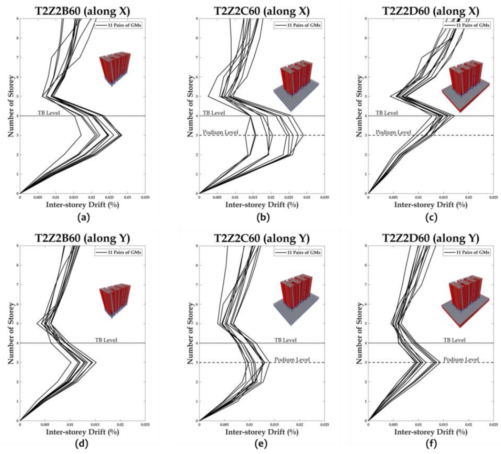

(ii) T2_60s

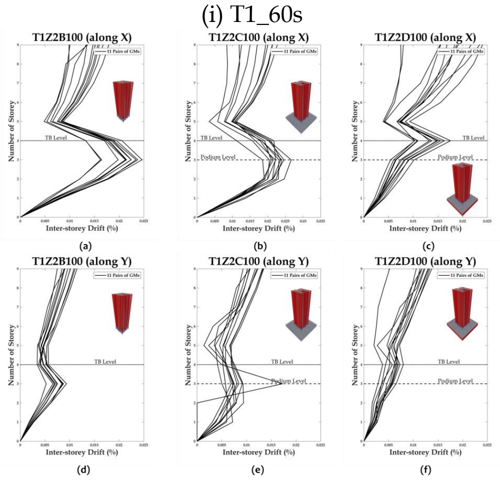

(iii) T1_100s

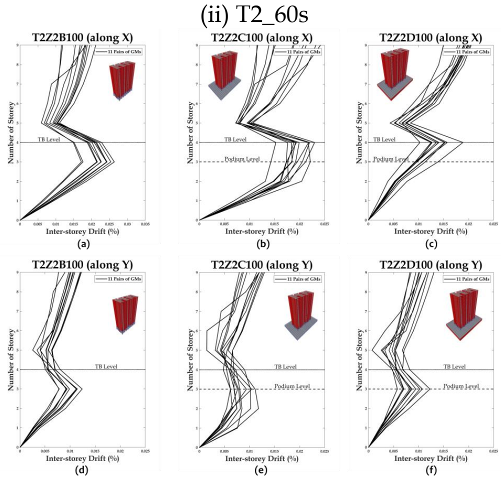

(iv) T2_100s

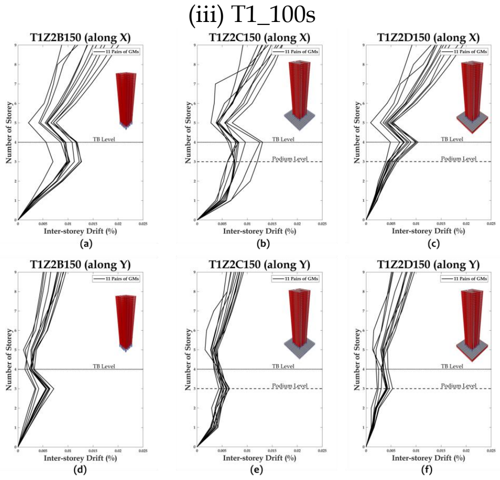

(v) T1_150s

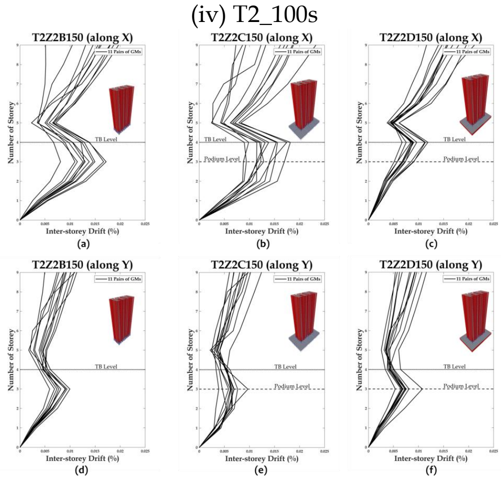

(vi) T2_150s

Figure 4.15: LTHA IDR profile for lower storeys for all the buildings

4.3.4 Column PMM Capacity Ratio

Under the action of gravity and lateral load, structural members such as a column are subjected to combinations of axial force (P) and biaxial bending moments (M_2, M_3). They are, therefore, designed for the P-M interaction envelope curve as per SP:16 (SP 16, 1980). With the advancement of computational capabilities, generating 3D interaction capacity surface (PMM interaction) is possible. The methodology for the design of the column is discussed in 3.3.6.

Columns subjected to high axial force typically have brittle failure when this axial force is coupled with relatively small moment. For columns to behave in a ductile manner, they need to have a large axial area, and their axial stress should be way below the balanced point in the P-M interaction diagram under the combined action of dead, live and earthquake loads (Murty et al., 2012). Hence, while doing performance evaluation, it is desirable that the combined demand of design axial compressive force and bending moment sit in the lower third of their compression P-M interaction diagrams (Figure 4.16). In the absence of any code recommendation value on this aspect, the suggested guideline is followed for the evaluation.

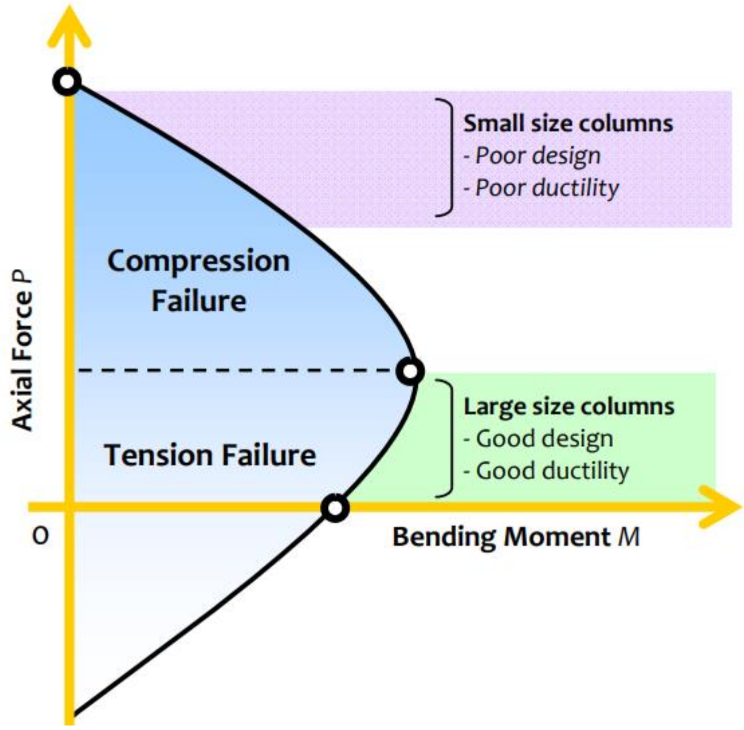

Figure 4.16: Schematic of P-M Interaction diagram of RC columns (Murty et al., 2012)

The PM or PMM capacity ratio is a factor that indicates the stress condition of the column with respect to the capacity of the column. For example, one P-M interaction curve is generated (Figure 4.17 a) for a square RC column having details as given in Table 4.8. The black line indicates the capacity curve or P-M interaction curve. The combined demand (P and M_3) due to lateral load combination is plotted as a circular dot. If P and M_3 keep on increasing linearly with the same proportion, then RC column can take P-M_3 combination as shown as a square mark. For a quick comparison of P-M curves of different sizes of columns or same size columns with different reinforcement detailing, it is common practice to convert this P-M interaction curve axis into a normalised axis, as shown in Figure 4.17 b. The demand is also converted and plotted. Now, the PM capacity ratio is nothing but the ratio of length between the origin to demand point (circular mark) to the length between the origin to capacity point (square mark).

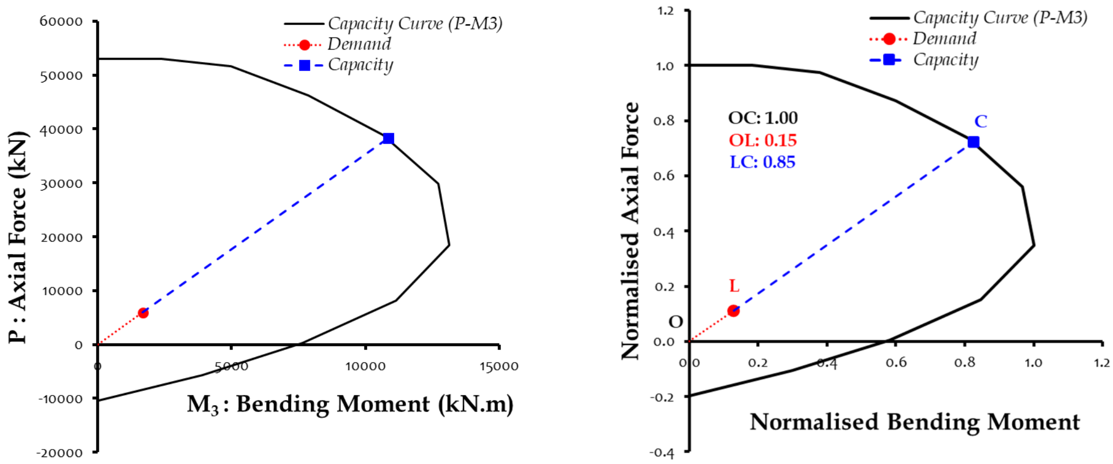

(a) Actual (b) Normalised

Figure 4.17: Example of computation of PM capacity ratio

Table 4.8: RC column detail of PM capacity ratio example

INFORMATION FOR CAPACITY		
Geometry	Shape: Square	Dimensions: 1800mmx1800mm
Materials	Concrete: M35	Steel: HYSD 415
Reinforcement Detailing	Main: 36 – 32 ϕ (On each face: Along X=10 & Along Y= 8)	Secondary: 3 Legged 12 ϕ @ 175mm c/c (Both direction)
INFORMATION FOR DEMAND		
LTHA Bhuj X	Axial: 5942 kN	Bending Moment: 1684 kNm

Similarly, software (Computer and Structures Inc., 2020) used for the study can generate a 3D surface of P-M2-M3 (Figure 4.18). The PMM capacity ratio is computed as follows:

a. Generation of P-M_2-M_3 curves starting from 0 degrees to 360 degrees at every 15-degree orientation.
b. Extract the P-M2-M3 demand for various load combinations.
c. Generate an additional curve when the demand point is not exactly at a multiple of 15 degrees. For this, linear interpolation is used to derive the value.
d. In Figure 4.18, the demand is plotted as points L. Point C is derived based on generated curves and the location of L. Point C is defined as the point where the line OL (if extended outwards) will intersect the failure surface. This point

is determined by three-dimensional linear interpolation between the points that define the failure surface.

e. The PMM capacity ratio, CR, is given by the ratio OL/OC.
    a. If OL = OC (or CR = 1), the point lies on the interaction surface, and the column is stressed to capacity.
    b. If OL < OC (or CR < 1), the point lies within the interaction volume, and the column capacity is adequate.
    c. If OL > OC (or CR > 1), the point lies outside the interaction volume and the column is overstressed.

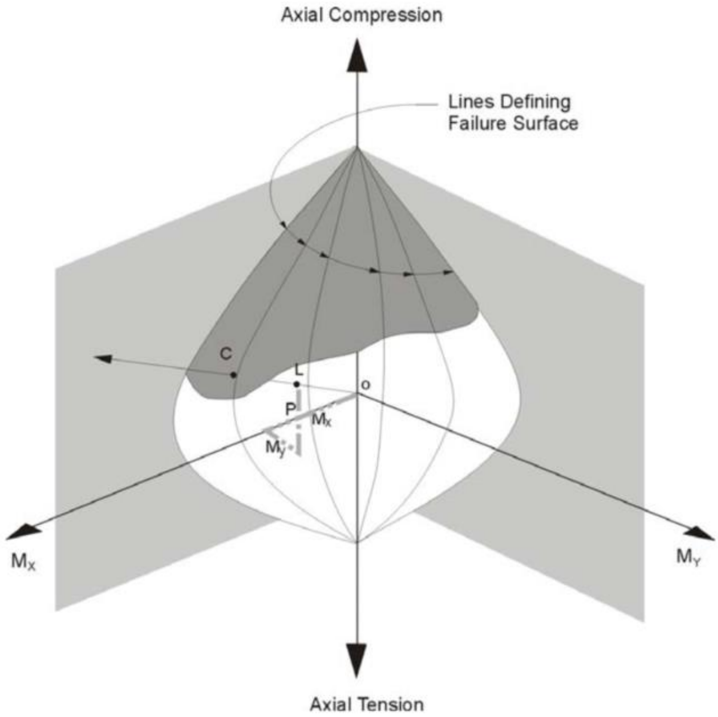

Figure 4.18: Geometric representation of column PMM capacity ratio (CSI, 2020a)

Table 4.9: Sizes of Transfer columns

Model ID	*Transfer Column Size*		*Model ID*	*Transfer Column Size*	
	Square	*Circular*		*Square*	*Circular*
T1ZIIB60	1800 × 1800	1400	T2ZIIB60	1900 × 1900	1500
T1ZIIC60	1800 × 1800	1400	T2ZIIC60	1900 × 1900	1500
T1ZIID60	1800 × 1800	1400	T2ZIID60	1900 × 1900	1500
T1ZIIB100	1800 × 1800	1400	T2ZIIB100	1900 × 1900	1500
T1ZIIC100	1800 × 1800	1400	T2ZIIC100	1900 × 1900	1500
T1ZIID100	1800 × 1800	1400	T2ZIID100	1900 × 1900	1500
T1ZIIB150	2500 × 2500	1800	T2ZIIB150	2100 × 2100	1500
T1ZIIC150	2500 × 2500	1800	T2ZIIC150	2100 × 2100	1500
T1ZIID150	2500 × 2500	1800	T2ZIID150	2100 × 2100	1500

Note: All dimensions are in mm

In this way, PMM capacity ratios are computed for all the transfer columns of eighteen buildings. Table 4.9 shows the details of transfer columns, and Figure 4.19 shows the maximum PMM capacity ratio from a storey one to four. The plot shows that the maximum PMM capacity ratio does not exceed 0.30. This indicates the possibility of column failure in tension. Further, there is no drastic change in PMM demands for buildings of similar height. Hence, the effect of podium configurations (*type* C and D) is not visible. The exact values of PMM capacity ratios are given in Table 4.10.

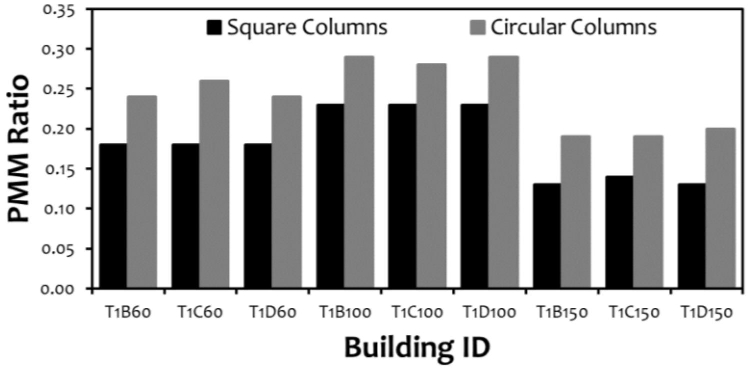

(a) Tower 1

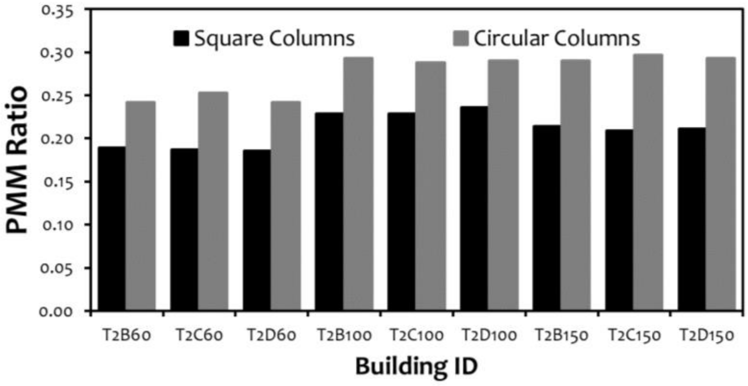

(b) Tower 2

Figure 4.19: Maximum LTHA PMM capacity ratio (storey 1-4) for all buildings

Table 4.10: Maximum LTHA PMM capacity ratio (storey 1-4) for all buildings

Model ID	*Max. PMM Ratio*		*Model ID*	*Max. PMM Ratio*	
	Square	*Circular*		*Square*	*Circular*
T1ZIIB60	0.18	0.24	T2ZIIB60	0.19	0.24
T1ZIIC60	0.18	0.26	T2ZIIC60	0.19	0.25
T1ZIID60	0.18	0.24	T2ZIID60	0.19	0.24
T1ZIIB100	0.23	0.29	T2ZIIB100	0.23	0.29
T1ZIIC100	0.23	0.28	T2ZIIC100	0.23	0.29
T1ZIID100	0.23	0.29	T2ZIID100	0.24	0.29
T1ZIIB150	0.13	0.19	T2ZIIB150	0.21	0.29
T1ZIIC150	0.14	0.19	T2ZIIC150	0.21	0.30
T1ZIID150	0.13	0.20	T2ZIID150	0.21	0.29

4.3.5 *Column Shear Demand/Capacity Ratio*

The shear force demand in transfer columns is usually high owing to the large height of buildings and a limited number of columns. The shear demand to capacity ratio of columns is computed manually by extracting shear demand from various load combinations from software and computing shear capacity as per IS 456 for a given reinforcement detailing. The maximum shear demand to capacity ratio for all columns (square and circular) in the bottom four stories is plotted in Figure 4.20. The maximum value of the shear D/C ratio is 0.387 and 0.505 for buildings of *Tower 1* and *Tower 2*, respectively. Also, for most cases, a slight increase in shear D/C ratio is observed for type C and D buildings compared to *type B.* This indicates that podium configuration slightly alters the lateral force distribution for lower locations. However, it is important to note that the variation in the shear D/C ratio is not large (Table 4.11).

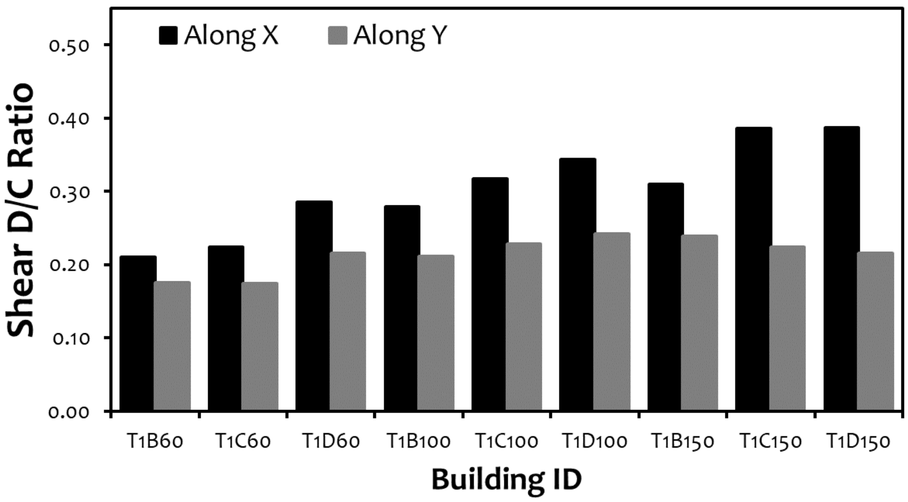

(a) Tower 1

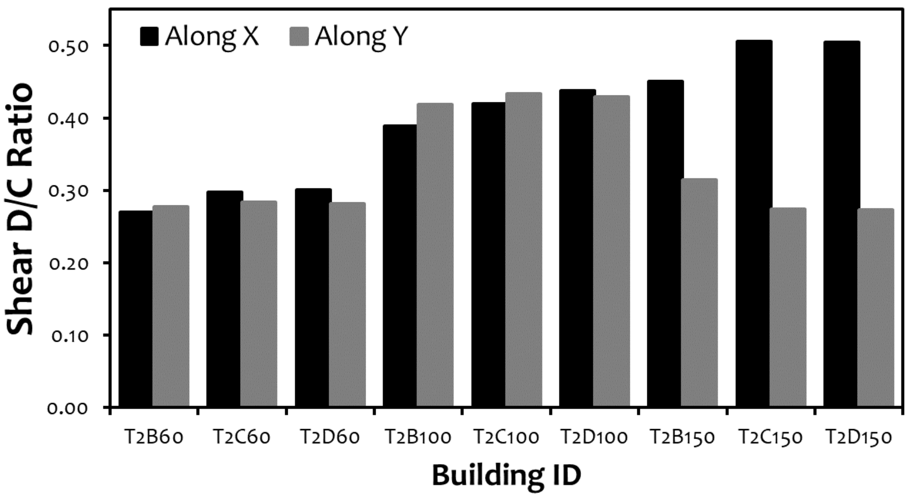

(b) Tower 2

Figure 4.20: Maximum LTHA shear demand/capacity ratio (storey 1-4) for all buildings

Table 4.11: Maximum LTHA shear demand/capacity ratio (storey 1-4) for all buildings

Model ID	Max. Shear D/C Ratio		Model ID	Max. Shear D/C Ratio	
	Square	*Circular*		*Square*	*Circular*
T1ZIIB60	0.211	0.175	T2ZIIB60	0.270	0.278
T1ZIIC60	0.224	0.175	T2ZIIC60	0.298	0.284
T1ZIID60	0.286	0.216	T2ZIID60	0.301	0.282
T1ZIIB100	0.279	0.212	T2ZIIB100	0.389	0.419
T1ZIIC100	0.318	0.229	T2ZIIC100	0.420	0.434
T1ZIID100	0.344	0.242	T2ZIID100	0.438	0.429
T1ZIIB150	0.310	0.239	T2ZIIB150	0.450	0.315
T1ZIIC150	0.386	0.224	T2ZIIC150	0.506	0.275
T1ZIID150	**0.387**	0.216	T2ZIID150	**0.505**	0.274

4.4 Summary

The current chapter deals with assessing eighteen buildings discussed in the previous chapter. The assessment of these buildings is carried out based on LTHA for eleven ground motions (GMs). It is ideal to select ground motions representing the time history experienced by the building at its location. However, the study focuses on zone II, which is spread across a larger region, making it impossible to narrow down the selection to a few ground motions. Moreover, a limited number of Indian earthquakes have been recorded and are publicly available, so significant earthquakes occurring outside India, except for the Bhuj earthquake, were chosen for the study. As IS 1893 does not provide detailed guidelines for spectral matching methods, the ASCE 7-16 guidelines are used to modify the ground motions and make them compatible with the design acceleration spectrum of IS 1893.

These modified ground motions are applied to the lateral direction of buildings at the foundation level. The response of the building is then evaluated using cracked section property, and three global parameters, namely base shear, displacements and inter-storey drift ratio, and two local parameters for transfer columns, namely PMM capacity ratio and shear demand to capacity ratio, are considered as performance indicators of buildings with transfer beams.

After studying several performance indicators, the following salient observations are made:

a) The uniqueness of structural configuration and modification of GMs tailored to the natural periods of each building leads to a varied range of design as well as LTHA base shear. The base shear ratio of LTHA to RSA (design) was found to vary in the range of 0.57-1.19 and 0.53-1.32 for tower 1 and 2 buildings, respectively. However, cracked section property and partial safety factors used in the assessment are believed to take care of the ill effects of increased LTHA base shear demand.

b) The roof displacement for all the buildings is less, indicating that the general performance of buildings is well controlled. Further, similar maximum displacements of buildings with the same height indicate that podium configurations (type C and D) influence is negligible on LTHA displacements.
c) IDR:
    a. The enormous stiffness of the structural wall configuration above the transfer storey and the massive proportions of transfer elements at lower levels can keep IDR value much lower than code specified limits. This was not captured in the displacement profile. Hence, IDR is a better indicator of measuring the effect of podium configuration.
    b. The continuation of more number of structural walls along the Y direction is further able to restrict the IDR profile of buildings along the Y direction compared to X. Hence, a continuation of a few vertical structural walls at strategic locations will help in improving the performance of buildings.
    c. Close observation of the IDR profile only at lower levels to compare IDR values of storeys near the vicinity of transfer storey (storey 4) to reveal the effects of podium configurations indicated that:
        i. For *type B* buildings, the maximum IDR demand is observed to be at one storey below the transfer storey, i.e. at storey 3.
        ii. Increased stiffness of the podium without retaining walls (*type C*) can reduce the difference in IDR of TB level (storey 4) and a level below (podium level = storey 3). Still, in most cases, the IDR demand at the podium level is higher than the IDR demand at the TB level.
        iii. This scenario changes for *type D* buildings where increased stiffness due to retaining wall is shifting maximum IDR demand to TB level (storey 4) for all buildings, except four buildings along the Y direction.
        iv. The amplitude of maximum IDR tends to reduce from configuration *B* to *D*.
d) The PMM capacity ratio for all transfer columns is computed, and based on the suggested literature, it was observed that the demand from LTHA analysis is falling at the lower $1/3^{rd}$ portion of the PMM curve; hence columns have the sufficient reserved capacity to take additional loads. Moreover, the failure of columns will be non-brittle in nature.
e) Shear Demand to Capacity Ratio:

a. The shear demand to capacity ratio in transfer columns is found to reach up to 50%. Which indicates there is still reserved capacity is left.
b. Podium configurations alter the shear demands; however, the variation is insignificant.

Table 4.12: Summary of LTHA results

Parameters	***Overall***	***Effect of Podium Configurations***
Global Parameters:		
Base Shear	No specific pattern	-
Displacements	Overall displacements were less	Negligible effect
IDR	Max. IDR did not cross 1/5th of Code specified limit of 0.2%	The Amplitude of IDR tends to reduce from configuration *B* to *D*
Local parameters for Transfer columns:		
PMM capacity Ratio	Demand from LTHA analysis is falling at the lower 1/3rd portion of the PMM curve	-
Shear demand to capacity ratio	Reached up to 50%	Not significant alteration

…

Chapter 5. Summary, Conclusions and Future Work

5.1 Summary

The present research aimed to evaluate the effect of RC transfer beam on the seismic performance of tall residential buildings located in a low seismic zone (II) of India. The second aim of this study was to evaluate the advantage or disadvantages of constructing podiums in buildings under focus and propose guidelines that could be incorporated into IS 16700. To achieve these goals, eighteen buildings of height 60 to 150m are designed and assessed using widely used finite element commercial software in the structural engineering community of India.

The investigation results indicate that transfer beams essentially introduce mass and stiffness irregularities, which are difficult to alter since they are inherent in such buildings. Although stiffness and mass irregularities can be altered to a certain extent, complete elimination is impossible. Moreover, this configuration can also cause deviation in modal mass and modal period compared to an ideal regular building. While it is difficult to make a generalized statement about the relation between natural period and modal mass from the current study, it was found that the difference between the least lateral fundamental lateral period and torsion period tends to decrease with an increase in the height of the tower or attachment of podiums with retaining walls. Furthermore, most buildings in the current sample had 65% of modal mass participation in the first three modes, indicating the absence of irregular oscillation modes in the two principal plan directions.

The study used the amplitude of roof displacements, maximum inter-storey drift ratios, and base shear values obtained from linear time history assessment was used as indicators of seismic performance. The roof displacements and maximum inter-storey drifts were well within the limiting values prescribed by the code for irregular buildings. Furthermore, the base shear due to various ground motions increased by 30% for a couple of buildings. Despite this variation in base shear, the buildings performed well.

The performance of transfer columns supporting transfer beams was studied in detail by observing the PMM capacity ratio and shear demand to capacity ratio. The maximum PMM capacity ratio was found to be no not more than 0.30, and all the LTHA demands were found to be sitting on the lower one-third portion of the PMM curve. Another observation that emerged from this study is that the shear demand to capacity ratio reached about 0.5 for columns supporting the transfer. This finding suggests that shear force governs the fixing dimensions of columns.

The study could not meet the aim of developing a concise analysis and design provisions that can be directly incorporated into the IS 16700. The reason being even after getting qualified for several irregularities, the building performance was found to be satisfactory under LTHA; hence, the need to revise code defined limits got eliminated. Further, limited access to data of actual plans of such configuration and the amount of computation time that goes for analysis and design of buildings additional buildings were not added in this work.

5.2 Significant Observations and Conclusions

The following conclusions can be drawn from the present study:

1) Analysis:
    a. Complete elimination of stiffness irregularity by bringing the stiffness difference between two consecutive floors to less than 30% is quite challenging. However, continuing a few structural walls other than the core walls down to the foundation level will be beneficial.
    b. The contribution of stiffness increase due to *type C* is relatively less. A significant increase in stiffness occurs when *type D* configuration is present. However, the percentage of increase in stiffness depends on the number and orientation of walls continuing from the top to the foundation.
    c. Mass irregularity occurs between level below TB level and TB level due to a large mass of TB level due to TB. If necessary, this irregularity can be eliminated by modelling podium configurations.
2) LTHA behaviour:
    a. The increase in base shear demand due to LTHA did not cause any significant change in performance parameters such as displacements and IDR.
    b. Building displacements are minimal, and the effect of podium configurations on displacements is insignificant.
    c. IDR demands are also well within the code specified limits. Further, IDR can better capture the influence of podium configuration in a better manner. The amplitude of maximum IDR tends to reduce from configuration *B* to *D*.
    d. The transfer column PMM capacity ratios are in the interaction curve's lower third, indicating column failure's non-brittle nature.
    e. The effect of podium configurations on transfer column shear demand to capacity ratio is insignificant, and up to 50-60% of shear capacity is reserved for transfer columns.
3) Design Provisions:

a. Even after qualifying for several irregularities, the building performance was satisfactory under LTHA, thus eliminating the need to revise the code limits for inter storey drift ratio.

4) Other:
   a. Residential buildings with RC transfer beams can perform well in seismic zone II when all analysis and design criteria are properly followed.
   b. The impact of podium configurations (*Type C* and *Type D*) on the seismic resistance of buildings is negligible. Thus, architects and structural engineers can choose whether or not to include a separation joint based solely on functional and execution requirements.

5.3 Significance of the findings

1) The insights gained from this study could assist the Bureau of Indian Standards (BIS) and building approval body at the municipal/town level in improving building codes and bylaws, which permit the construction of residential buildings with floating members in seismic zone II. Further, allowing such buildings in the lower seismic zone will promote development in seismic zone II and prevent them from being built in higher seismic zones (III-V).
2) The present study lays the groundwork for future research on assessing and retrofitting existing buildings with transfer stories located in zones III to V, which is a significant step toward building a seismically resilient city.
3) The present study has advanced our understanding of infrastructure development while ensuring seismic safety, creating a new possibility for constructing buildings above railway stations located in seismic zone II across the country. These buildings can be used as railway passenger lounges, railway operation offices, railway booking counters and can be rented or sold as commercial space.

5.4 Scope for future work

The following are some potential areas for future research:

1) Investigating the local behaviour of individual members and their interaction with each other should be a priority. This could involve experimental work to explore the stress and deformation within transfer beams, as well as the effect of the deformation of the transfer beam on the floating members and transfer columns and walls. Additionally, determining the values of cracked RC section properties for transfer elements would also be helpful.

2) Since the current study was limited to buildings in seismic zone II, future research could assess the performance of such buildings in seismic zone III to V. Additionally, the effect of vertical ground motion, which was not considered in zone II buildings, could be studied.
3) The study could also be extended to include detailed information on existing building stock with transfer beams constructed for functional utility beyond residential purposes. More broadly, research is also needed to determine the performance of transfer elements made from steel and composite materials.

…

References

Abdelbasset, Y. M., Sayed-Ahmed, E. Y., & Mourad, S. A. (2014). High-Rise Buildings with Transfer Floors: Drift Calculations. *IABSE Symposium Report*, *102*(35), 637–644. https://doi.org/10.2749/222137814814028278

Abdlebasset, Y. M., Sayed-Ahmed, E. Y., & Mourad, S. A. (2016). High-rise buildings with transfer floors: Linear versus nonlinear seismic analysis. *Electronic Journal of Structural Engineering*, *16*(1), 8–16.

Abdlebasset, Y., Sayed-Ahmed, E., & Mourad, S. (2016). Inter-Storey Drift and Seismic Response of High-Rise Buildings with Transfer Slabs. *Journal of Al-Azhar University Engineering Sector*, *11*(40), 913–926. https://doi.org/10.21608/auej.2016.19414

Ahmed, N. (2020). *The Chedi Mumbai - a GHM Hotel*. https://goo.gl/maps/Aer3Bmm6YTRBkaBD6

Ahn, B., Kang, T. H.-K., Kang, S.-M., & Yoon, J. K. (2020). Punching Shear Stress in Post-Tensioned Transfer Plate of Multi-Story Buildings. *Applied Sciences*, *10*(17), 6015. https://doi.org/10.3390/app10176015

Arnold, C. (1984). Building configuration The architecture of seismic design. *Bulletin of the New Zealand Society for Earthquake Engineering*, *17*(2), 83–89. https://doi.org/10.5459/bnzsee.17.2.83-89

ASCE 7-16, S. (2016). ASCE STANDARD ASCE/SEI 7-16 Minimum Design Loads and Associated Criteria for Buildings and Other Structures. In *ANSI/ASCE Standard* (Issue 7 98). American Society of Civil Engineers.

Balasubramanian, K., & Jaya, K. P. (2022). *Reverse Cyclic Loading Effect on RCC Wall-Floor Slab-Deep Beam Connection*. https://doi.org/10.1155/2022/8497173

Balasuriya, S. S., Bandara, K. M. K., Ekanayake, S. D., & Jayasinghe, M. T. R. (2007). The Influence of Transfer Plates on the Lateral Behaviour of Apartment Buildings. *Engineer: Journal of the Institution of Engineers, Sri Lanka*, *40*(4), 22. https://doi.org/10.4038/engineer.v40i4.7150

Carpenter, L. D., Naeim, F., Lew, M., Youssef, N. F., Rojas, F., Saragoni, G. R., & Adaros, M. S. (2011). Performance of tall buildings in Viña del Mar in the 27 February 2010 offshore Maule, Chile earthquake. *The Structural Design of Tall and Special Buildings*, *20*(1), 17–36. https://doi.org/10.1002/tal.672

Colaco, J. P., Dravid, G., & Kasliwal, V. (2012). The design and construction of the Palais Royale, Mumbai, India. *CTBUH 2012 9th World Congress*, 687–692.

Computer and Structures Inc. (2020). *ETABS: Analysis Reference Manual* (19.1.0). Computer and Structure Inc.

Coull, A. (1966). Composite action of walls supported on beams. *Building Science*, *1*(4), 259–270. https://doi.org/10.1016/0007-3628(66)90001-6

CSI. (2020a). *Concrete Frame Design Manual IS 456:2000 For ETABS*.

CSI. (2020b). *Shear Wall Design Manual IS 456:2000 and IS 13920:1993 For ETABS*.

Deshpande, H. (2023, January 9). How Fast-Tracking Of Redevelopment Projects Brought Haze To Mumbai's Skyline, Displacement To People's Lives. *Outlook*. https://www.outlookindia.com/national/how-fast-tracking-of-redevelopment-projects-brought-polluting-haze-to-mumbai-skyline-displacement-to-people-lives-news-252271

El-Abbasya, A. A., Sharaky, I. A., & Sallam, H. (2017). Misuse of transfer plate / floor concept in the traditional buildings in KSA. *International Engineering Conference and Exhibition IECE*.

Elassaly, M., & Nabil, M. (2017). Seismic Damage Assessment of RC Building with The Transfer Slab System. *WIT Transactions on the Built Environment*, *172*, 83–95. https://doi.org/10.2495/ERES170081

Elawady, A. K., Okail, H. O., Abdelrahman, A. A., & Sayed-Ahmed, E. Y. (2014). Seismic behaviour of high-rise buildings with transfer floors. *Electronic Journal of Structural Engineering*, *14*(January), 57–70.

FEMA 454. (2006). Designing for Eartqhuakes A Manual for Architects. In *FEMA* (Issue December).

Gampathi, G. A. P., & Peiris, P. P. P. (2010). Computer Aided Design of Modern High-Rise Building. *Engineer: Journal of the Institution of Engineers, Sri Lanka*, *43*(3), 57. https://doi.org/10.4038/engineer.v43i3.6975

GB18306-2001. (2001). *Seismic Ground Motion Parameter Zonation Map of China*. China National Standards.

GoI. (2015a). *About Smartcities*. https://smartcities.gov.in/about-the-mission

GoI. (2015b). *Pradhan Mantri Awas Yojana – Urban*. https://pmay-urban.gov.in/about

GoI. (2021). *Light House Project*. https://ghtc-india.gov.in/Content/LHP.html

Green, D. R. (1972). The interaction of solid shear walls and their supporting structures. *Building Science*, *7*(4), 239–248. https://doi.org/10.1016/0007-3628(72)90005-9

Gwalani, P., Singh, Y., & Varum, H. (2023). Seismic vulnerability of reinforced concrete buildings with discontinuity in columns. *Earthquake Engineering & Structural Dynamics*, *52*(1), 204–225. https://doi.org/10.1002/eqe.3757

Hindustan Times. (2016). *Vashi Station image having transfer beam*. https://www.hindustantimes.com/mumbai-news/emr-outside-vashi-station-to-be-ready-by-january-2017/story-LKaG0HO3SxnryHnRU1VzsO.html

HK Buildings Department. (2020). *Code of Practice for Structural Use of Concrete 2013 (2020 Edition)* (2020 Editi). Buildings Department. https://www.bd.gov.hk/doc/en/resources/codes-and-references/code-and-design-manuals/OldVersions/CoP_Concrete_ov.zip

Ho, Y. B. (2009). *Seismic Vulnerability Assessment of Tall Buildings with Transfer Storeys* [PhD Thesis]. The Hong Kong University of Science and Technology.

Huynh, T., & Panahshahi, N. (2020). Seismic Performance of Transfer Story Reinforced Concrete Buildings. *The 17th World Conference on Earthquake Engineering*.

IS 456:2000. (2000). *Plain and Reinforced Concrete - Code of Practice*. Bureau of Indian Standards (BIS).

IS 875 (Part 1) : 1987. (1987). *Code of Practice for Design Loads (Other Than Earthquake) for Buildings and Structures Part 1 Dead Loads - Unit Weights of Building Materials and Stored Materials [Reaffirmed 2003]* (Reaffirmed 2003). Bureau of Indian Standards.

IS 875 (Part 2) : 1987. (1987). *Code of Practice for Design Loads (Other Than Earthquake) for Buildings and Structures Part 2 Imposed Loads [Reaffirmed 2003]* (Reaffirmed 2003). Bureau of Indian Standards.

IS 875 (Part 3) : 2015. (2015). *Design Loads (Other than Earthquake) for Buildings and Structures - Code of Practice part 3 Wind Loads* (Third Revi, Vol. 875, Issue April). Bureau of Indian Standards (BIS).

IS 1893(Part 1):2016. (2016). *Criteria for Earthquake Resistant Design of Structures Part 1 General Provision and Buildings*. Bureau of Indian Standards (BIS).

IS 13920:2016. (2016). *Ductile Design and Detailing of Reinforced Concrete Structures Subjected to Seimsic Forces - Code of Practice*. Bureau of Indian Standards (BIS).

IS 16700. (2017). *Criteria for Structural Safety of Tall Concrete Buildings*. Bureau of Indian Standards (BIS).

IS 16700. (2023). *Criteria for Structural Safety of Tall Concrete Buildings*. Bureau of India Standards (BIS) .

Jayasinghe, M. T. R., Hettiarachchi, D. S., & Gunawardena, D. S. R. T. N. (2012). Performance of Tall Buildings with and without Transfer Plates under Earthquake Loading. *Engineer: Journal of the Institution of Engineers, Sri Lanka*, *45*(2), 13–22. https://doi.org/10.4038/engineer.v45i2.6937

Jeong, S. Y., Kang, T. H. K., Yoon, J. K., & Klemencic, R. (2020). Seismic performance evaluation of a tall building: Practical modeling of surrounding basement structures. *Journal of Building Engineering*, *31*(April), 101420. https://doi.org/10.1016/j.jobe.2020.101420

JGJ 3-2010 China. (2010). *Technical Specification for Concrete Structures of Tall Building*. Ministry of Housing and Urban-Rural Development of the People's Republic of China.

Kuang, J. S., & Li, S. (2001). Interaction-based design tables for transfer beams supporting in-plane loaded shear walls. *The Structural Design of Tall Buildings*, *10*(2), 121–133. https://doi.org/10.1002/tal.171

Kuang, J. S., & Li, S. (2005). Interaction-Based Design Formulas for Transfer Beams: Box Foundation Analogy. *Practice Periodical on Structural Design and Construction*, *10*(2), 127–132. https://doi.org/10.1061/(ASCE)1084-0680(2005)10:2(127)

Kuang, J. S., & Puvvala, J. (1996). Continuous transfer beams supporting in-plane loaded shear walls in tall buildings. *The Structural Design of Tall Buildings*, *5*(4), 281–293. https://doi.org/10.1002/(SICI)1099-1794(199612)5:4<281::AID-TAL79>3.0.CO;2-P

LATBSDC. (2017). *An Alternative Procedure for Seismic Analysis and Design of Tall Buildings Located in the Los Angeles Region*.

Li, C. S. (2005). *Response of Transfer Plate When Subjected to Earthquake* [PhD Thesis]. The Hong Kong Polytechnic University.

Li, C. S., Lam, S. S. E., Zhang, M. Z., & Wong, Y. L. (2006). Shaking Table Test of a 1:20 Scale High-Rise Building with a Transfer Plate System. *Journal of Structural Engineering*, *132*(11), 1732–1744. https://doi.org/10.1061/ASCE0733-94452006132:111732

Li, J. H., Su, R. K. L., Chandler, A. M., & Lam, N. T. K. (2002). Seismic assessment of low-rise building with transfer structure. In *Advances in Building Technology* (Vol. 1, pp. 747–754). Elsevier. https://doi.org/10.1016/B978-008044100-9/50094-2

Li, S. (2000). *Transfer Beams Supporting In-plane Loaded Shear Walls in Tall Buildings* [Master of Philosophy in Civil Engineering]. The Hong Kong University of Science and Technology.

Looi, D. T. W., & Su, R. K. L. (2018). Seismic axial collapse of short shear span RC shear walls above transfer structure. *IOP Conference Series: Materials Science and Engineering*, *431*(12), 122005. https://doi.org/10.1088/1757-899X/431/12/122005

Lu, X., Chen, Y., & Mao, Y. (2012). Shaking table model test and numerical analysis of a supertall building with high-level transfer storey. *The Structural Design of Tall and Special Buildings*, *21*(10), 699–723. https://doi.org/10.1002/tal.632

Murty, C. V. R., Goswami, R., Vijayanarayanan, A. R., & Mehta, V. v. (2012). *Some Concepts in Earthquake Behaviour of Buildings*. Gujarat State Disaster Management Authority.

Mwafy, A., & Khalifa, S. (2017). Effect of vertical structural irregularity on seismic design of tall buildings. *The Structural Design of Tall and Special Buildings*, *26*(18), e1399. https://doi.org/10.1002/tal.1399

NDMA GoI. (2021). *NDMA Annual Report 2020-2021*.

O. El-Mahdy, O., M. Refat, H., M. Abd El-Salamc, A., & Z. El-Bayome, E.-S. (2022). Towards Seismic Performance of Tall Buildingswith Transfer Floors. *Engineering Research Journal - Faculty of Engineering (Shoubra)*, *51*(1), 56–72. https://doi.org/10.21608/erjsh.2022.224292

Osman, A., & Azim, M. ohamed A. (2015). Analysis and Behavior of High-rise Buildings with Transfer Plate System. *13th Arab Structural Engineering Conference*, *December*.

Osman, A., & Saad, T. (2015). Progressive Collapse in High-rise Buildings with Transfer Plate System. *14th International Conference on Structural & Geotechnical Engineering, ICSGE2015*, *December*.

PIB Delhi. (2022, December 27). *Amrit Bharat Station Scheme for Indian Railways*. https://pib.gov.in/PressReleasePage.aspx?PRID=1886884

PIB Delhi. (2023, February 8). *1275 railway stations have been identified under Amrit Bharat Station scheme*. Minister of Railways, Communications and Electronic &

Information Technology, Shri Ashwini Vaishnaw. https://pib.gov.in/PressReleaseIframePage.aspx?PRID=1897382

Puvvala, J. (1996). *Analysis and Behaviour of Transfer Girder Systems in Tall Buildings* [Master of Philosophy in Civil and Structural Engineering]. The Hong Kong University of Science and Technology .

Ramancharla, P. K., & Murty, C. V. R. (2014). Earthquake Safety of Houses in India: Understanding the Bottlenecks in Implementation. *Indian Concrete Journal*, *88*(9), 51–63.

Ribeiro, G., Almeida, J., & Lobo, P. (2022). Analysis and construction of transfer structures: a case study. *Procedia Structural Integrity*, *37*(C), 89–96. https://doi.org/10.1016/j.prostr.2022.01.063

Ribeiro, G. X. S. (2018). *Structural Design of Transfer Structures* (Issue November). Tecnico Lisboa.

R.K.L. Su. (2008). Seismic Behaviour of Buildings with Transfer Structures in Low-to-Moderate Seismicity Regions. *Electronic Journal of Structural Engineering*, *01*, 99–109. https://doi.org/10.56748/ejse.9001

Seismosoft. (2020). *SeismoMatch* (2020).

Shan, Z., Looi, D. T. W., Cheng, B., & Su, R. K. L. (2020). Simplified seismic axial collapse capacity prediction model for moderately compressed reinforced concrete shear walls adjacent to transfer structure in tall buildings. *The Structural Design of Tall and Special Buildings*, *29*(12), e1752. https://doi.org/10.1002/tal.1752

SP 16. (1980). *Design Aids for Reinforced Concrete to IS 456:1978*. Bureau of Indian Standards (BIS).

Su, R. K. L. (2019). *Reference Materials on Seismic Detailing for Concrete Buildings in Hong Kong*. Construction Industry Council. http://www.cic.hk/files/page/148/CIC_Reference Materials_Ray SU.pdf

Su, R. K. L., & Cheng, M. H. (2009). Earthquake-induced shear concentration in shear walls above transfer structures. *The Structural Design of Tall and Special Buildings*, *18*(6), 657–671. https://doi.org/10.1002/tal.458

Su, R. K. L. K. L., Chandler, A. M. M., Li, J. H. H., & Lam, N. T. K. T. K. (2002). Seismic assessment of transfer plate high rise buildings. *Structural Engineering and Mechanics*, *14*(3), 287–306. https://doi.org/10.12989/sem.2002.14.3.287

Tang, T. O., & Su, R. K. L. (2015). Gravity-induced shear force in reinforced concrete walls above transfer structures. *Proceedings of the Institution of Civil Engineers - Structures and Buildings*, *168*(1), 40–55. https://doi.org/10.1680/stbu.13.00092

TBI. (2017). *Guidelines for Performance-Based Seismic Design of Tall Buildings* (Issue May).

Velani, P. D., & Ramancharla, P. K. (2023). Approximate natural period expression for reinforced concrete tall buildings in India. *Current Science*, *124*(12), 1412–1421.

VRSCCL. (2019). *Vashi Railway Station Building from outside*. https://vrsccl.com/assets/img/slides/nivo/01_r1.JPG

Wikimedia Foundation. (2005). https://commons.wikimedia.org/wiki/Category:1971_San_Fernando_earthquake#/media/File:USGS_-_1971_San_Fernando_earthquake_-_Olive_View_Hospital_-_Detached_stairways.jpg

Yacoubian, M., Lam, N., Lumantarna, E., & Wilson, J. (2016). Seismic performance of high-rise buildings featuring a transfer plate taking into account displacement-controlled behaviour. *Australian Earthquake Engineering Society 2016 Conference*, 1–13.

Yacoubian, M., Nelson, T. K., & Lumantarna, E. (2018). Simplified Design Checks for Buildings with a Transfer Structure in Regions of Low Seismicity. In T. K. Nelson & T.-M. Chan (Eds.), *Design of Buildings and Structures in Low to Moderate Seismicity Regions* (pp. 113–140).

Zhang, Z. (2000). *Analysis and Behaviour of Transfer Plate-Shear Wall Systems* [Master of Philosophy in Civil Engineering]. The Hong Kong University of Science and Technology .

Zhou, X., & Xu, Y. L. (2007). Multi-hazard performance assessment of a transfer-plate high-rise building. *Earthquake Engineering and Engineering Vibration*, *6*(4), 371–382. https://doi.org/10.1007/s11803-007-0780-9

Appendix A. Details of Analysis and Design of Tall Buildings

A.1 Building Plans

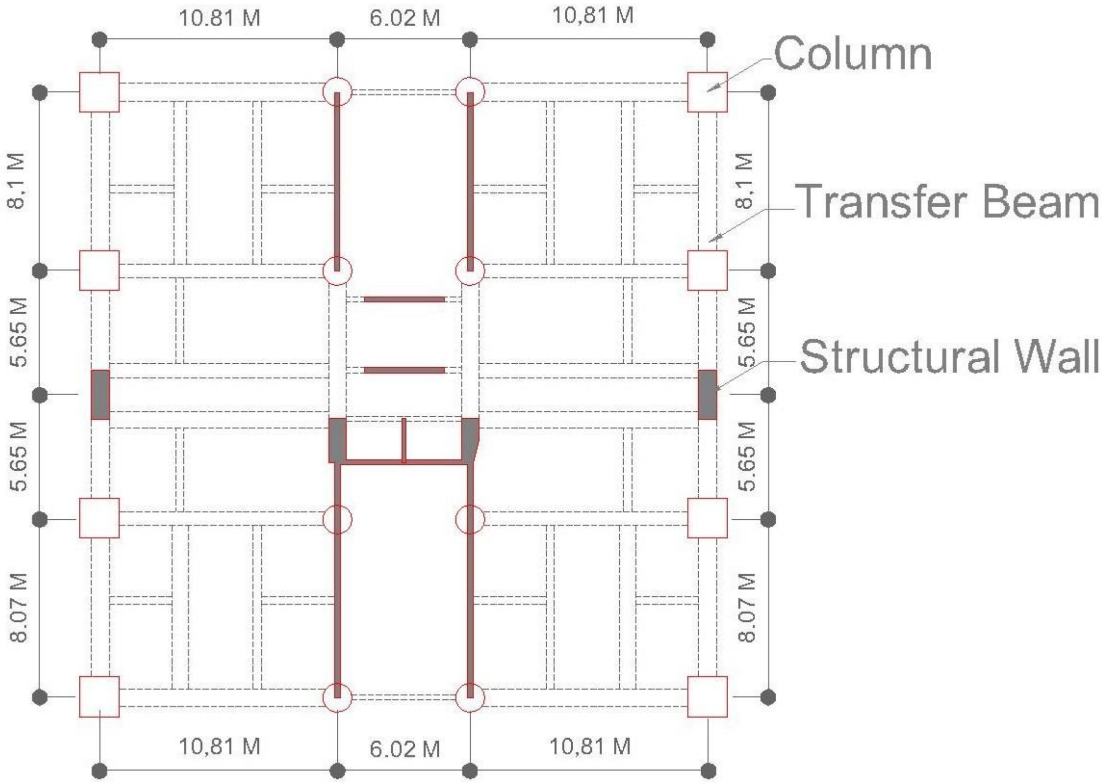

Figure A.1: Structural layout of transfer storey for Tower 1

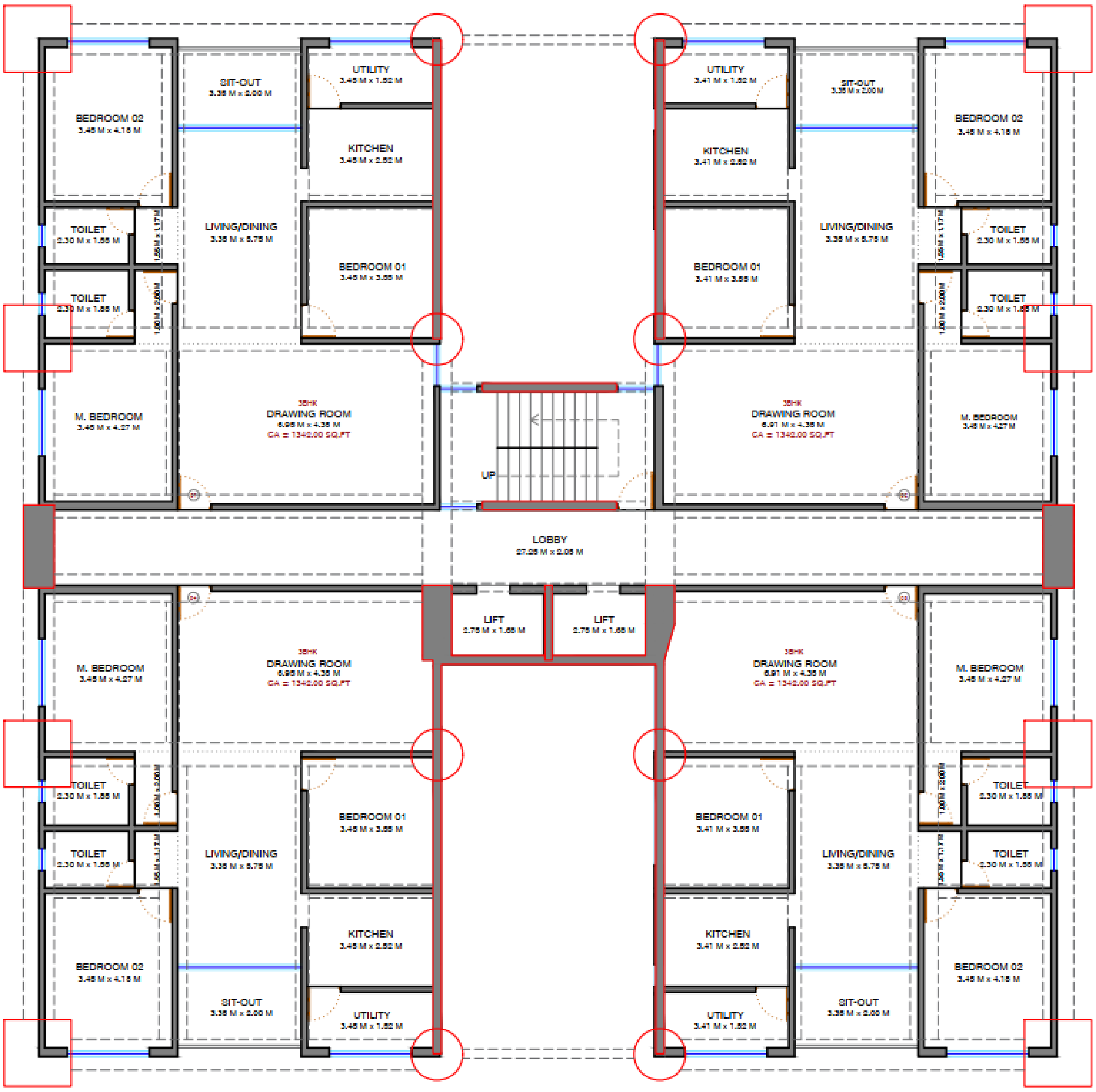

Figure A.2: Structural layout and architectural plan of tower 1

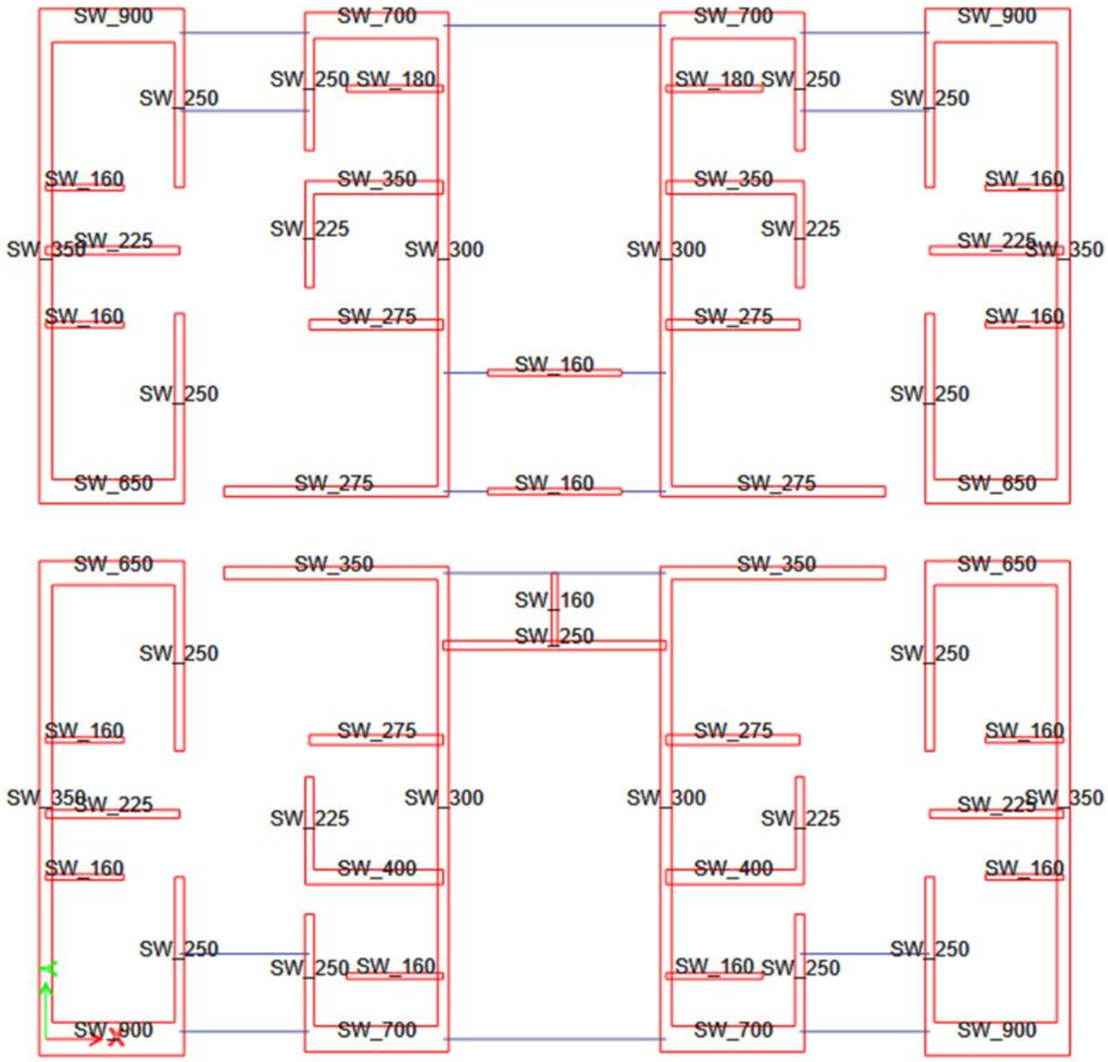

Figure A.3: Typical floor layout of a numerical model showing location of structural walls and beam of tower 1

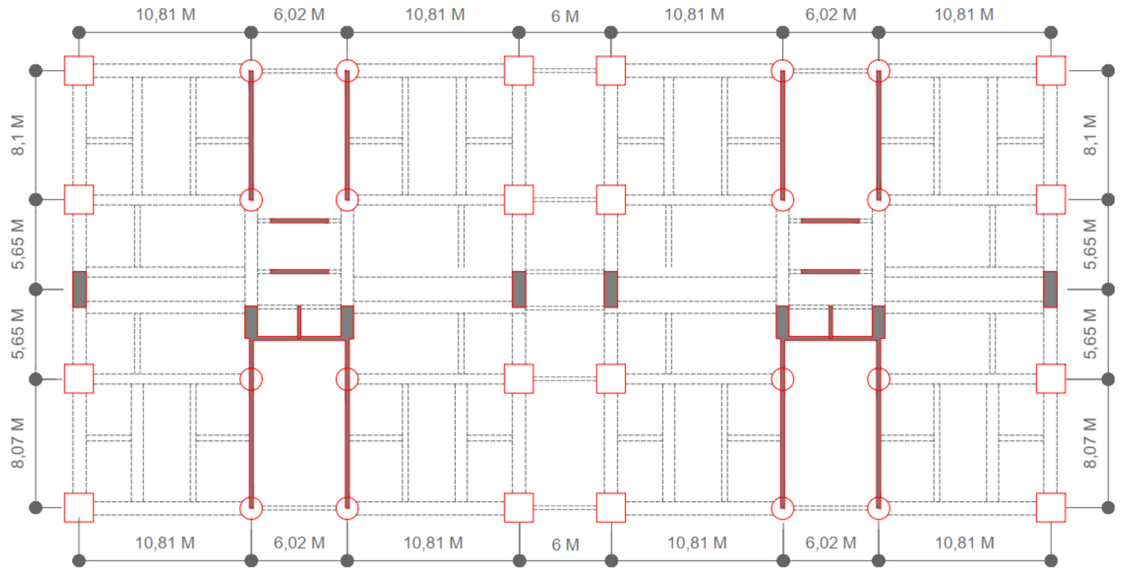

Figure A.4: Structural layout of transfer storey for Tower 2

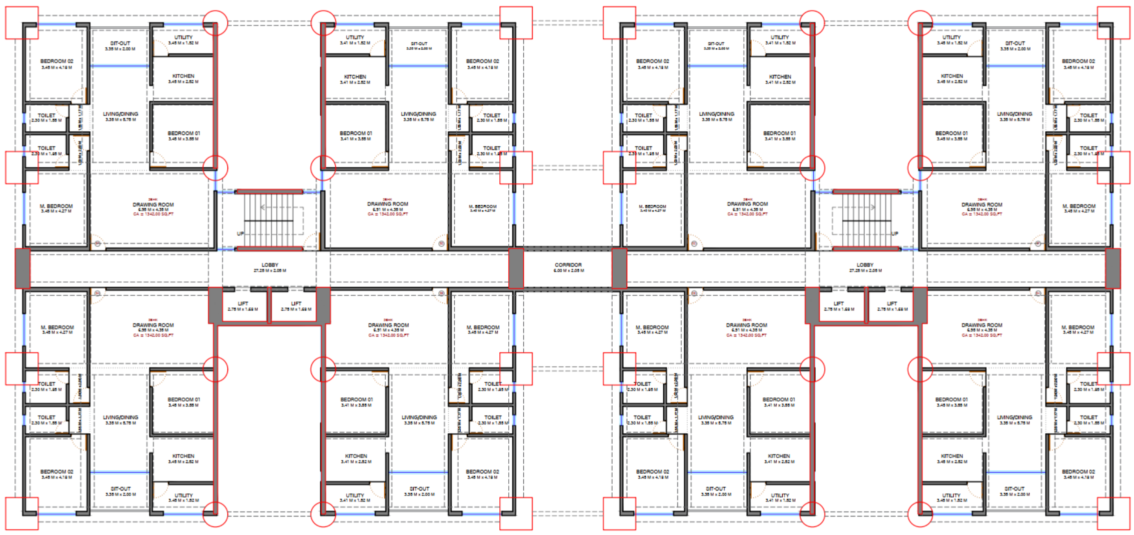

Figure A.5: Structural layout and architectural plan of tower 2

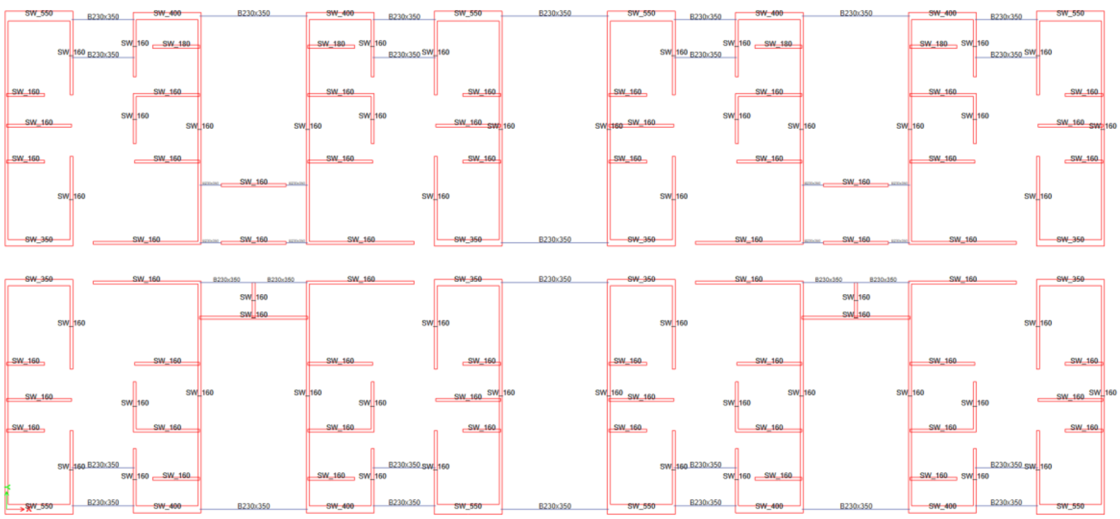

Figure A.6: Typical floor layout of a numerical model showing location of structural walls and beam of tower 2

A.2 Element sizes

Table A.1: Story wise Beam sizes in all buildings

Model ID	***Storey***		
	1 to 3	***4***	***5 and above***
T1ZIIB60	B230x350 FB375x700 FB450x700	B230x350 TGP600x1400 TGP750x1400 TGP800x2100 TGS 300x400 TGS2 600x1100	B230x350
T1ZIIC60	B230x350 FB375x700 FB450x700	B230x350 TGP600x1400 TGP750x1400 TGP800x2100 TGS 300x400 TGS2 600x1100	B230x350
T1ZIID60	B230x350 FB375x700 FB450x700	B230x350 TGP600x1400 TGP750x1400 TGP800x2100 TGS 300x400 TGS2 600x1100	B230x350
T1ZIIB100	B230x350 FB375x700	B230x350 TGP600x1400 TGP750x1400 TGP800x2100 TGS 300x400 TGS2 600x1100	B230x350
T1ZIIC100	B230x350 B250x350 FB375x700	B230x350 B250x350 TGP600x1400 TGP750x1400 TGP800x2100 TGS 300x400 TGS2 600x1100	B230x350 B250x350
T1ZIID100	B230x350 B250x350 FB375x700	B230x350 B250x350 TGP600x1400	B230x350 B250x350

Model ID	Storey		
	1 to 3	4	5 and above
		TGP750x1400 TGP800x2100 TGS 300x400 TGS2 600x1100	
T1ZIIB150	B230x350 FB375x700	B230x350 TGP750x1400 TGP800x1600 TGP900x2300 TGS 400x500 TGS2 750x1300	B230x350
T1ZIIC150	B230x350 B250x350 FB375x700	B230x350 B250x350 TGP750x1400 TGP800x1600 TGP900x2300 TGS 400x500 TGS2 750x1300	B230x350 B250x350
T1ZIID150	B230x350 B250x350 FB375x700	B230x350 B250x350 TGP750x1400 TGP800x1600 TGP900x2300 TGS 400x500 TGS2 750x1300	B230x350 B250x350
T2ZIIB60	B230x350 B250x350 FB375x600 FB375x700 FB400x750 FB400x800	B230x350 B250x350 TGP1000x2000 TGP1000x2200 TGP750x1200 TGP800x1400 TGP800x1600 TGP900x1900 TGP900x2100 TGS 350x450 TGS2 750x900	B230x350 B250x350
T2ZIIC60	B230x350	B230x350	B230x350

Model ID	Storey		
	1 to 3	4	5 and above
	B250x350	B250x350	B250x350
	B250x400	B250x400	B250x400
	FB375x600	TGP1000x2000	
	FB375x700	TGP1000x2200	
	FB400x750	TGP750x1200	
		TGP800x1400	
		TGP800x1600	
		TGP900x1900	
		TGP900x2100	
		TGS 350x450	
		TGS2 750x900	
T2ZIID60	B230x350	B230x350	B230x350
	B250x350	B250x350	B250x350
	B250x400	B250x400	B250x400
	FB375x600	TGP1000x2000	
	FB375x700	TGP1000x2200	
	FB400x750	TGP750x1200	
		TGP800x1400	
		TGP800x1600	
		TGP900x1900	
		TGP900x2100	
		TGS 350x450	
		TGS2 750x900	
T2ZIIB100	B230x350	B230x350	B230x350
	B250x350	B250x350	B250x350
	FB375x600	TGP1000x1800	
	FB375x700	TGP1000x2000	
		TGP1000x2400	
		TGP750x1000	
		TGP800x1200	
		TGP800x1400	
		TGP900x1700	
		TGP900x1900	
		TGS 350x450	
		TGS2 400x850	
		TGS2 750x800	
T2ZIIC100	B230x350	B230x350	B230x350
	B250x350	B250x350	B250x350
	FB375x600	TGP1000x1800	

Model ID	Storey		
	1 to 3	4	5 and above
	FB375x700	TGP1000x2000	
		TGP1000x2400	
		TGP750x1000	
		TGP800x1200	
		TGP800x1400	
		TGP900x1700	
		TGP900x1900	
		TGS 350x450	
		TGS2 750x800	
T2ZIID100	B230x350	B230x350	B230x350
	B250x350	B250x350	B250x350
	FB375x600	TGP1000x1800	
	FB375x700	TGP1000x2000	
		TGP1000x2400	
		TGP750x1000	
		TGP800x1200	
		TGP800x1400	
		TGP900x1700	
		TGP900x1900	
		TGS 350x450	
		TGS2 750x800	
T2ZIIB150	B230x350	B230x350	B230x350
	B250x350	B250x350	B250x350
	FB375x600	TGP1000x2200	
	FB375x700	TGP1000x2400	
		TGP1300x2800	
		TGP750x1400	
		TGP800x1400	
		TGP800x1600	
		TGP900x1700	
		TGP900x2100	
		TGP900x2300	
		TGS 350x500	
		TGS 400x500	
		TGS2 400x850	
		TGS2 750x1100	

Model ID	Storey		
	1 to 3	*4*	*5 and above*
T2ZIIC150	B230x350 B250x350 FB375x600 FB375x700	B230x350 B250x350 TGP1000x2200 TGP1000x2400 TGP1100x2300 TGP750x1400 TGP750x1500 TGP800x1500 TGP800x1600 TGP900x1700 TGP900x2100 TGP900x2200 TGP900x2300 TGS 350x500 TGS2 750x1100	B230x350 B250x350
T2ZIID150	B230x350 B250x350 FB375x600 FB375x700 FB375x600 FB375x700	B230x350 B250x350 TGP1000x2200 TGP1000x2400 TGP1100x2300 TGP750x1400 TGP800x1600 TGP900x1700 TGP900x2100 TGP900x2300 TGS 350x500 TGS2 750x1100	B230x350 B250x350

Note:

1. *All dimensions are in mm*
2. *FB: Floor Beam; B=Beam; TGP = Transfer Girder Primary; TGS = Transfer Girder Secondary;*
3. *E.g. FB375 ×600 indicates Floor beam of size 375mm width and 600mm depth*

Table A.2: Structural walls thickness

Model ID	*Storey*	*Wall thickness (mm)*
T1ZIIB60	1 to 4	160, 225, 250, 800
	5 to 7	160, 200, 250, 350
	8 & beyond	160
T1ZIIC60	1 to 4	160, 225, 250, 300, 800

Model ID	*Storey*	*Wall thickness (mm)*
	5 to 7	160, 200, 250, 300, 400
	8 & beyond	160
T1ZIID60	1 to 4	160, 225, 250, 800
	5 to 7	160, 200, 250, 350
	8 & beyond	160
T1ZIIB100	1 to 4	160, 200, 225, 250, 800
	5 to 11	160, 200, 225, 250, 300, 400, 500
	11 & beyond	160
T1ZIIC100	1 to 4	160, 225, 250, 300, 800
	5 to 10	160, 200, 250, 300, 400, 500
	10 & beyond	160
T1ZIID100	1 to 4	160, 225, 250, 300, 800
	5 to 10	160, 200, 250, 300, 400, 500
	10 & beyond	160
T1ZIIB150	1 to 4	225, 300, 350, 450, 500, 550, 800, 1000,1200
	5 to 13	160, 180, 200, 225, 250, 275, 300, 400, 450, 500, 550, 600, 650, 700, 800, 850, 900
	14 & beyond	160
T1ZIIC150	1 to 4	225, 300, 350, 450, 550, 800,1000
	5 to 13	160, 180, 200, 225, 250, 300, 350, 400, 450, 500, 550, 600, 700, 800, 850, 900
	14 & beyond	160
T1ZIID150	1 to 4	225, 300, 350, 500, 550, 800, 1000, 1200
	5 to 13	160, 180, 200, 225, 250, 275, 300, 350, 400, 450, 500, 550, 600, 650, 700, 800, 850, 900
	14 & beyond	160

A.3 Modal Analysis Results

Table A.3: Modal Analysis results for T1ZIIB60

Mode		*X Period*	*Modal Mass (%)*		*Y Period*	*Modal Mass (%)*		*T Period*	*Modal Mass (%)*
1	X1	1.072	65.66	Y1	0.691	60.08	T1	0.759	72.85
2	X2	0.355	21.90	Y2	0.200	26.97	T2	0.287	16.09
3	X3	0.158	02.44	Y3	0.097	02.34	T3	0	0
4	X4	0.098	00.53	Y4	0.083	01.31	T4	0	0
5	X5	0.077	04.58	Y5	0.058	02.67	T5	0	0
6	X6	0.040	03.16	Y6	0.047	03.62	T6	0	0
		Total	98.27			96.99			88.94

Table A.4: Modal Analysis results for T1ZIIC60

Mode		*X Period*	*Modal Mass (%)*		*Y Period*	*Modal Mass (%)*		*T Period*	*Modal Mass (%)*
1	X1	1.050	46.21	Y1	0.685	42.34	T1	0.709	36.32
2	X2	0.182	09.04	Y2	0.214	37.24	T2	0.374	24.19
3	X3	0.121	05.69	Y3	0.120	10.33	T3	0.356	19.19
4	X4	0.085	03.13	Y4	0.087	02.59	T4	0.169	8.22
5	X5	0.065	02.48	Y5	0.073	02.06	T5	0	0
6	X6	0.039	01.61	Y6	0.060	02.53	T6	0	0
7	X7	0.000	00.00	Y7	0.046	01.50	T7	0	0
8	X8	0.000	00.00	Y8	0.023	01.05	T8	0	0
		Total	96.41			97.80			88.93

Table A.5: Modal Analysis results for T1ZIID60

Mode		*X Period*	*Modal Mass (%)*		*Y Period*	*Modal Mass (%)*		*T Period*	*Modal Mass (%)*
1	X1	0.985	35.79	Y1	0.663	35.63	T1	0.625	11.86
2	X2	0.278	19.03	Y2	0.178	24.32	T2	0.182	6.75
3	X3	0.144	09.03	Y3	0.094	13.29	T3	0.140	0.05
4	X4	0.092	17.77	Y4	0.069	15.71	T4	0	0
5	X5	0.080	05.49	Y5	0.039	03.98	T5	0	0
6	X6	0.056	02.78	Y6	0.021	02.50	T6	0	0
7	X7	0.051	02.57	Y7	0	0	T7	0	0
8	X8	0.033	04.70	Y8	0	0	T8	0	0
		Total	97.16			95.43			18.66

Table A.6: Modal Analysis results for T1ZIIB100

Mode		*X Period*	*Modal Mass (%)*		*Y Period*	*Modal Mass (%)*		*T Period*	*Modal Mass (%)*
1	X1	2.101	62.08	Y1	1.534	57.85	T1	1.435	63.04
2	X2	0.569	22.36	Y2	0.346	23.86	T2	0.441	26.26
3	X3	0.290	07.31	Y3	0.167	09.45	T3	0.209	03.22
4	X4	0.172	01.41	Y4	0.103	01.93	T4	0	0
5	X5	0.111	00.66	Y5	0.066	01.12	T5	0	0
6	X6	0.072	02.96	Y6	0.048	03.27	T6	0	0
7	X7	0.038	02.05	Y7	0.025	01.63	T7	0	0
		Total	98.83			99.11			92.52

Table A.7: Modal Analysis results for T1ZIIC100

Mode		***X Period***	***Modal Mass (%)***		***Y Period***	***Modal Mass (%)***		***T Period***	***Modal Mass (%)***
1	X1	2.085	46.54	Y1	1.529	43.32	T1	1.391	24.28
2	X2	0.562	22.83	Y2	0.346	23.49	T2	0.447	44.71
3	X3	0.304	13.68	Y3	0.178	18.32	T3	0.265	14.28
4	X4	0.186	04.81	Y4	0.118	06.36	T4	0	0
5	X5	0.130	04.69	Y5	0.089	02.21	T5	0	0
6	X6	0.091	03.17	Y6	0.072	02.20	T6	0	0
7	X7	0.055	02.23	Y7	0.053	01.83	T7	0	0
		Total	97.95			97.73			83.27

Table A.8: Modal Analysis results for T1ZIID100

Mode		***X Period***	***Modal Mass (%)***		***Y Period***	***Modal Mass (%)***		***T Period***	***Modal Mass (%)***
1	X1	2.037	42.69	Y1	1.512	41.18	T1	1.345	17.51
2	X2	0.508	14.52	Y2	0.328	17.50	T2	0.325	06.94
3	X3	0.249	09.75	Y3	0.155	12.34	T3	0.132	03.36
4	X4	0.160	05.77	Y4	0.101	07.71	T4	0	0
5	X5	0.107	05.98	Y5	0.073	10.10	T5	0	0
6	X6	0.083	13.50	Y6	0.063	05.11	T6	0	0
7	X7	0.040	04.21	Y7	0.049	02.31	T7	0	0
8	X8	0	0	Y8	0.028	02.38	T8	0	0
		Total	96.42			98.63			27.81

Table A.9: Modal Analysis results for T1ZIIB150

Mode		***X Period***	***Modal Mass (%)***		***Y Period***	***Modal Mass (%)***		***T Period***	***Modal Mass (%)***
1	X1	3.161	56.90	Y1	2.442	53.42	T1	2.101	53.09
2	X2	0.804	16.86	Y2	0.536	19.17	T2	0.534	20.72
3	X3	0.376	10.15	Y3	0.234	10.85	T3	0.148	09.55
4	X4	0.239	06.75	Y4	0.143	06.66	T4	0	0
5	X5	0.163	02.78	Y5	0.097	03.64	T5	0	0
6	X6	0.067	03.49	Y6	0.043	03.93	T6	0	0
		Total	96.93			97.67			83.36

Table A.10: Modal Analysis results for T1ZIIC150

Mode		*X Period*	*Modal Mass (%)*		*Y Period*	*Modal Mass (%)*		*T Period*	*Modal Mass (%)*
1	X1	3.175	46.04	Y1	2.460	43.3	T1	2.072	24.16
2	X2	0.810	14.43	Y2	0.541	16.72	T2	0.532	15.15
3	X3	0.384	11.17	Y3	0.240	12.99	T3	0.290	33.88
4	X4	0.252	10.41	Y4	0.154	11.92	T4	0	0
5	X5	0.180	04.58	Y5	0.111	05.24	T5	0	0
6	X6	0.130	02.45	Y6	0.077	04.56	T6	0	0
7	X7	0.093	04.93	Y7	0.045	03.84	T7	0	0
8	X8	0.055	04.18	Y8	0	0	T8	0	0
		Total	98.19			98.57			73.19

Table A.11: Modal Analysis results for T1ZIID150

Mode		*X Period*	*Modal Mass (%)*		*Y Period*	*Modal Mass (%)*		*T Period*	*Modal Mass (%)*
1	X1	3.157	44.01	Y1	2.452	41.67	T1	2.053	19.96
2	X2	0.794	12.21	Y2	0.534	14.78	T2	0.507	06.35
3	X3	0.366	06.97	Y3	0.231	09.07	T3	0.231	03.35
4	X4	0.228	05.50	Y4	0.142	08.52	T4	0	0
5	X5	0.164	05.47	Y5	0.103	05.78	T5	0	0
6	X6	0.124	02.82	Y6	0.060	05.38	T6	0	0
7	X7	0.095	02.18	Y7	0.048	07.35	T7	0	0
8	X8	0.065	10.36	Y8	0	0	T8	0	0
		Total	89.52			92.55			29.66

Table A.12: Modal Analysis results for T2ZIIB60

Mode		*X Period*	*Modal Mass (%)*		*Y Period*	*Modal Mass (%)*		*T Period*	*Modal Mass (%)*
1	X1	1.045	65.22	Y1	0.665	62.18	T1	0.675	65.65
2	X2	0.352	22.85	Y2	0.211	25.61	T2	0.276	04.43
3	X3	0.080	03.61	Y3	0.096	02.68	T3	0.238	10.60
4	X4	0.049	04.13	Y4	0.060	03.27	T4	0	0
		Total	95.81			93.74			80.68

Table A.13: Modal Analysis results for T2ZIIC60

Mode		*X Period*	*Modal Mass (%)*		*Y Period*	*Modal Mass (%)*		*T Period*	*Modal Mass (%)*
1	X1	1.033	50.76	Y1	0.662	47.99	T1	0.660	38.10
2	X2	0.360	28.23	Y2	0.221	32.11	T2	0.286	35.30
3	X3	0.172	07.13	Y3	0.120	05.71	T3	0.253	04.30
4	X4	0.115	06.01	Y4	0.070	06.41	T4	0.142	06.62
5	X5	0.073	04.32	Y5	0.040	02.56	T5	0	0
6	X6	0.042	02.55	Y6	0	0	T6	0	0
		Total	99.00			94.78			84.32

Table A.14: Modal Analysis results for T2ZIID60

Mode		*X Period*	*Modal Mass (%)*		*Y Period*	*Modal Mass (%)*		*T Period*	*Modal Mass (%)*
1	X1	0.929	39.89	Y1	0.613	42.51	T1	0.582	22.82
2	X2	0.278	22.35	Y2	0.191	26.90	T2	0.175	15.34
3	X3	0.144	06.99	Y3	0.098	07.90	T3	0	0
4	X4	0.084	10.76	Y4	0.063	11.48	T4	0	0
5	X5	0.067	10.48	Y5	0.033	05.02	T5	0	0
6	X6	0.037	07.59	Y6	0	0	T6	0	0
		Total	98.06			93.81			38.16

Table A.15: Modal Analysis results for T2ZIIB100

Mode		*X Period*	*Modal Mass (%)*		*Y Period*	*Modal Mass (%)*		*T Period*	*Modal Mass (%)*
1	X1	2.097	62.22	Y1	1.501	58.02	T1	1.460	58.79
2	X2	0.570	22.29	Y2	0.353	25.04	T2	0.379	26.36
3	X3	0.290	07.28	Y3	0.172	06.84	T3	0	0
4	X4	0.172	01.13	Y4	0.102	01.79	T4	0	0
5	X5	0.106	00.86	Y5	0.049	04.86	T5	0	0
6	X6	0.060	04.27	Y6	0	0	T6	0	0
		Total	98.05			96.55			85.15

Table A.16: Modal Analysis results for T2ZIIC100

Mode		*X Period*	*Modal Mass (%)*		*Y Period*	*Modal Mass (%)*		*T Period*	*Modal Mass (%)*
1	X1	2.083	50.68	Y1	1.489	47.18	T1	1.439	34.03
2	X2	0.568	22.56	Y2	0.353	25.14	T2	0.379	32.52
3	X3	0.299	11.22	Y3	0.180	13.33	T3	0.238	03.13
4	X4	0.181	03.69	Y4	0.117	04.17	T4	0.235	08.70
5	X5	0.128	03.28	Y5	0.079	04.32	T5	0	0
6	X6	0.102	03.42	Y6	0.050	03.42	T6	0	0
7	X7	0.058	03.59	Y7	0	0	T7	0	0
		Total	98.44			97.56			78.38

Table A.17: Modal Analysis results for T2ZIID100

Mode		*X Period*	*Modal Mass (%)*		*Y Period*	*Modal Mass (%)*		*T Period*	*Modal Mass (%)*
1	X1	1.900	44.81	Y1	1.390	43.78	T1	1.324	27.49
2	X2	0.487	15.60	Y2	0.327	20.70	T2	0.313	11.97
3	X3	0.237	10.29	Y3	0.161	12.50	T3	0	0
4	X4	0.157	04.85	Y4	0.105	03.58	T4	0	0
5	X5	0.108	01.50	Y5	0.047	05.94	T5	0	0
6	X6	0.076	12.20	Y6	0	0	T6	0	0
		Total	89.25			86.50			39.46

Table A.18: Modal Analysis results for T2ZIIB150

Mode		*X Period*	*Modal Mass (%)*		*Y Period*	*Modal Mass (%)*		*T Period*	*Modal Mass (%)*
1	X1	3.326	60.27	Y1	2.625	56.93	T1	2.457	56.78
2	X2	0.853	17.70	Y2	0.577	10.52	T2	0.577	10.87
3	X3	0.411	10.08	Y3	0.256	10.81	T3	0.273	10.99
4	X4	0.265	04.93	Y4	0.158	05.35	T4	0	0
5	X5	0.182	01.43	Y5	0.109	01.73	T5	0	0
6	X6	0.129	00.53	Y6	0.073	00.93	T6	0	0
7	X7	0.079	00.86	Y7	0.039	03.29	T7	0	0
8	X8	0.046	02.88	Y8	0	0	T8	0	0
		Total	98.68			89.56			78.64

Table A.19: Modal Analysis results for T2ZIIC150

Mode		*X Period*	*Modal Mass (%)*		*Y Period*	*Modal Mass (%)*		*T Period*	*Modal Mass (%)*
1	X1	3.340	52.05	Y1	2.630	49.01	T1	2.457	37.00
2	X2	0.857	16.04	Y2	0.577	18.17	T2	0.573	16.44
3	X3	0.413	11.20	Y3	0.257	12.42	T3	0.278	21.19
4	X4	0.269	07.29	Y4	0.159	08.80	T4	0	0
5	X5	0.189	02.85	Y5	0.114	03.60	T5	0	0
6	X6	0.133	02.02	Y6	0.075	03.36	T6	0	0
7	X7	0.096	03.92	Y7	0.047	03.63	T7	0	0
8	X8	0.052	03.31	Y8	0	0	T8	0	0
		Total	98.68			98.99			74.63

Table A.20: Modal Analysis results for T2ZIID150

Mode		*X Period*	*Modal Mass (%)*		*Y Period*	*Modal Mass (%)*		*T Period*	*Modal Mass (%)*
1	X1	3.140	47.63	Y1	2.441	45.09	T1	2.287	31.87
2	X2	0.796	13.16	Y2	0.538	16.27	T2	0.524	10.85
3	X3	0.369	07.51	Y3	0.147	08.45	T3	0.229	06.10
4	X4	0.232	06.48	Y4	0.102	04.74	T4	0	0
5	X5	0.166	04.83	Y5	0.064	06.65	T5	0	0
6	X6	0.122	02.41	Y6	0.040	06.46	T6	0	0
7	X7	0.076	05.14	Y7	0	0	T7	0	0
8	X8	0.047	10.11	Y8	0	0	T8	0	0
		Total	97.27			87.66			48.82

Appendix B. LTHA Results

B.1 Storey Shear

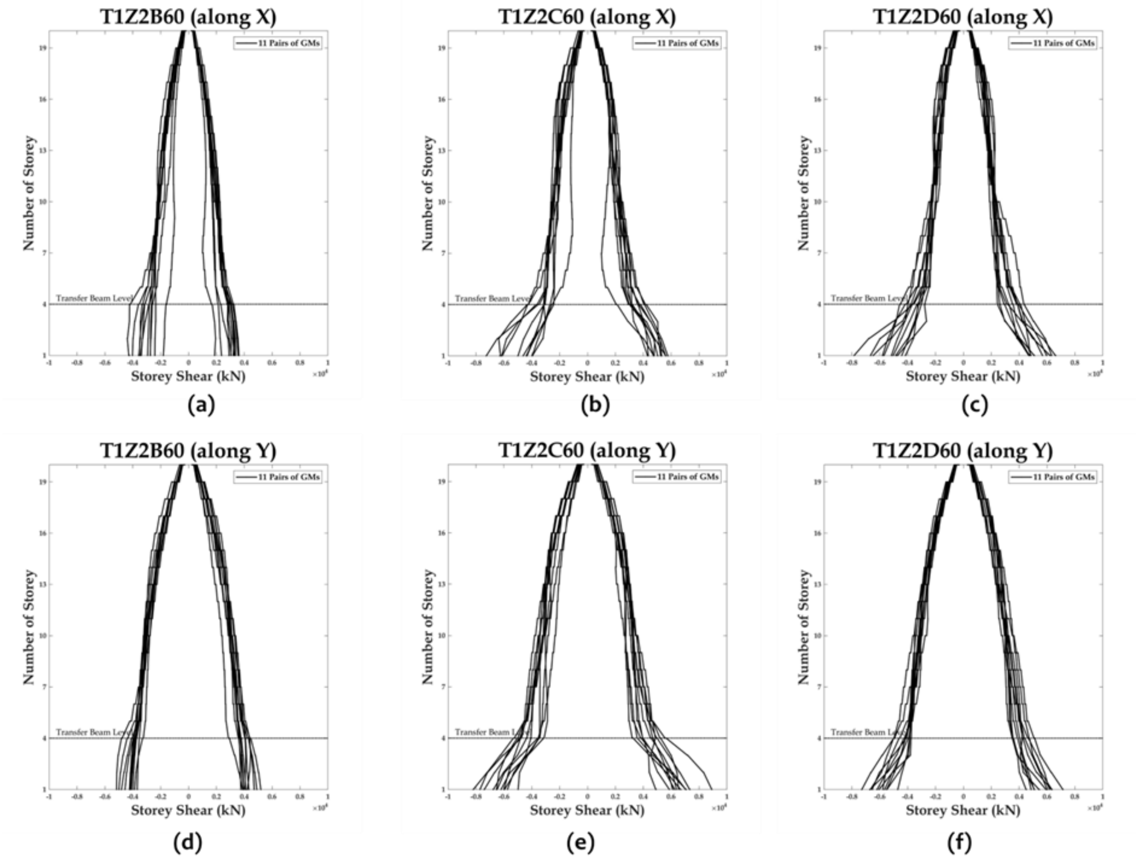

Figure B.1: LTHA Storey Shear of T1_60s

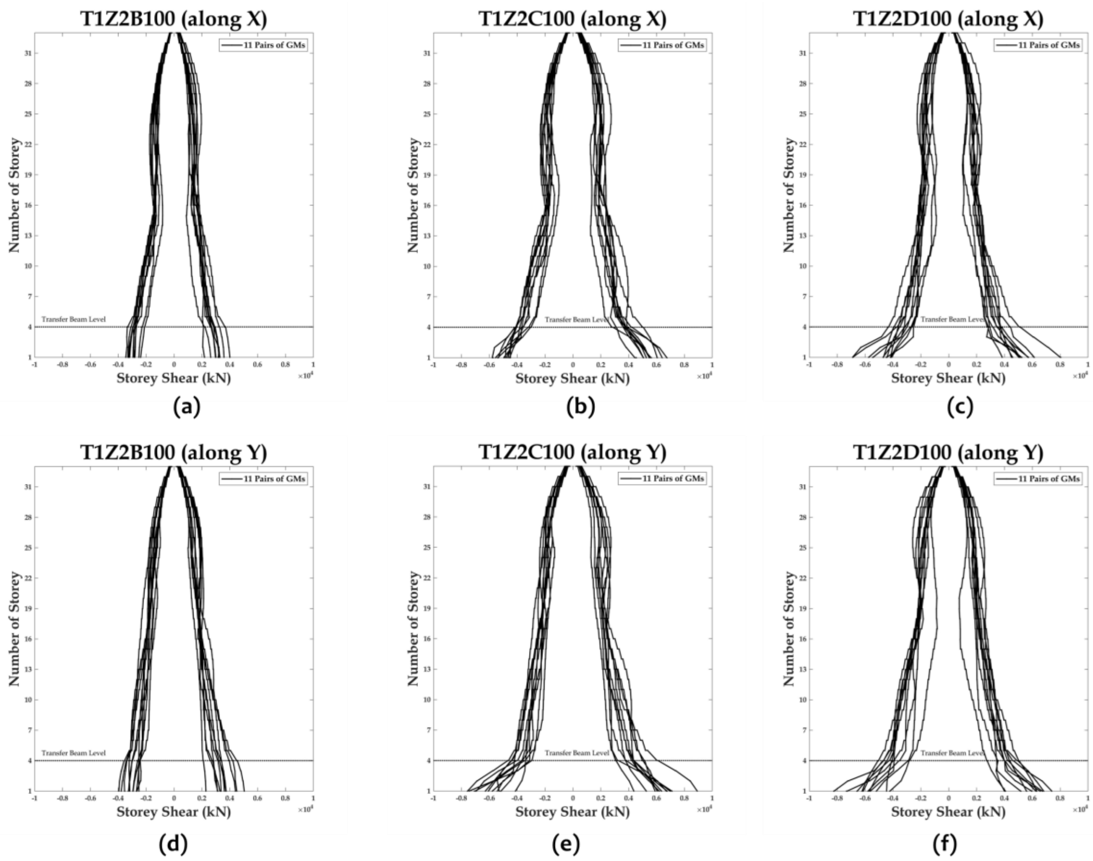

Figure B.2: LTHA Storey Shear of T1_100s

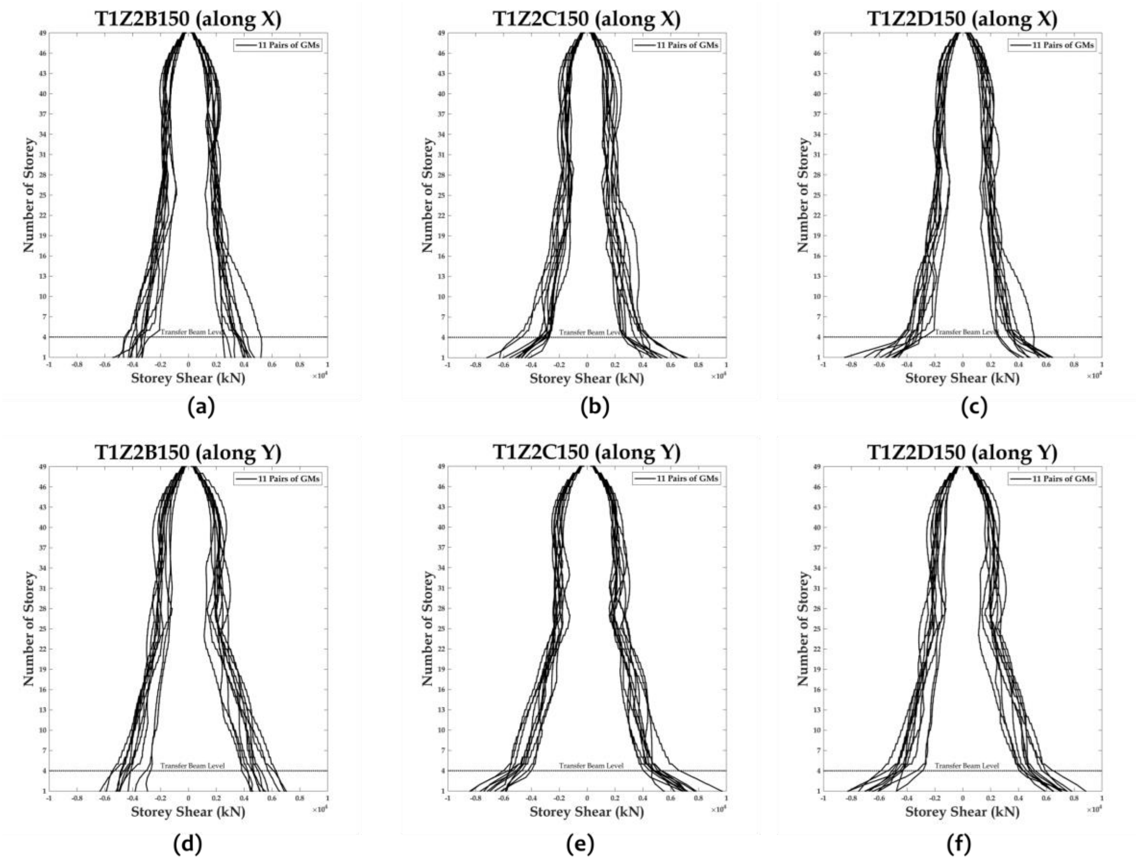

Figure B.3: LTHA Storey Shear of T1_150s

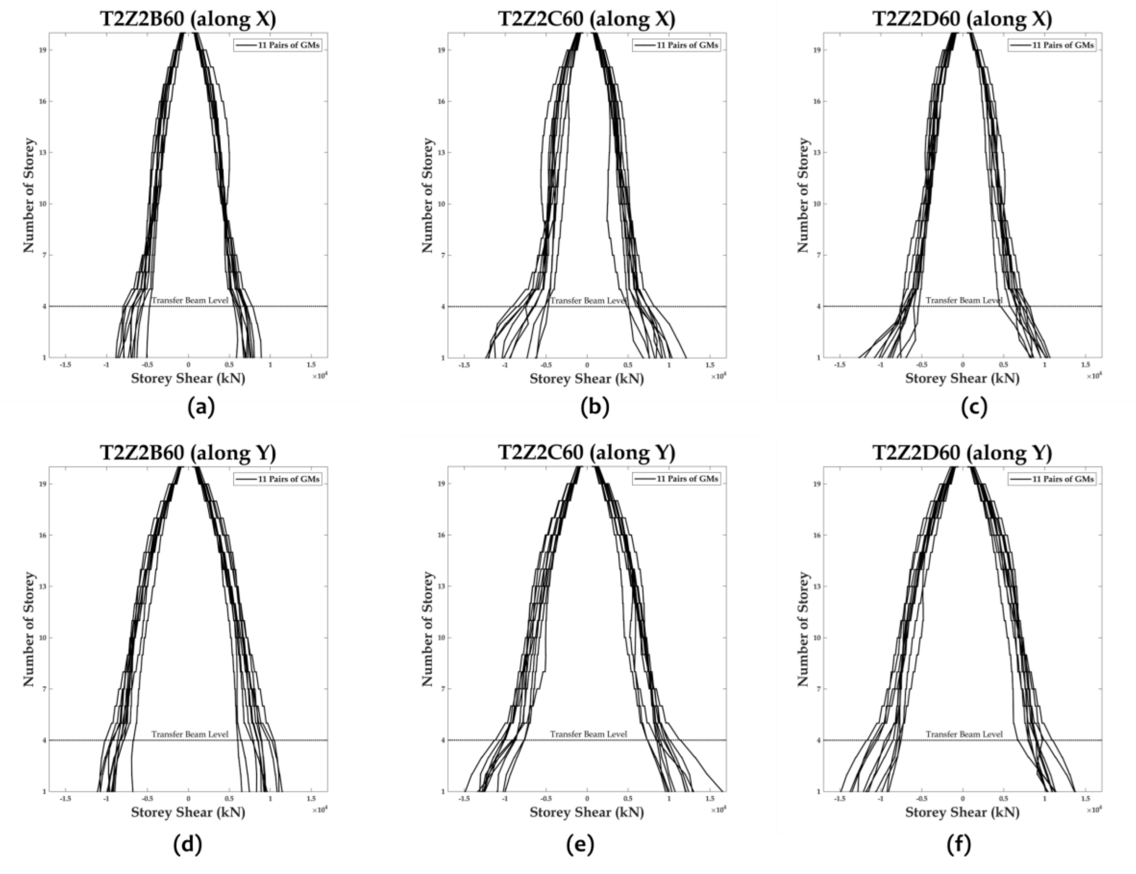

Figure B.4: LTHA Storey Shear of T2_60s

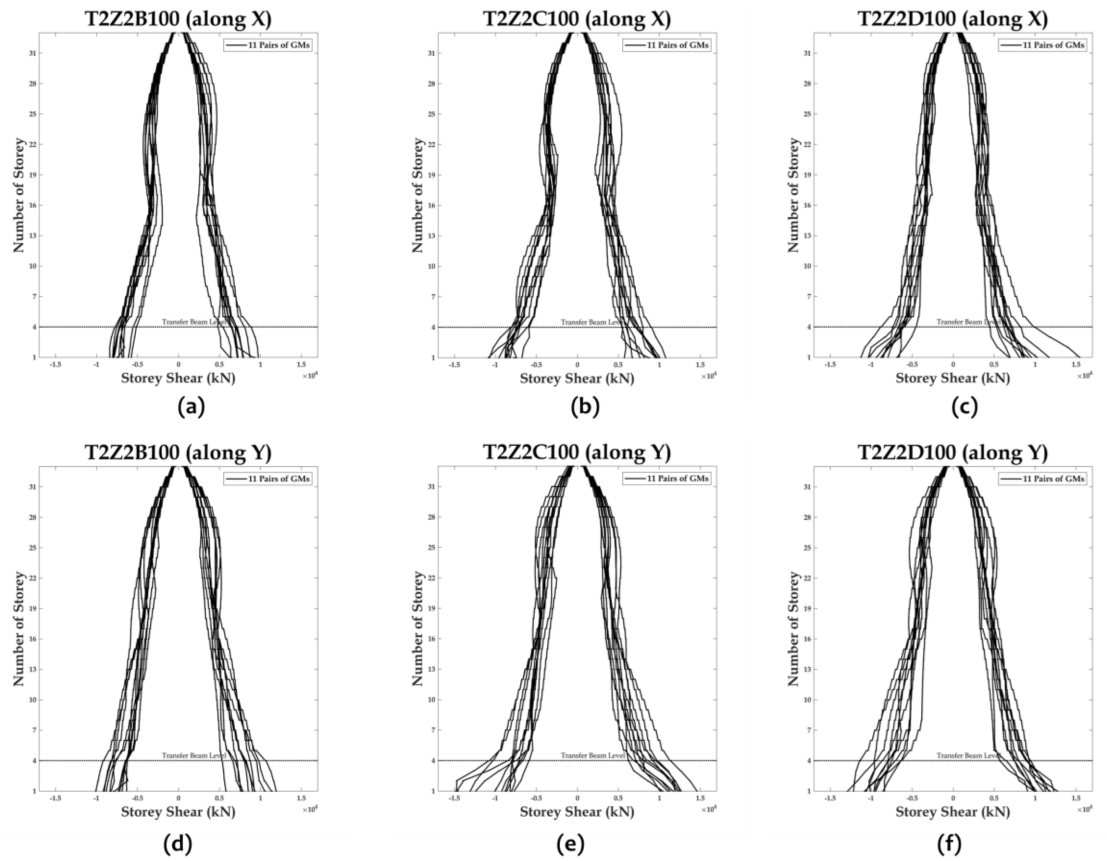

Figure B.5: LTHA Storey Shear of T2_100s

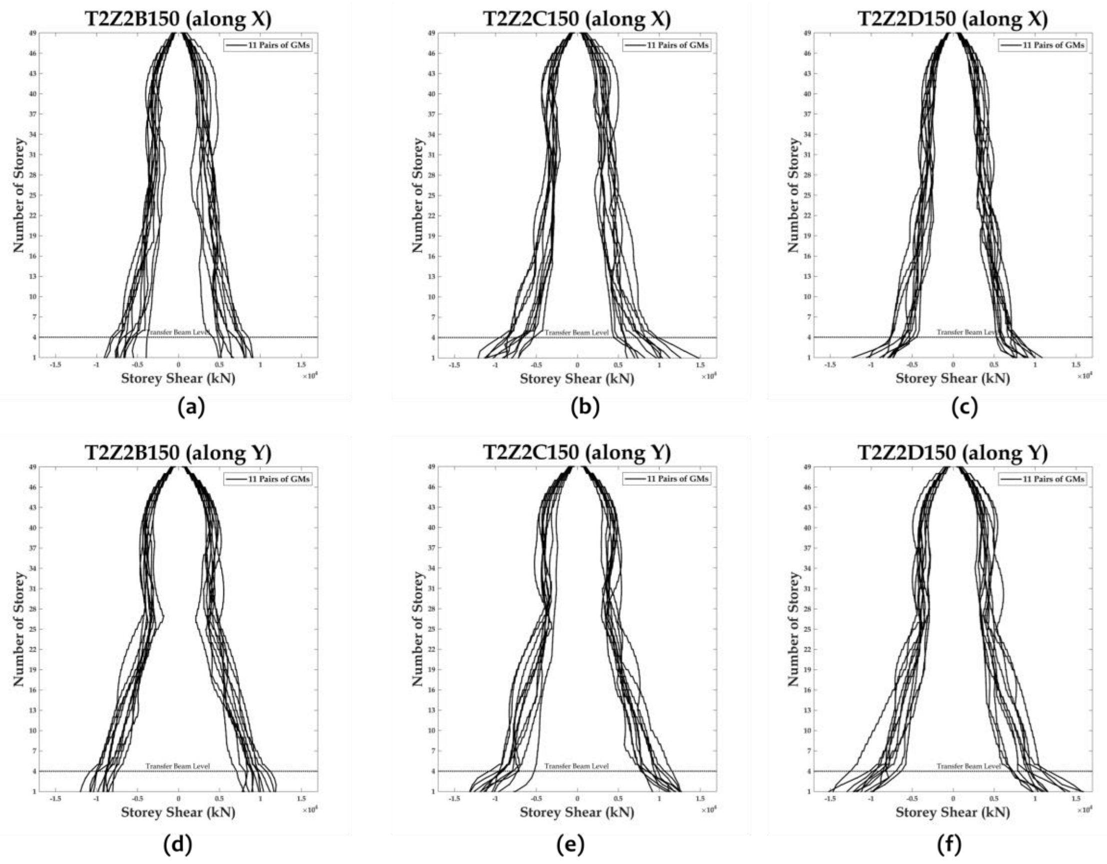

Figure B.6: LTHA Storey Shear of T2_150s

B.2 Displacements

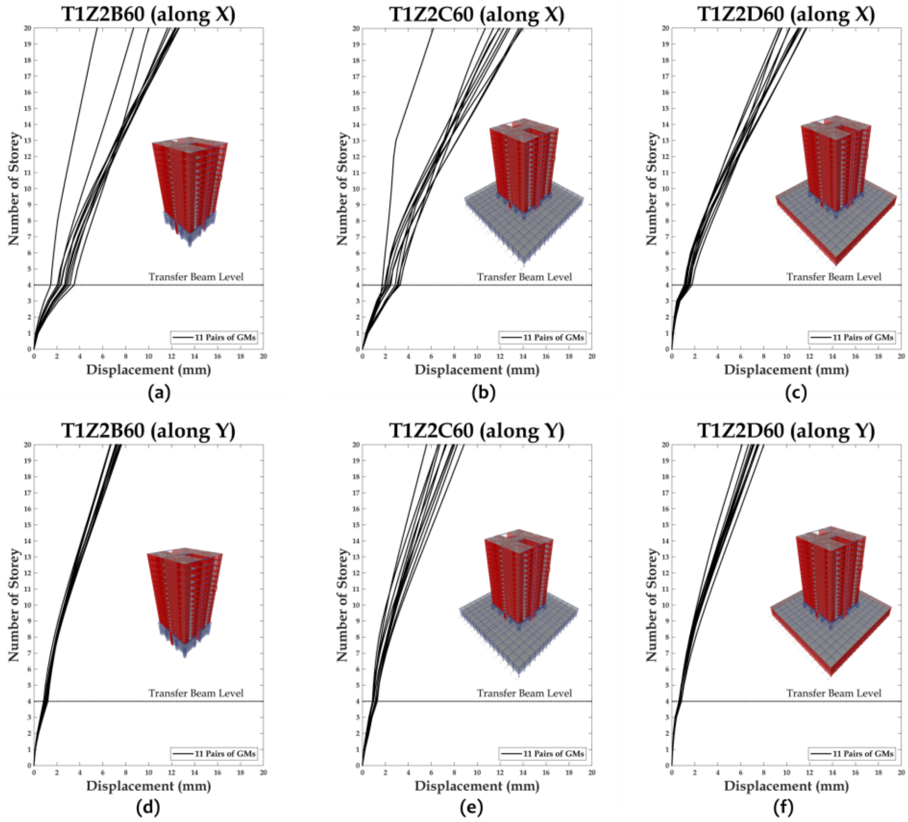

Figure B.7: LTHA Displacements of T1_60s

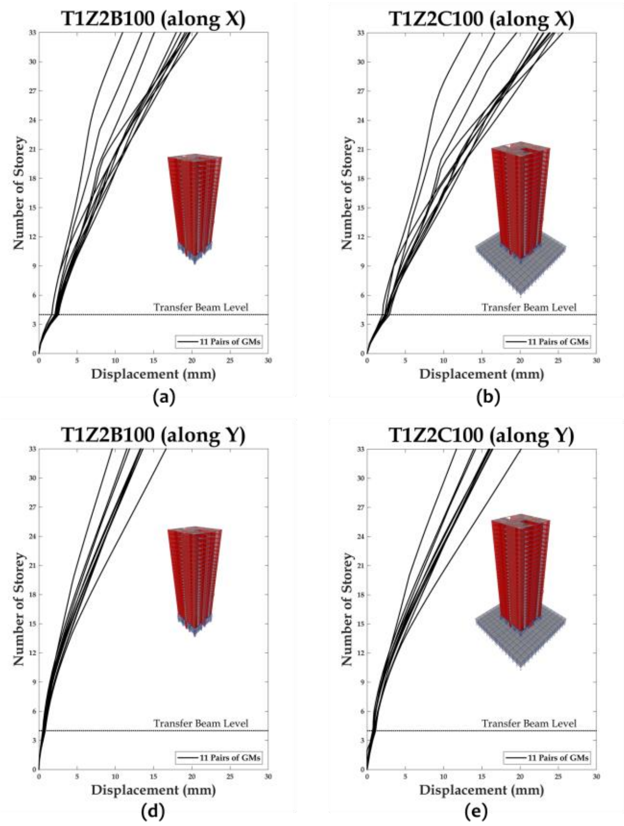

Figure B.8: LTHA Displacements of T1_100s

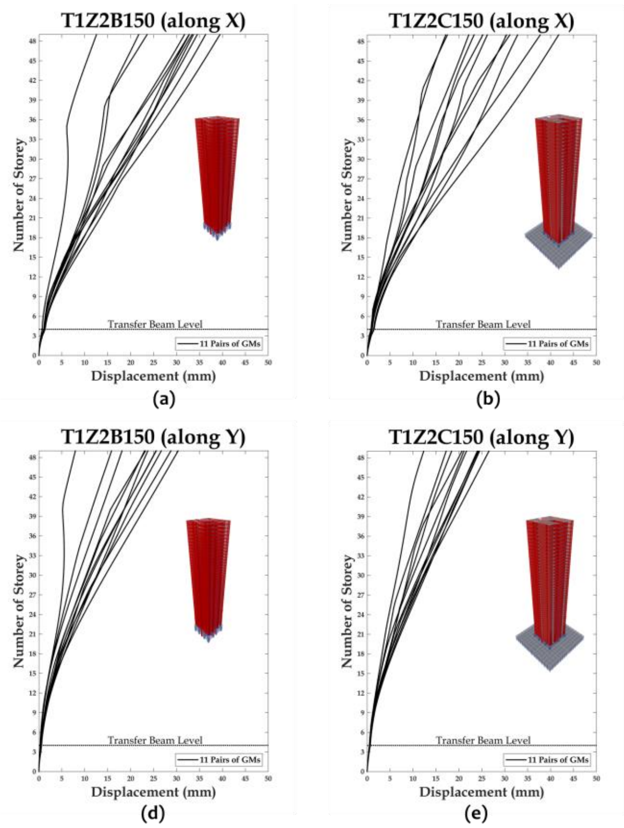

Figure B.9: LTHA Displacements of T1_150s

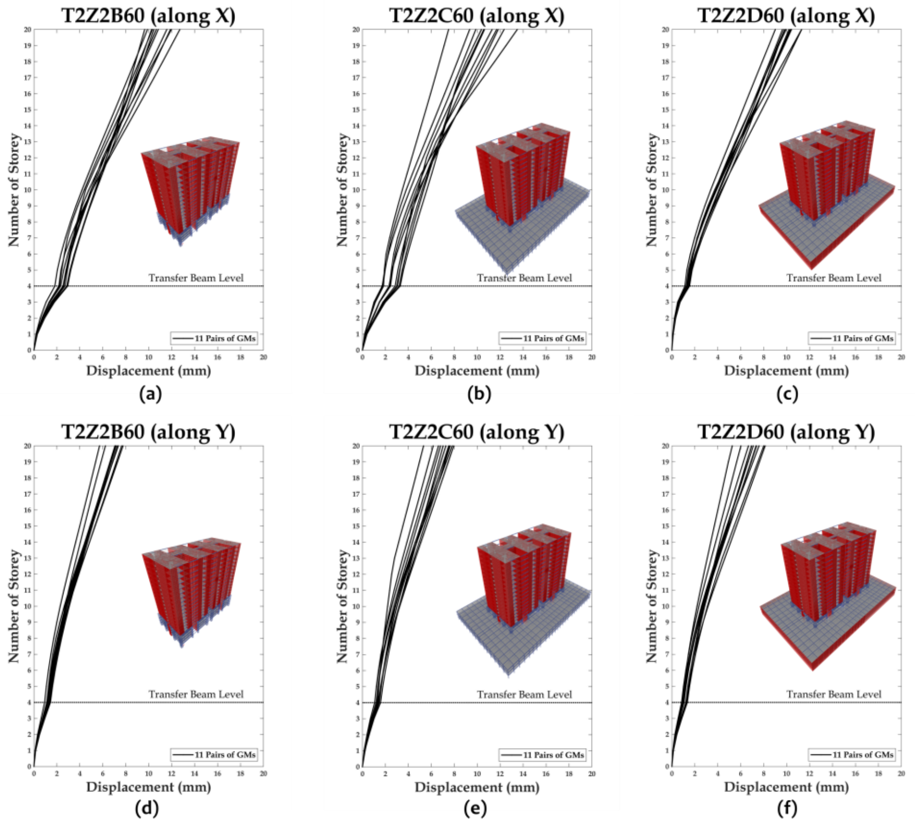

Figure B.10: LTHA Displacements of T2_60s

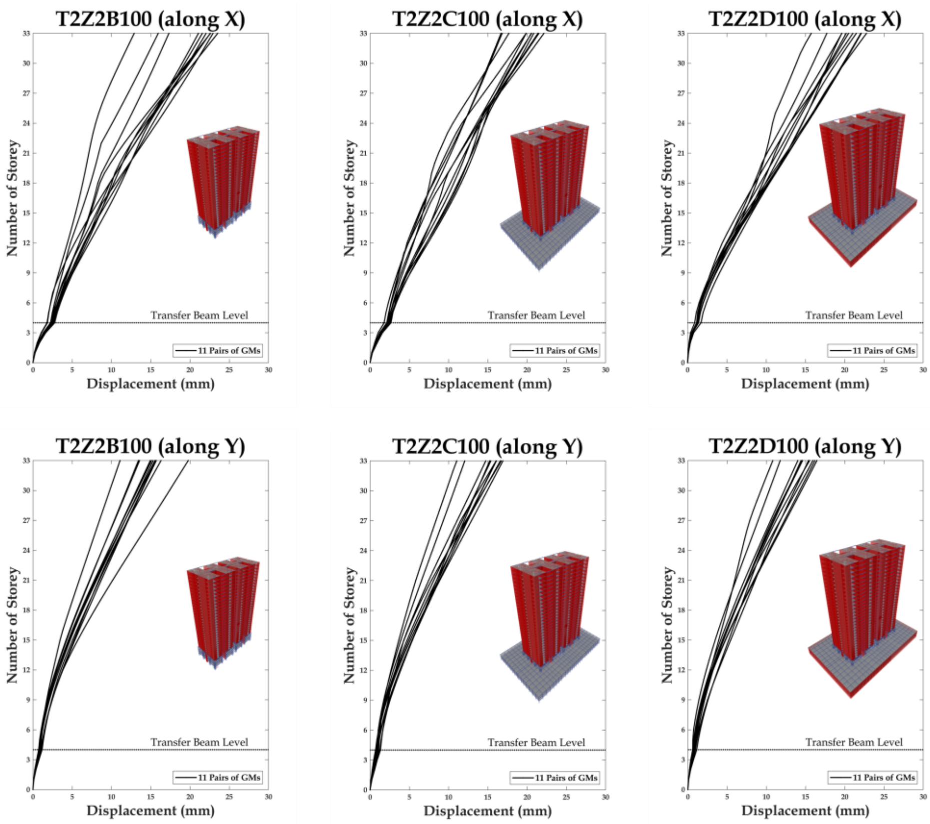

Figure B.11: LTHA Displacements of T2_100s

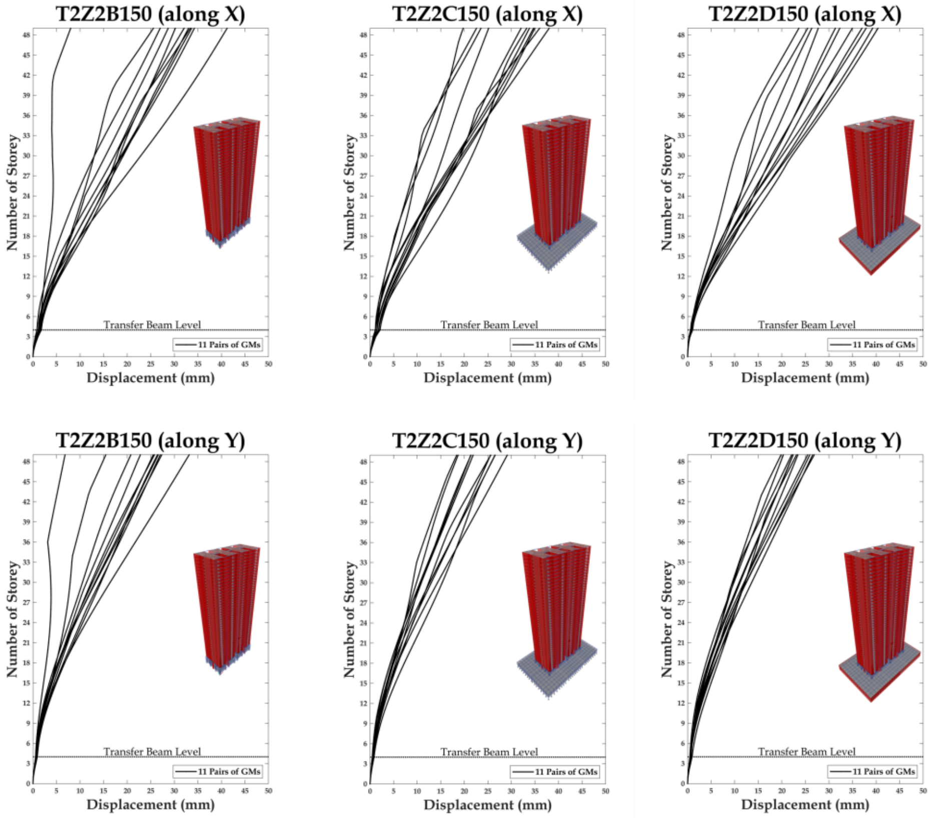

Figure B.12: LTHA Displacements of T2_100s

B.3 Building Drift

The building drifts in percentage are computed using equation B.1, and computed values are given in Table B.1.

$$Building\ Drift\ (\%) = 100 \times \frac{Roof\ Displacement}{Building\ Height} = 100 \times \frac{\Delta_{roof}}{H} \qquad \text{B.1}$$

Table B.1: Maximum LTHA Building Drift (%)

Model ID	*LTHA Building Drift (%)*		*Model ID*	*LTHA Building Drift (%)*	
	X Max	*Y Max*		*X Max*	*Y Max*
T1ZIIB60	0.0204	0.0123	T2ZIIB60	0.0205	0.0125
T1ZIIC60	0.0225	0.0143	T2ZIIC60	0.0218	0.0128
T1ZIID60	0.0189	0.0129	T2ZIID60	0.0182	0.0131
T1ZIIB100	0.0205	0.0165	T2ZIIB100	0.0233	0.0196
T1ZIIC100	0.0253	0.0199	T2ZIIC100	0.0219	0.0168
T1ZIID100	0.0264	0.0171	T2ZIID100	0.0225	0.0163
T1ZIIB150	0.0265	0.0204	T2ZIIB150	0.0277	0.0222
T1ZIIC150	0.0413	0.0263	T2ZIIC150	0.0376	0.0288
T1ZIID150	0.0264	0.0205	T2ZIID150	0.0271	0.0180

B.4 Inter-storey Drift

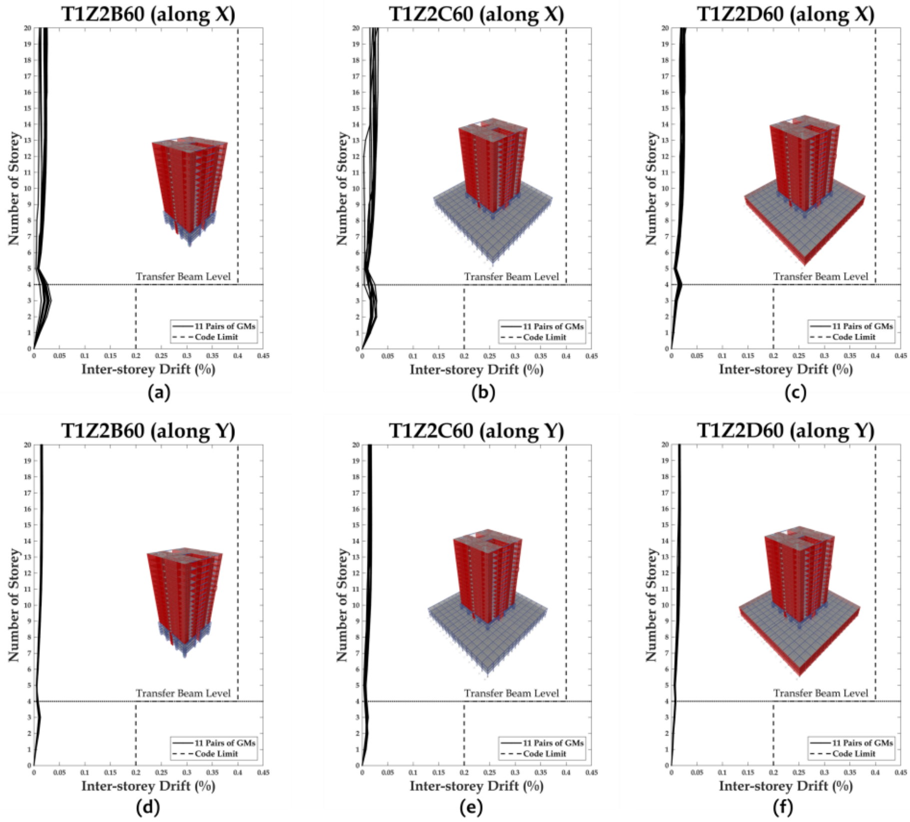

Figure B.13: LTHA IDR of T1_60s

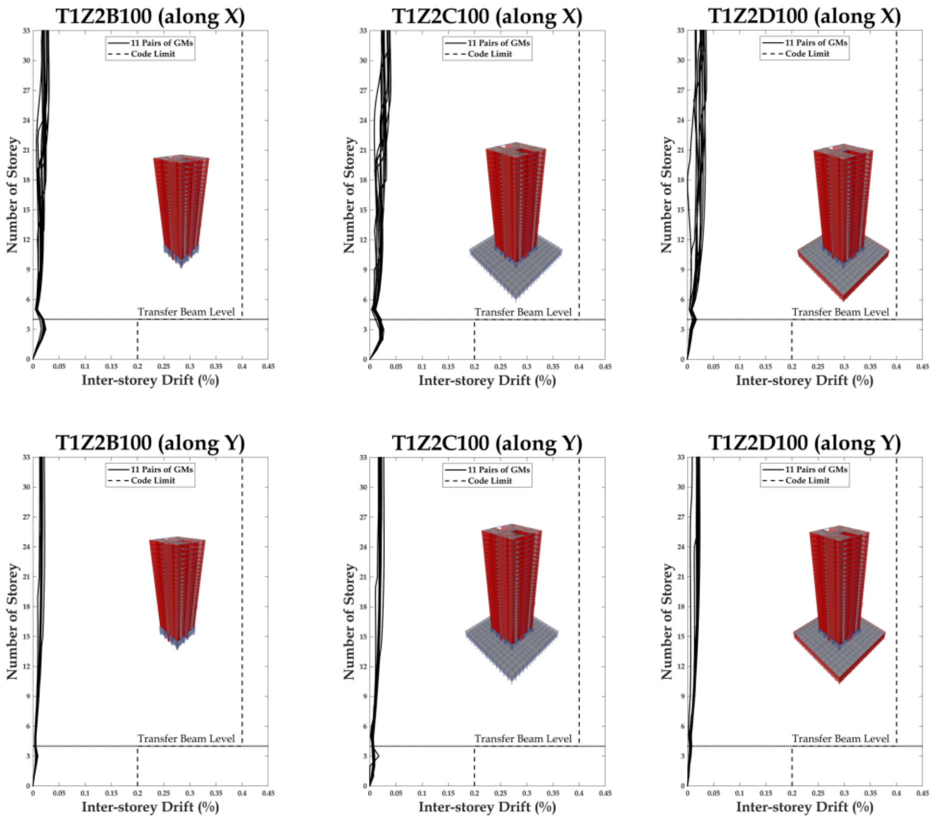

Figure B.14: LTHA IDR of T1_100s

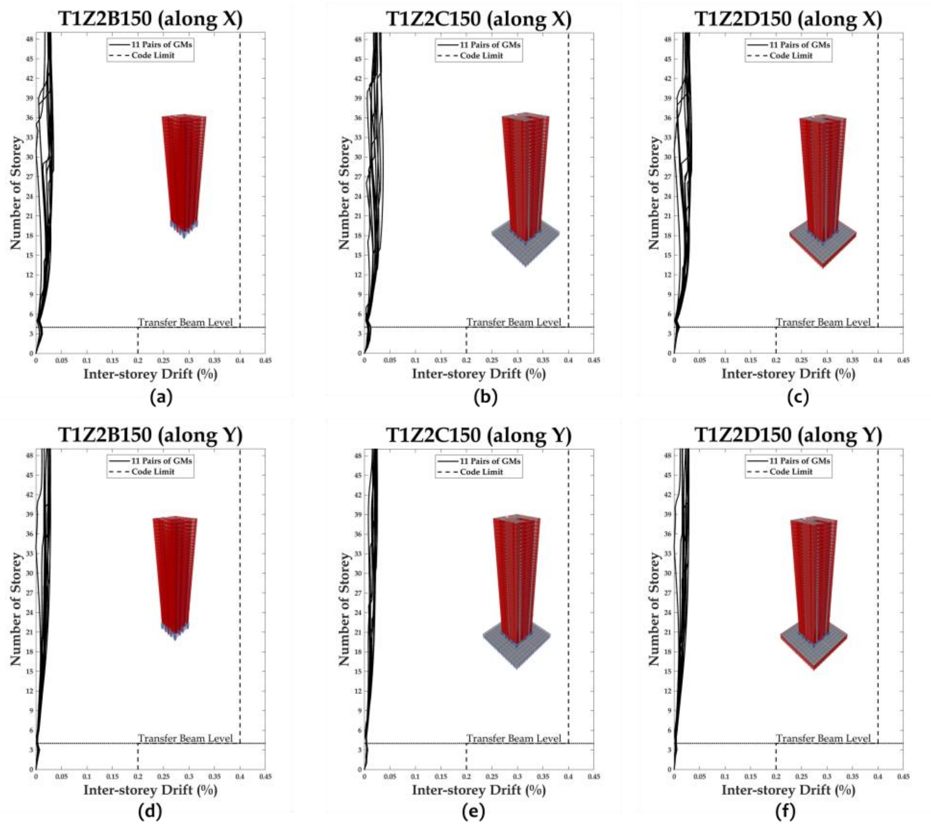

Figure B.15: LTHA IDR of T1_150s

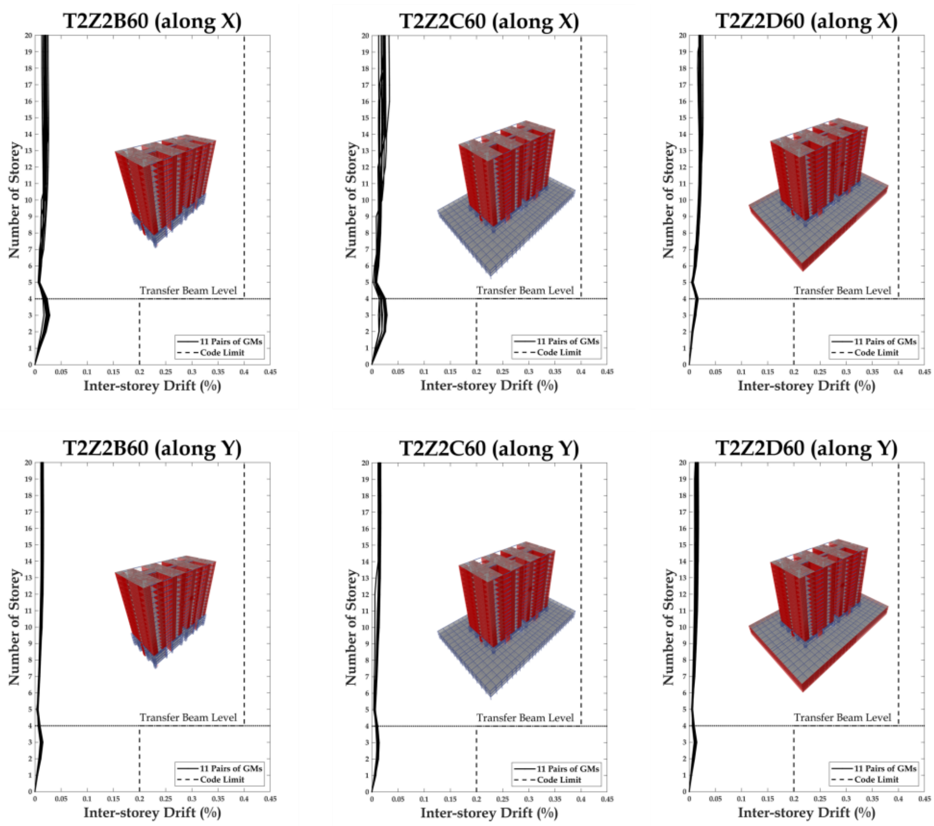

Figure B.16: LTHA IDR of T2_60s

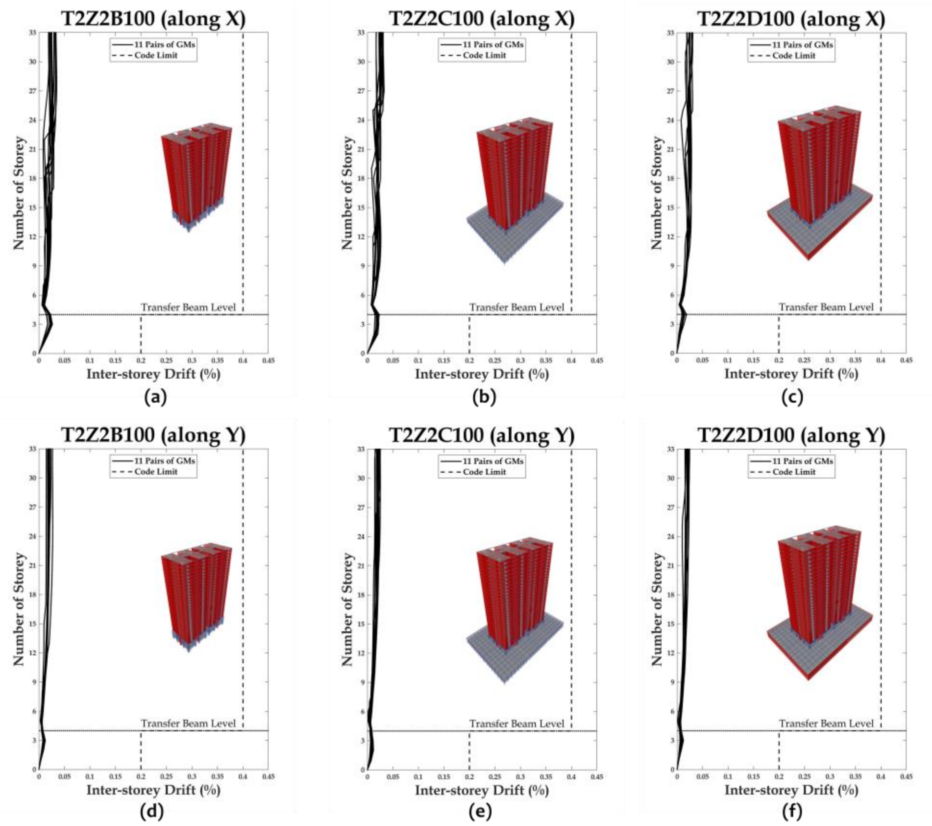

Figure B.17: LTHA IDR of T2_100s

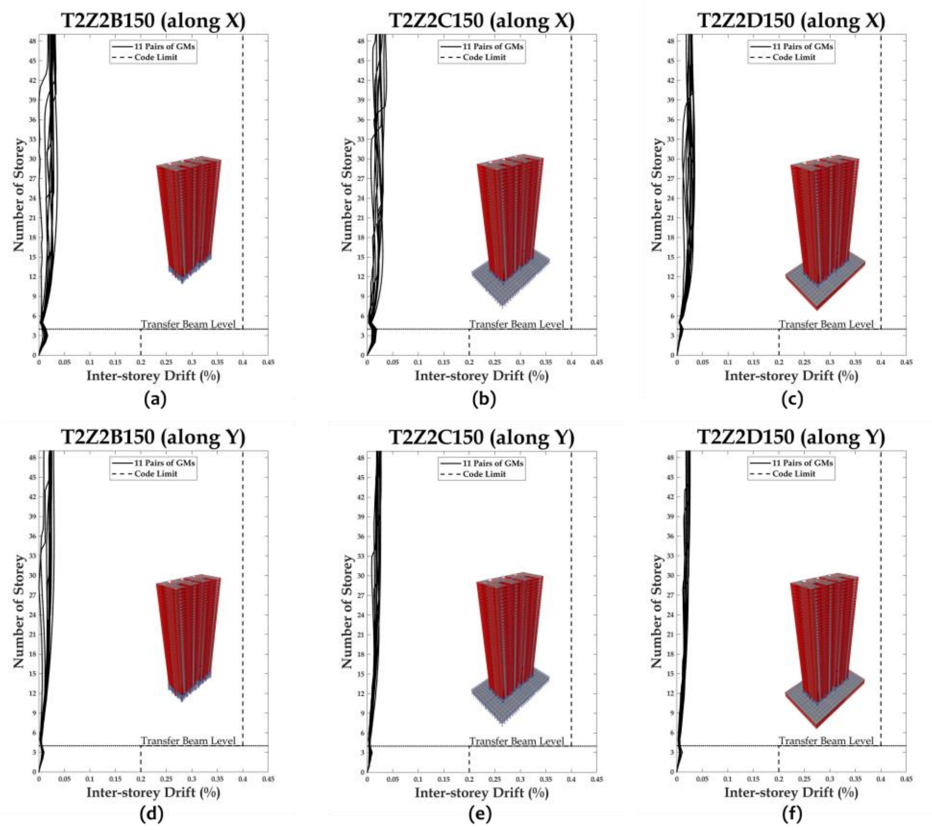

Figure B.18: LTHA IDR of T2_150s

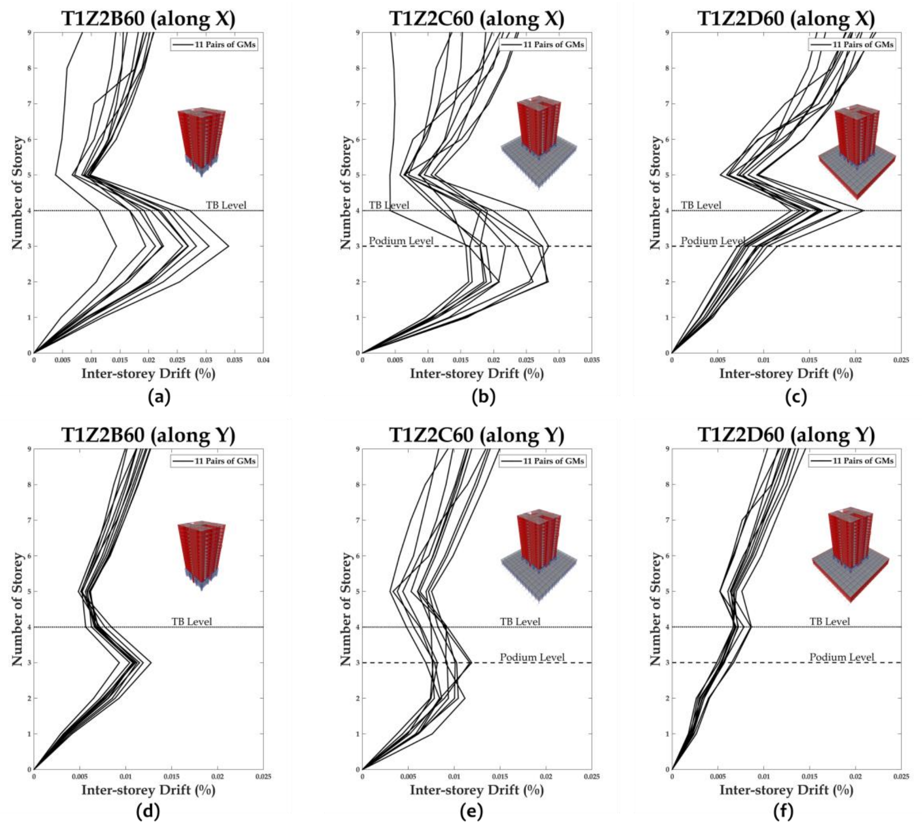

Figure B.19: LTHA IDR of T1_60s at lower levels

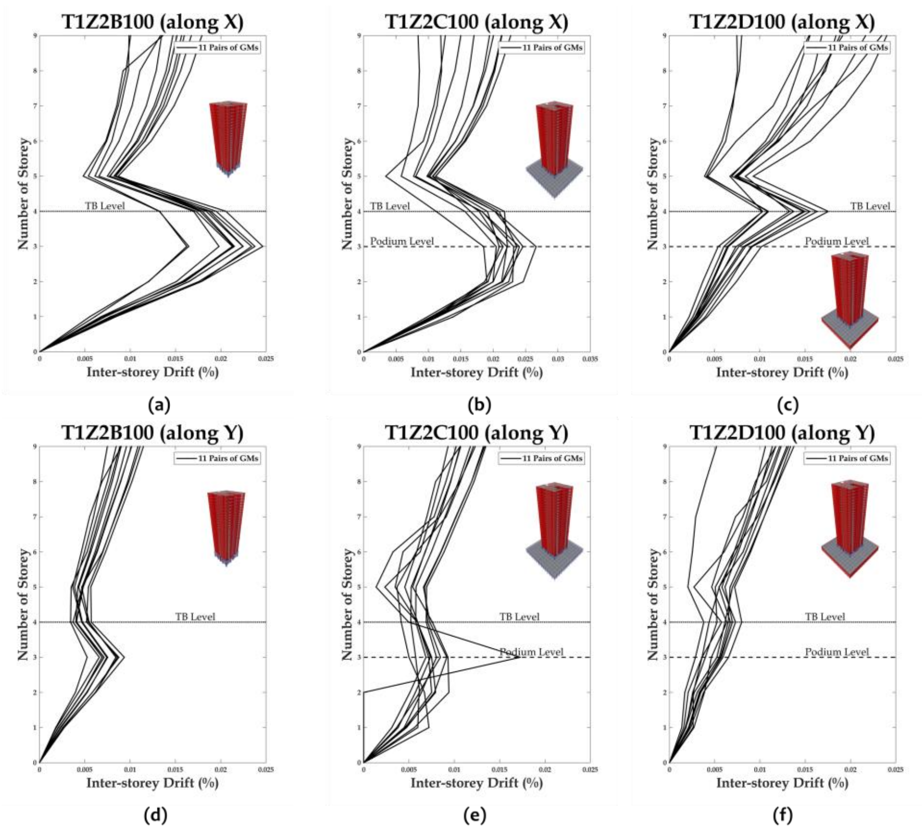

Figure B.20: LTHA IDR of T1_100s at lower levels

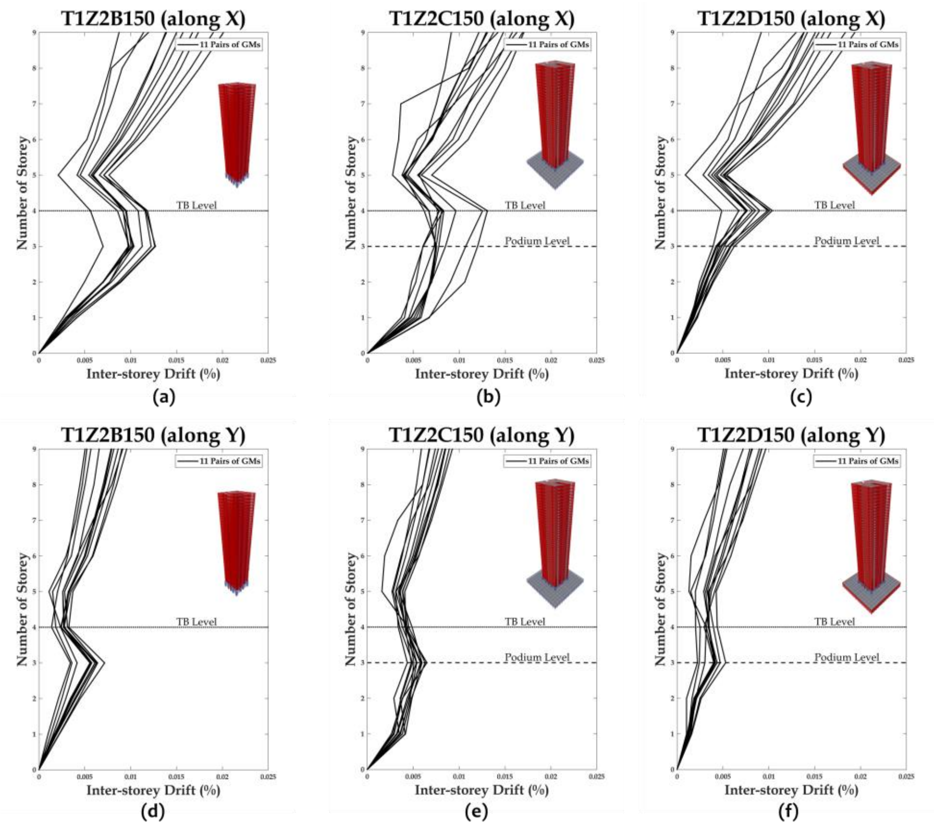

Figure B.21: LTHA IDR of T1_150s at lower levels

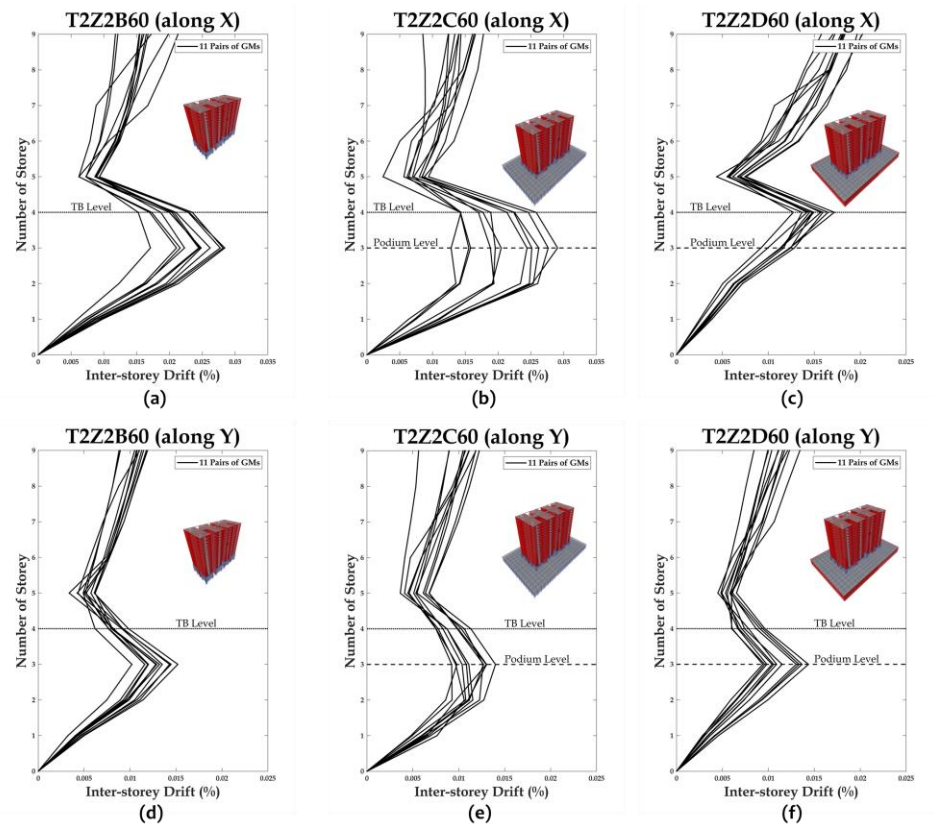

Figure B.22: LTHA IDR of T2_60s at lower levels

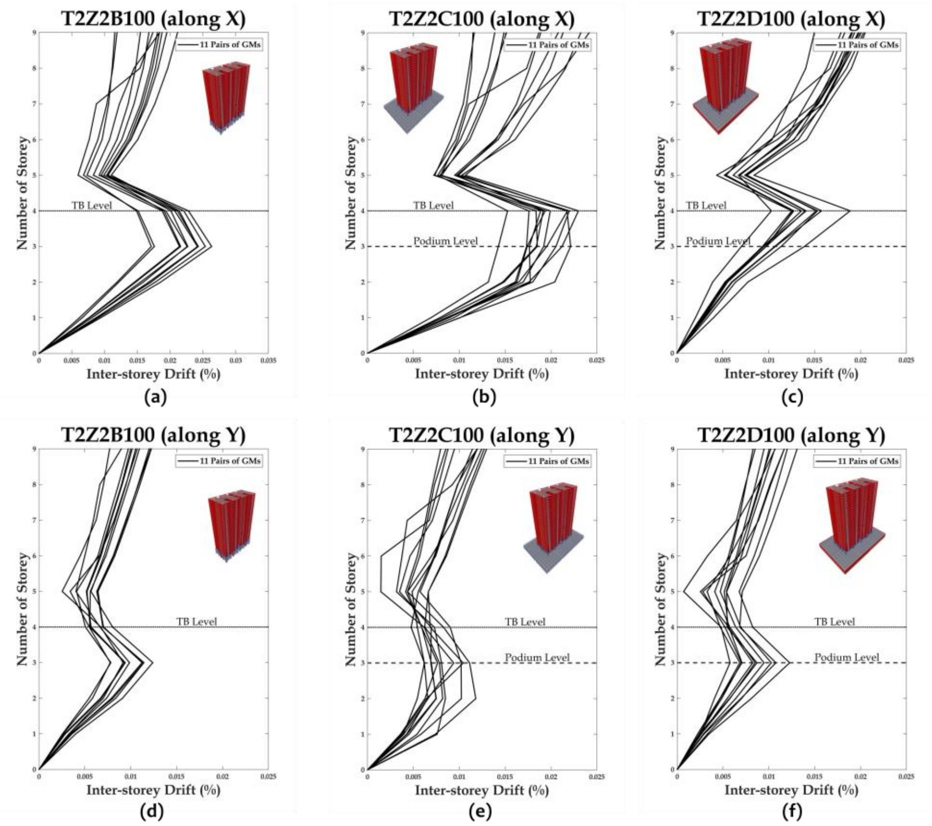

Figure B.23: LTHA IDR of T2_100s at lower levels

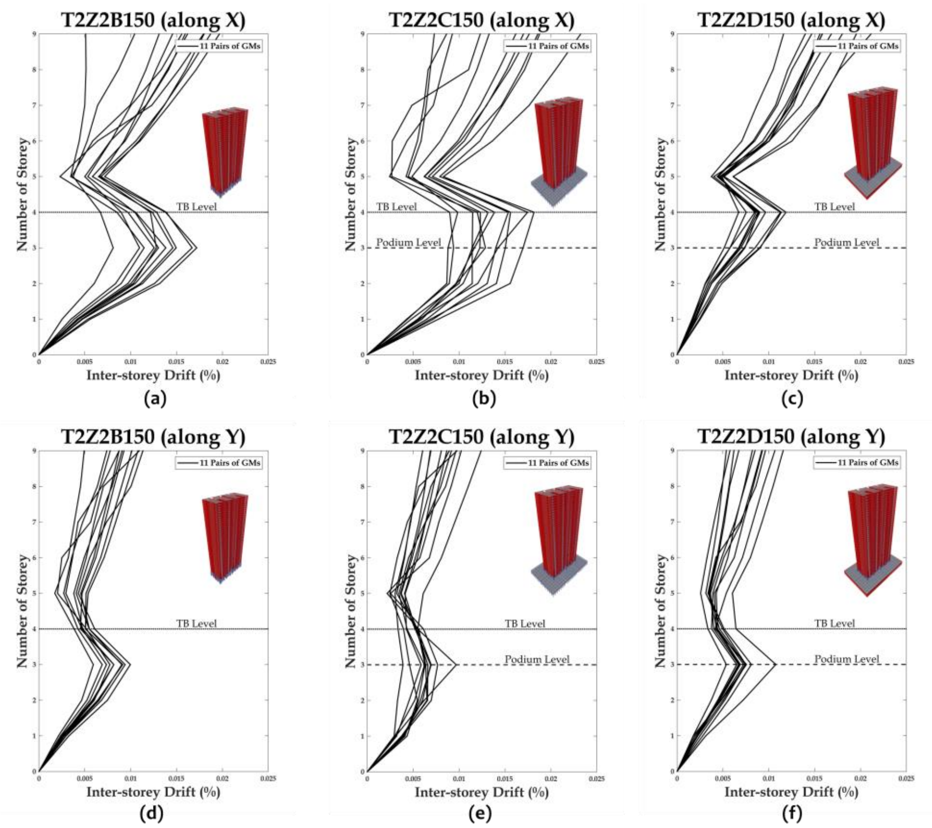

Figure B.24: LTHA IDR of T2_150s at lower levels